THE UNIVERSITY OF MICHIGAN

INDUSTRY PROGRAM OF THE COLLEGE OF ENGINEERING

CONDENSATION HEAT TRANSFER

Herman Merte, Jr.

Department of Mechanical Engineering
University of Michigan
Ann Arbor, Michigan

December 1971

IP-840

TABLE OF CONTENTS

LIST OF FIGURES v

NOMENCLATURE ix

I INTRODUCTION 1

II NUCLEATION 4

A. Surface Tension 5
B. Latent Heat 16
C. Equilibrium Across a Curved Surface 18
D. Bulk Phase Nucleation 29
E. Nucleation on Solid Phase 35

III LIQUID-VAPOR INTERFACE PHENOMENA 53

IV BULK CONDENSATION RATES 64

A. Condensation on Drops 64
1. Supersaturated Vapor 65
2. Subcooled Liquid Drop 67
B. Condensation in Liquid Bulk 69

V SURFACE CONDENSATION RATES 71

A. Prediction of Mode 71
B. Dropwise 77
1. Non-Condensables 77
2. Promotors 77
3. Effect of Surface Thermal Properties 79
4. Droplet Removal 80
5. Correlations 85
6. Effect of Vapor Velocity 94
C. Film Condensation 98
1. Classical Derivation 98
2. Laminar Film Condensation 102
a. Gravity Body Force 102
b. Forced Convection 118
c. Rotating Condensation 123
d. Miscellaneous Liquid Film Removal 125
3. Turbulent Film Condensation 126

VI MIXTURES 130

VII SIMILARITIES BETWEEN BOILING AND CONDENSATION 131

REFERENCES 135

List of Figures

1. Intermolecular forces at a surface
2. Pressure difference across a curved interface
3. Work of adhesion
4. Contact angles
5. Vapor-liquid drop equilibrium
6. Vapor-liquid drop equilibrium states
7. Free energy of formation of a liquid drop
8. Supersaturation limit in a nozzle with nitrogen. (Ref. 13)
9. Supersaturation ratio versus condensation temperature with nitrogen. (Ref. 13)
10. Rate of formation of condensation nuclei in water vapor. (Ref. 14)
11. Nucleation rate for water vapor. (Ref. 14)
12. Comparison of dropwise and film condensation of steam at atmospheric pressure on vertical copper surface. (Ref. 20)
13. Several models for dropwise condensation.
14. Measurements of intensity of reflected polarized light for detecting thin liquid film. (Ref. 19)
15. Heat flux during dropwise condensation of water on a horizontal surface (Ref. 33)
16. Summary of published results of heat transfer coefficient for dropwise condensation nucleation cavities. (Ref. 48)
17. Model for determining effective nucleating site.
18. Effective size range of condensation nucleation cavities. (Ref. 29)
19. Continuum representation of liquid-vapor interface.
20. Condensation coefficient of potassium versus saturation pressure (Ref. 42)
21. Dropwise bulk condensation
22. Application of a spray-type condenser to Rankin-cycle power plant

List of Figures (Cont.)

23. Interface surface free energy

24. Definition of critical surface tension. (Ref. 60)

25. Effect of nearby drops on drop growth rate. P(water vapor) = 19 mm Hg. (Ref. 33)

26. Correlation of growth rates of condensation water drops on copper promoted by benzyl mercaptan. (Ref. 33)

27. Average condensation water drop distribution for maximum diameters between 500 -3000 microns. (Ref. 33)

28. Theoretical curves from a computer model relating heat transfer coefficient to nucleation site density and maximum drop size. (Ref. 68)

29. Comparison of condensation heat transfer coefficients from correlation with independent data for steam. (Ref. 33)

30. Comparison of correlation for dropwise condensation with independent data for Ethylene Glycon. (Ref. 32)

31. Improved correlation for dropwise condensation on vertical surfaces. (Ref. 32)

32. Comparison of steam condensation drop growth with quasi-steady predictions. (Ref. 19)

33. Comparison of calculated and experimental values of condensation heat transfer coefficient. (Ref. 31)

34. Effect of mean vapor velocity on dropwise condensation. (Ref. 72)

35. Physical model for film condensation.

36. Local heat transfer from solution of complete boundary layer equation. (Ref. 76)

37. Local heat transfer for low Pr numbers from solution of complete boundary layer equation. (Ref. 76)

38. The effect of interfacial shear stress on heat transfer, $Pr > 1$. Laminar film condensation on vertical surface. (Ref. 77)

39. Effect of interfacial shear stress on heat transfer, liquid metal range. (Ref. 77)

40. Theoretical heat transfer - laminar film condensation on a vertical surface. (Ref. 78)

List of Figures (Cont.)

1. Comparison with data and theories for liquid metals. (Ref. 78)

2. Experimental data for condensation of saturated and superheated steam on a vertical surface. (Ref. 84)

3. Heat flux versus temperature difference for film condensation of saturated n-butyl alcohol on a vertical surface. (Ref. 85)

4. Variation of condensing film coefficient with Re for vertical tubes. (Ref. 148)

5. Condensing heat transfer data with horizontal tubes compared. (Ref. 148)

6. Variation of condensing film coefficient with tube inclination. (Ref. 148)

7. Correlation of condensation with forced convection in horizontal tubes. (Ref. 108)

8. Local heat transfer coefficient with condensation of steam. (Ref. 109)

9. Heat transfer with condensation on a vertical surface. (Ref. 126)

10. Turbulent condensation on vertical surfaces for various Prandtl numbers. (Ref. 127)

11. Effect of non-condensable gas on the steam-side heat transfer coefficient. (Ref. 130)

12. Effect of vent position on the steam-to-surface temperature difference for fixed venting rate. (Ref. 63)

NOMENCLATURE

Unless defined otherwise locally, the following apply:

a	Acceleration
A	Area, or defined below Eq. (57)
B_o	Bond number, Eq. (2)
C_p	Specific heat
D	Diameter
f	Fractional Area covered by drops
F	Force
g	Acceleration due to gravity, Gibbs free energy per mole
G	Total free energy, mass velocity
h	Heat transfer coefficient
h_{f_g}	Latent heat of vaporization
J	Rate of formation of condensation nuclei, Eq. (54)
k	Thermal conductivity, Boltzmann constant
L	Length
m	Mass per molecule
M	Mass, molecular weight
n	Number of moles
No	Avagadros' number
Nr	Distribution of embryos of radius r, Eq. (53)
Nu	Nusselt number
P	Pressure
Pr	Prandtl number
q	Heat transfer Rate
q_s	Latent heat of surface, Eq. (6)
r,R	Radius
R	Universal gas constant
r*	Critical radius
Re	Reynold's number
S	Spreading Coefficient, Eqs. (11,87)
Sc	Schmidt number
Sh	Sherwood number
t	Time
T	Temperature
v	Velocity

NOMENCLATURE (Continued)

v	Specific volume
w	Mass flow rate
W	Work
α, θ	Angles
β, γ	Defined parameters
γ	Specific heat ratio
δ	Film thickness
ϵ_s	Total surface energy, Eq. (5)
Γ	Eq. (71)
π_E	Equilibrium film pressure, Eq. (84)
σ	Surface tension, condensation coefficient
ρ	Density
μ	Dynamic viscosity
ν	Kinematic viscosity

Subscripts

c	condensed, solid
cr	critical
e	emitted
i	liquid-vapor interface, incipient
ℓ	liquid
L	based on length L
m	mean
s	"normal" saturation
v	vapor
v_∞	bulk vapor
w	wall

I. INTRODUCTION

Condensation is the change in phase from the vapor state to the liquid or solid state. It can be considered as taking place either within a bulk material or on a cooled surface, and is accompanied by simultaneous heat and mass transfer.

Condensation plays a significant role in the heat rejection parts of the Rankine power generation cycle and the vapor compression refrigeration cycle, which generally involve single components (pure substances). Dehumidification in air conditioning and the production of liquified petroleum gases, liquid nitrogen and liquid oxygen are examples in which condensation in mixtures take plaee.

Condensation is initiated by a nucleation process, either in a bulk vapor or on a solid surface. Fog and clouds are droplets which have grown from nuclei in a gas-vapor mixture. The energy release or latent heat removal with condensation in clouds, under certain conditions, serves as the driving force for the severe thunder storms, with which we are all familiar.

Cryopumping and vacuum depositing of metals are examples of condensation in which the vapor-solid phase change takes place. Condensation takes place during the collapse phase of the cavitation process, and in the boiling of subcooled liquids.

The development of the heat pipe, which can provide an almost infinite effective thermal conductivity, depends on the high rate of heat transfer possible with condensation.

After consideration of the processes of nucleation, a moderately detailed examination of the liquid-vapor interface, and a brief discussion of bulk condensation, the majority of effort in this writing will be devoted to condensation on solid surfaces, since this has the greatest engineering significance.

Condensation on a cooled solid surface occurs in one of two ways; film or dropwise condensation.

In film condensation the liquid condensate forms a continuous film which covers the surface, and takes place when the liquid "wets" the surface. This film flows over the surface under the action of gravity or other body forces, surface rotation, and/or shear stresses due to vapor flow. Heat transfer to the solid surface takes place through the film, which forms the greatest part of the thermal resistance.

In dropwise condensation the vapor impinges on the cool wall, decreasing its energy and thereby liquifying, and forming drops which grow by direct condensation of vapor on the drops and by coalescence with neighboring droplets until the drops are swept off the surface by the action of gravity or other body forces, surface rotation, and/or shear stresses due to vapor flow. As the drops move they coalesce with other droplets in their path, sweeping a portion of the surface clean so that condensation can begin anew. The details of dropwise condensation are not completely understood, but it is known to take place under circumstances where the liquid does not "wet" the surface. Dropwise condensation of steam has heat transfer coefficients over 10 times as large as film condensation[1]. However, it has been difficult to sustain dropwise condensation commercially for long periods of time, so conservative designs must be based on operation with film condensation.

Efforts are continuing on means to predict the heat transfer coefficient for condensation more accurately, and to increase the heat transfer coefficient. This will result in reduced condenser sizes and would increase significantly the attractiveness of condensers in applications such as steam cars. The increase in the heat transfer coefficient will result if dropwise condensation can be sustained, or if the liquid film can be reduced in thickness in the case of film condensation.

Condensation heat transfer can be studied from either the macroscopic or microscopic point of view, as is the case in other physical phenomena. The ultimate objective for the engineer is to understand the phenomena so it can be described, and hence its behavior predicted for design purposes. The macroscopic viewpoint considers matter as a continuum, and requires the introduction of certain phenomenological laws, the macroscopic transport equations, in addition to the conservation equations of mass, energy, and momentum, in order to deal with rate processes. On a microscopic level, dealing with molecules, atoms, and sub-atomic particles, only the conservation principles need be introduced. However, because of limitations in describing these particles and in relating the large numbers of particles which constitute a reasonable size system one resorts to concepts of statistical and quantum mechanics. Both points of view, macroscopic and microscopic, will be introduced here as appropriate where it aids in understanding the phenomena of condensation.

II. NUCLEATION

Nucleation involves a nucleus-a starting point for growth. Nucleation and subsequent condensation can occur only if energy of the vapor is removed or reduced such that the temperature is sufficiently below the saturation temperature. This can be considered in one of two categories, depending on how the energy removal takes place: bulk nucleation, and solid surface nucleation.

Bulk nucleation occurs within the bulk of the vapor away from solid boundaries, and takes place either as homogeneous nucleation in the absence of any other phases such as entrained foreign particles, or as heterogeneous nucleation on foreign particles entrained in the vapor, such as dust[2]. Bulk nucleation of a pure vapor can occur only by an adiabatic expansion, such that a transformation of energy from internal energy to other forms takes place. The vapor then becomes supersaturated until nuclei spontaneously form. Such an expansion in a nozzle produces a so-called condensation shock, and can occur within the low pressure stage of a steam turbine, or in expansions to very low pressures as in space. The strange particles observed outside of the spacecraft by the astronauts in the Appollo flights are believed to be solid condensed vapors. The Wilson cloud chamber, used to detect cosmic radiation, is an example of a non-flow adiabatic expansion to produce a supersaturated vapor. The path of the charged particles is made visible by the condensation trail left behind.

In a mixture of vapor and "non-condensable" gases, such as water vapor and air, bulk nucleation can also take place by expansion of the mixture, as is the case with pure vapors mentioned above. Meteorologically, the clouds in the center of a low-pressure region are in part a consequence of this expansion; one rarely observes clouds in the center of a high pressure area. The temperature of a mixture can also be reduced by a mixing process, by intro-

ducing a cold constituent to the mixture. The condensable component is then cooled below its saturation condition by a combination of mass and thermal diffusion and turbulent mixing. The consequences of mixing of this type on a meteorological scale, the meeting of a "warm" and "cold" front, are quite familiar. In addition,the cooling and bulk nucleation of both pure vapors and mixtures can occur by the radiant emission of energy to the cooler boundaries, for certain substances.

Nucleation on solid surfaces can be placed in the category of heterogeneous nucleation, where nucleation takes place on a foreign substance, or homogeneous nucleation, where the solid is the same substance as the vapor. In this case, however, as contrasted to bulk nucleation, the energy removal from the vapor can take place by heat transfer through the solid phase in addition to the vapor phase. Nucleation results in interfaces between phases and substances, and thus requires that certain interfacial phenomena be examined in some detail first. Extensive treatments of this subject are found in Adam[3] and Davies and Rideal[4].

A. Surface Tension

A commonly observed property of liquid surfaces is that they tend to contract spontaneously to the smallest possible surface area. Surfaces of minimum area are described at any point by[3]

$$\frac{1}{R_1} + \frac{1}{R_2} = \text{Constant} \qquad (1)$$

where R_1 and R_2 are the principal radii at a point. The driving forces for this minimum area are intermolecular, as illustrated in Fig. 1.

Liquids are distinguished from solids by the freedom of the molecules to move, and from gases by the larger cohesive forces between moelcules which inhibit their freedom of motion and hold them close together. In the interior

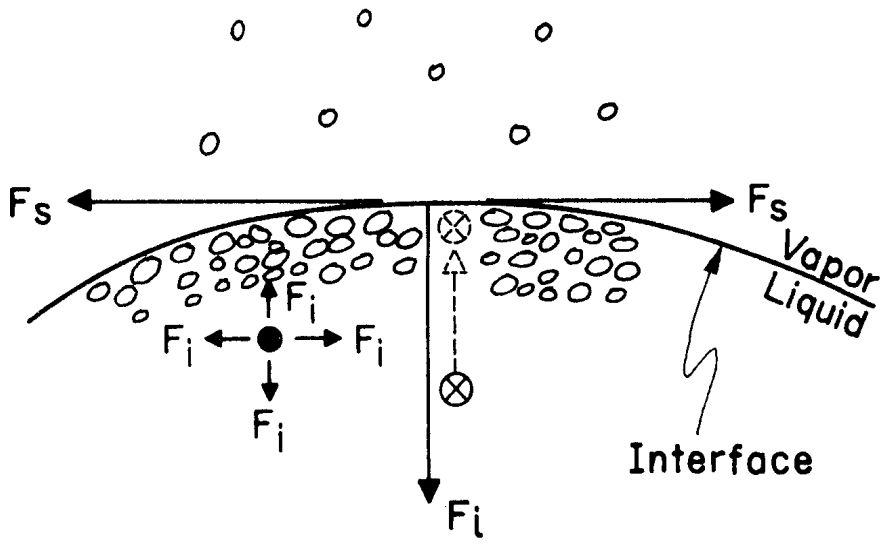

Figure 1. Intermolecular Forces at a Surface.

of the liquid in Fig. 1, each molecule is subject to the same attractive forces F_i in all directions. At the surface, the tangential molecular forces F_s cancel out, but because of the greater intermolecular spacing in the vapor the outward forces do not balance the inward ones. Hence, every surface molecule is subjected to a strong inward attraction, F_i, perpendicular to the surface. This force causes inward movement of the molecules until the maximum number are inside with a minimum on the outside, resulting in a minimum surface area.

That the liquid surface contracts spontaneously shows that thermodynamic "free energy" is associated with it. Any system which can undergo a spontaneous process possesses free energy, and can produce work. Converse to the spontaneous contraction of a surface above, the extending of a surface requires that work be done in order to bring additional molecules from the interior to the surface. This results in an increase in surface energy, the surface free energy.

Surface tension has been characterized[3] as a mathematical device introduced to simplify calculations. A hypothetical tension is substituted, acting in all directions parallel to the surface and equal to the surface free energy. One should be careful, however, and not think of surface tension as arising from a sort of stretched membrane at the surface since the physical basis for the tensile stress is different, and erroneous conclusions may be drawn. This is particularly true with regard to the vapor pressure about a curved surface, which will be considered shortly.

Another view of the source of surface tension is presented in Davies and Rideal[4]. Referring again to Fig. 1, equilibrium between the molecules at the interface and in the bulk requires that the free energies in both places be the same. If the forces F_i and F_s are identical the free energies will be unequal, and molecules at the surface will be attracted to the interior,

depleting somewhat the molecules at the surface. This increases the intermolecular spacing at the surface, resulting in added attractive forces between molecules in the surface which reduce their tendency to escape from the surface. The added attractive force at the interface thus constitutes the so-called surface tension phenomena.

Several important consequences arise from the phenomenon of surface free energy. First, a "flat" liquid-vapor interface is an unnatural state of affairs, and exists only because of the overwhelming magnitude of other forces compared to the surface energy-mainly gravity. For a very small drop the surface tension is large compared to the force of gravity, and it assumes a nearly spherical shape if it is non-wetting with the surface on which it rests. A large non-wetting liquid drop on the other hand will become spherical only under very low gravity. A liquid is wetting on a solid surface when the adhesive forces between the liquid and solid are greater than between the liquid particles itself, and conversely. A parameter describing the relation between the body or acceleration forces and the capillary or surface-tension forces is the Bond number, given by:

$$B_o = \frac{F_a}{F_c} = \frac{Ma}{\sigma L} = \frac{\rho L^2 a}{\sigma} \qquad (2)$$

L is some characteristic length of the system under consideration. The Bond number is useful for describing the conditions under which a wetting liquid will be settled at one end of a container under very low gravity fields, as in space[5].

The second consequence of surface free energy is that a pressure difference exists across a curved interface, with the pressure being smaller on the convex side. Consider the general surface A in Fig. 2, described by radii of curvature R_1 and R_2 with origins at O_1 and O_2. The displacement of surface A

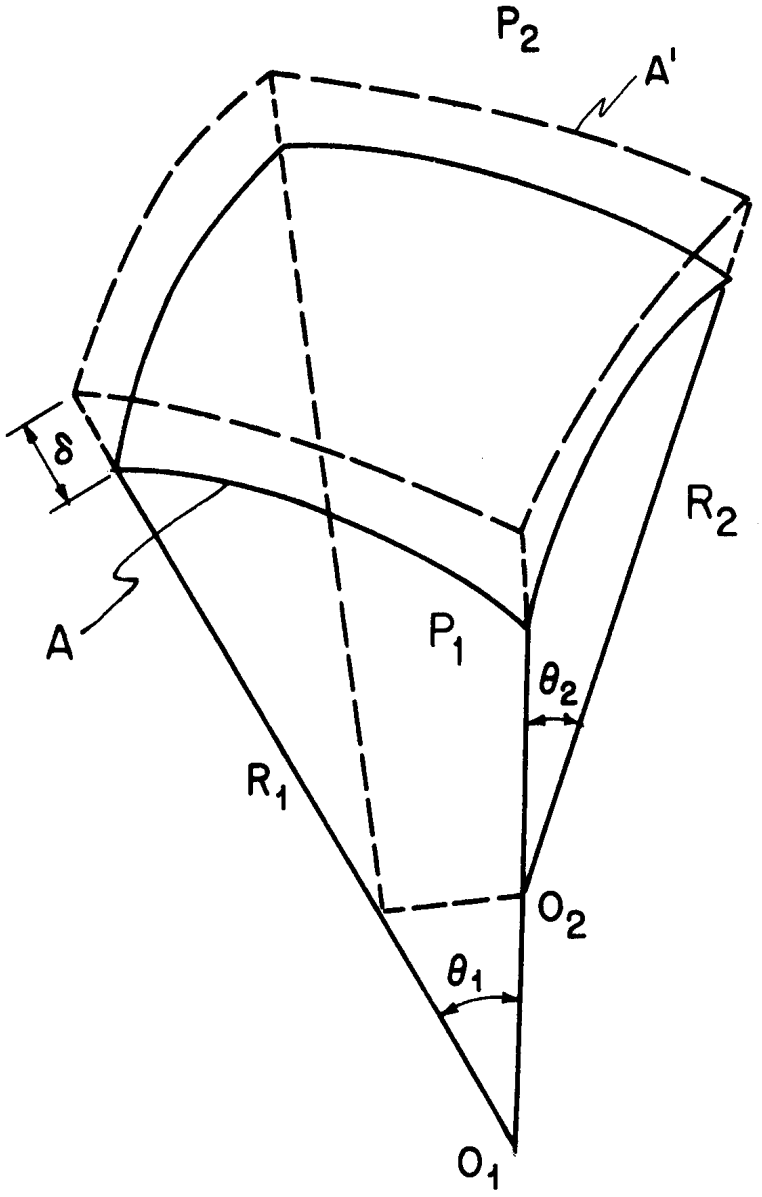

Figure 2. Pressure Difference Across a Curved Interface.

by a distance δ to A' parallel to itself requires the expenditure of work, since the surface area is increased. This work is supplied mechanically by the pressure difference (P_1-P_2). Evaluating the work in Fig. 2 results in the fundamental equation of capillarity[3]:

$$P_1 - P_2 = \sigma\left(\frac{1}{R_1} + \frac{1}{R_2}\right) \tag{3}$$

For a spherical surface $R_1 = R_2 = R$ and

$$P_1 - P_2 = \frac{2\sigma}{R} \tag{4}$$

Measurements show that for the great majority of substances that the surface tension decreases as temperature increases. Kelvin (given in Ref. (3)) showed that it follows that there must be an absorption of heat as a liquid surface is extended isothermally. By careful application of the energy equation to a liquid-vapor interface being extended isothermally, it can be shown that the total surface energy is given by

$$\epsilon_s = \sigma + q_s = \sigma - T\frac{d\sigma}{dT} \tag{5}$$

where

$$q_s = -T\frac{d\sigma}{dT} \tag{6}$$

q_s is the latent heat of the surface, since it represents the amount of heat which must be added to the surface to maintain its temperature during an isothermal expansion. The total energy ϵ_s of the surface (per unit area) then consists of two parts: the surface free energy σ and the latent heat $-T\, d\sigma/dT$. ϵ_s is the difference between the total energy per unit area of the molecules in the surface and the energy of the same number of molecules in the interior of the liquid. Heat is absorbed in extending a surface because molecules must

be brought from the interior against the inward attractive force in order to form the new surface. The inward attraction tends to retard the motion of the particles as they leave the interior, so that the temperature of the surface layers would be lower than that of the interior were heat not supplied from outside.

To compare the magnitudes of the surface free energy and the surface latent heat Eq. (5) is written as

$$\frac{\epsilon_s}{\sigma} - 1 = -\frac{T\frac{d\sigma}{dT}}{\sigma} \qquad (7)$$

Some values of the right hand side of Eq. (7) are listed in Table I, and show that the surface latent heat is of the same order as the surface free energy. For quantities of liquid of reasonable size, where the number of molecules in the interior of the liquid is large compared to the number in the surface, the contribution of the surface latent heat can be neglected. However, when considering small agglomerations of molecules which could serve as embryos for the onset of the nucleation under the appropriate conditions, the surface latent heat should be taken into account.

TABLE I. Comparison of the Surface Free Energy and Surface Latent Heat

LIQUID	TEMPERATURE	$\frac{\epsilon_s}{\sigma} - 1$
Ethyl Alcohol	80°F	0.82
n-hexane	120°F	3.63
H_2O	77°F	0.64
H_2O	200°F	1.28
Liquid Nitrogen	-320°F	1.82

Increasing the pressure of the vapor or a gas over the liquid surface decreases the surface tension by bringing a larger number of molecules closer to the surface on the vapor side. The attraction of these molecules neutralizes to some extent the inward attraction on the liquid surface molecules, hence decreasing the surface tension. For a pure substance this decreases to zero at the critical pressure and temperature. The surface tension at the interface between two non-mixing liquids likewise will be smaller than the surface tension of either liquid in equilibirum with its own vapor or a gas, because of the reduced net inward attraction on the molecules at the interface. If two liquids B and C, initially in contact with A, Fig. 3a, are brought into contact with each other the interfacial energy changes from $\sigma_{BA} + \sigma_{CA}$ in Fig. 3a to σ_{BC} in Fig. 3b. Substance A in Fig. 3 may be air, a vacuum, or any other defined material. The work required to separate them again is called the work of adhesion (Ref. (6), as presented in Ref. (3)):

$$W_{BC} = \sigma_{BA} + \sigma_{CA} - \sigma_{BC} \qquad (8)$$

As is obvious from Eq. (8), the work of adhesion is defined in terms of substance A (vapor, vacuum, etc.) and must be so understood. When the work of adhesion $W_{BC} < (\sigma_{BA} + \sigma_{CA})$, $\sigma_{BC} > 0$ and an interface between B and C is formed. If the interfacial tension σ_{BC} is zero or negative an interface between them cannot exist, since the work of adhesion is equal to or greater than the energy $(\sigma_{BA} + \sigma_{CA})$ required to form the two interfaces.

If the liquid B is the same as liquid C, then the work of adhesion is termed the work of cohesion, and $\sigma_{BA} = \sigma_{CA}$ and $\sigma_{BC} = 0$, and Eq. (8) gives:

$$W_{BB} = 2\sigma_{BA} \qquad (9)$$

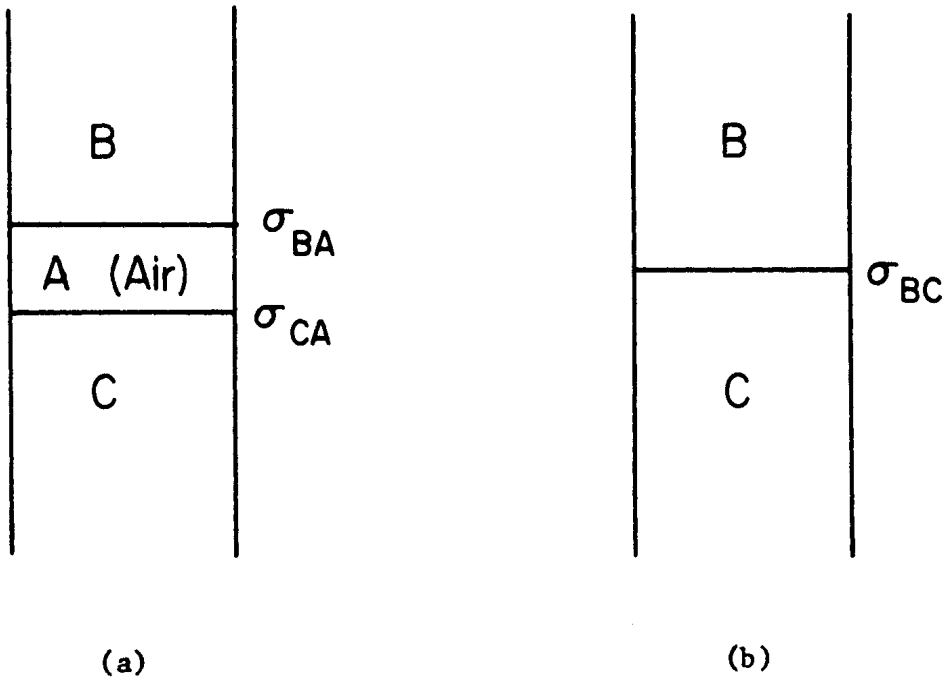

Figure 3. Work of Adhesion.

If, in Eq. (8)

$$\sigma_{CA} \geq \sigma_{BA} + \sigma_{BC} \tag{10}$$

then the energy will be decreased by B spreading on C, and liquid B will spread spontaneously on C. The difference between the left and right side of Eq. (10) is defined as the spreading coefficient S(3)

$$S = \sigma_{CA} - (\sigma_{BA} + \sigma_{BC}) \tag{11}$$

For $S \geq 0$, B will spread on C, while for $S < 0$, B will not spread, but form a drop.

If substrate C in Fig. 3 is a solid, Eq. (8) and Eq. (11) also apply as the work of adhesion and the spreading coefficient between liquid B and solid C. In addition, a particle of liquid resting on a solid surface will form an angle of contact θ at the triple interface, as in Fig. 4. Resolving the horizontal components in Fig. 4, at equilibrium

$$\sigma_{CA} = \sigma_{BC} + \sigma_{BA} \cos\theta \tag{12}$$

Combining Eq. (12) with Eq. (8):

$$W_{BC} = \sigma_{BA} (1 + \cos\theta) \tag{13}$$

Generally speaking, a liquid is considered non-wetting on a surface if $\theta > 90°$ and wetting if $\theta < 90°$.

σ_{CA} and σ_{BC} in Eq. (12) are difficult to measure directly, but measurement of the contact angle θ permits a convenient determination of the adhesion work, Eq. (13), which is related to the solid properties by Eq. (8). A procedure is presented [7] using drops on inclined planes which permits the straightforward calculation of the liquid-solid surface tension, σ_{BC} above.

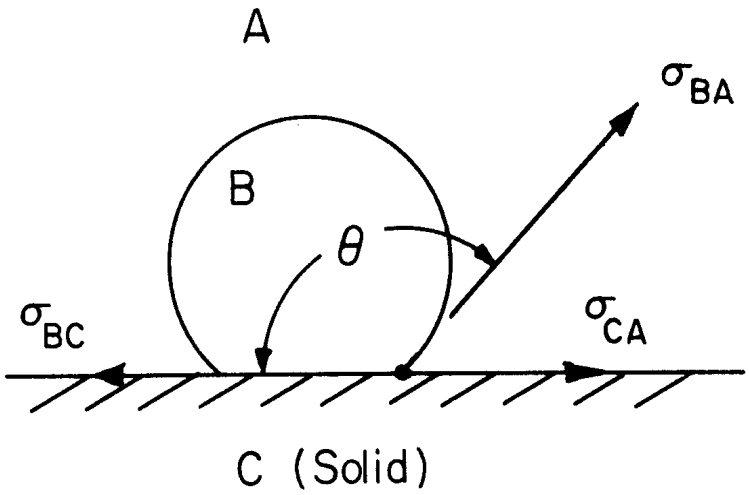

Figure 4. Contact Angles.

Data on the work of adhesion, spreading coefficient, contact angle and surface tension between various liquids and fluorinated polymers are presented in Ref. 8, along with a review of the rigorous solid-liquid interfacial relationships. These properties are of importance in the dropwise condensation process.

B. Latent Heat

The latent heat of evaporation, like surface energy, is a phenomena involving intermolecular forces, and a relation might be expected between them. This will be demonstrated on an order of magnitude basis. The total surface energy per unit area in Eq. (5), at the liquid surface, can be expressed as[9]

$$\epsilon_s = u(z - z')n' \tag{14}$$

where u = mutual potential energy of 2 neighboring molecules of mean spacing r.

z = no. of nearest neighbors within liquid bulk

z'= no. of nearest neighbors at liquid surface

n'= no. of surface particles per unit area ($\approx 1/r^2$)

To evaporate the liquid at the surface requires that the potential energy between the surface particles and those beneath must be overcome. The energy to accomplish this is the latent heat of evaporation, and can be expressed on a unit volume basis as:

$$\bar{h}_{fg}^{v} = \frac{1}{2} nzu \tag{15}$$

where n = no. of particles per unit volume ($\approx 1/r^3$).

The factor of 1/2 takes into account the fact that only the attractive forces of particles on the underside of the surface are effective. Dividing Eq. (14) by Eq. (15) and substituting the approximate values for n' and n:

$$\frac{\epsilon_s}{\bar{h}_{fg}^{v}} = \frac{2(z - z')}{z} r \approx r \approx 10^{-8} \text{ cm} \tag{16}$$

The intermolecular spacing of most liquids is on the order of 10^{-8} cm., and Eq. (16) has been verified for almost all liquids. Consider water at 100°C, for example:

$$\epsilon_s \cong \sigma \approx 60 \text{ dynes/cm } (\text{erg/cm}^2)$$

$$\bar{h}^v_{fg} \cong 330 \text{ cal/cm}^3 = 1.32 \times 10^{10} \text{ erg/cm}^3$$

Thus

$$\frac{\epsilon_s}{\bar{h}^v_{fg}} = \frac{60}{1.32 \times 10^{10}} = 0.45 \times 10^{-8} \text{ cm}$$

Another manifestation of surface tension is the ability of pure liquids to withstand great tensions. To estimate the tensile stress required to rupture a liquid, use is made of Eq. (9), which gives the minimum energy required to separate a liquid over area A at constant temperature is $2\sigma A$, since this is the amount by which the surface energy increases. It can be considered sufficient to rupture the liquid if the molecules are separated by an additional distance on the order of the molecular spacing r. The work of separation is then the product of this distance and the maximum tensile force (negative pressure x area) that the liquid can withstand without separating - i.e.

$$P_{max} \times A \times r \approx 2\sigma A \tag{17}$$

or

$$P_{max} \approx \frac{2\sigma}{r} \tag{18}$$

Again, for water at 100°C,

$$P_{max} \approx \frac{2 \times 60}{10^{-8}} = 1.2 \times 10^{10} \text{ dyne/cm}^2$$
$$\cong 10{,}000 \text{ atmospheres}$$

This is the theoretical upper limit for the process of bulk cavitation. That cavitation on solid surfaces occurs at much lower values is a consequence of

not only the different intermolecular forces between the liquid and solid, but the influence of foreign substances such as entrapped or dissolved gases and oil films.

C. Equilibrium Across a Curved Surface

The growth of a nucleus requires a non-equilibirum condition. To determine the required non-equilibrium condition it is necessary first to determine the equilibrium condition.

Consider a spherical drop of pure liquid of radius r at pressure P_ℓ and temperature T_ℓ somehow suspended inside an enclosure, as shown in Fig. 5. Surrounding the drop is a pure vapor of the same substance as the liquid, at pressure P_v and temperature T_v. Initially, take the vapor at P_v to be in equilibrium with a liquid at T_v, having a flat interface. The vapor is therefore saturated at P_v. Also, take the drop to be in thermal equilibrium with the liquid. Thus

$$T_\ell = T_v = T_s \tag{19}$$

From Eq. (4) which relates the pressures across a curved liquid-vapor interface,

$$P_\ell - P_v = \frac{2\sigma}{r} \tag{20}$$

Then $P_\ell > P_v$, and the liquid is compressed with respect to the "normal" saturation pressure corresponding to the temperature (or subcooled with respect to the "normal" saturation temperature corresponding to the liquid pressure). The presence of a curved interface influences equilibrium conditions in a liquid-vapor system, as was shown by Thomson[10]. To determine the necessary conditions for thermodynamic equilibrium the development will follow that of Frenkel[9].

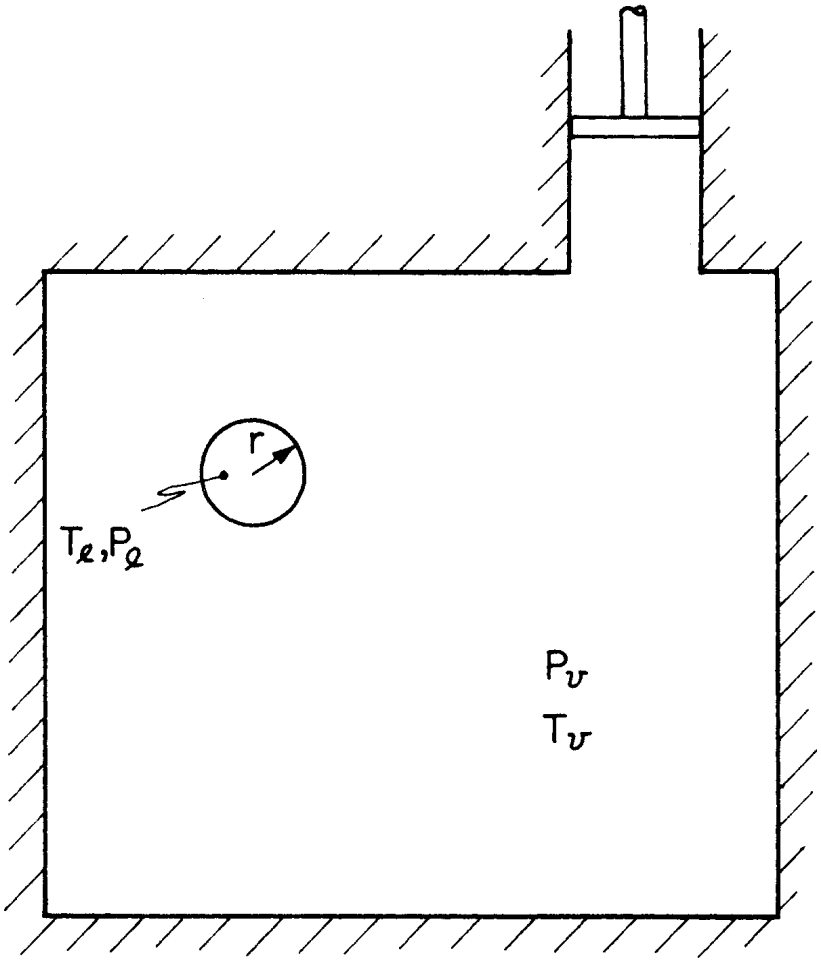

Figure 5. Vapor-Liquid Drop Equilibrium.

The total free energy (or Gibbs free energy, or thermodynamic potential) of the system in Fig. 5 is, for $T_\ell = T_v = T$:

$$G = n_v g_v(P_v, T) + n_\ell g_\ell (P_\ell, T) \tag{21}$$

n_v, n_ℓ = no. of moles of vapor and liquid

g_v, g_ℓ = Gibbs free energy of vapor and liquid per mole (chemical potential for a pure substance).

It should be noted that the surface energy is included in the last term of Eq. (21). P_ℓ in Eq. (21) is given from Eq. (20) as:

$$P_\ell = P_v + \frac{2\sigma}{r} = P_v + \Delta P \tag{22}$$

where $\Delta P = 2\ \sigma/r$. For thermodynamic equilibrium, at which state the system free energy is at a minimum;

$$dG(P,T=const) = 0 = n_v dg_v + g_v dn_v + n_\ell dg_\ell + g_\ell dn_\ell \tag{23}$$

If this occurs at a state where the system free energy is a minimum, we have a state of stable equilibirum. If this occurs at a maximum free energy a state of metastable equilibrium exists. A test will be conducted below to examine which form exists. Since $n_v + n_\ell$ = constant

$$dn_v = -dn_\ell \tag{24}$$

Also, at constant pressure and temperature,

$$dg_v = 0 \quad ; \quad dg_\ell = 0 \tag{25}$$

Substituting Eqs. (24) and (25) into Eq. (23), the requirement for equilibirum is given by the result:

$$g_v(P_v, T) = g_\ell(P_\ell, T) \tag{26}$$

or from Eq. (22)

$$g_v(P_v) = g_\ell(P_v + \Delta P) \tag{27}$$

Making a Taylor series expansion on the right side of Eq. (27);

$$g_v(P_v) = g_\ell(P_v) + \left(\frac{\partial g_\ell}{\partial P}\right)_T \cdot \Delta P \tag{28}$$

Employing the thermodynamic relation $v_\ell = (\partial g_\ell / \partial P)_T$;

$$g_v(P_v) = g_\ell(P_v) + v_\ell \cdot \frac{2\sigma}{r} \tag{29}$$

By comparing Eqs. (26) and (29)

$$g_\ell(P_\ell) = g_\ell(P_v) + v_\ell \frac{2\sigma}{r} \tag{30}$$

As $r \to \infty$, Eq. (29) gives

$$g_v(P_v) = g_\ell(P_v) \tag{31}$$

For a given value of T_v, Eq. (31) is satisfied at a certain pressure P_s, the "normal" vapor pressure. But for any value of r other than $r = \infty$ the value of P_v necessary to satisfy Eq. (29) will be different, depending on r. To determine this P_v, differentiate Eq. (29), holding T = constant.

$$dg_v - dg_\ell = 2\sigma v_\ell\, d\left(\frac{1}{r}\right) \tag{32}$$

For constant temperature the following thermodynamic relations apply;

$$\left.\begin{aligned} dg_v &= v_v\, dP \\ dg_\ell &= v_\ell\, dP \end{aligned}\right\} \tag{33}$$

Substituting Eq. (33) into Eq. (32),

$$(V_v - V_\ell)\, dP = 2\sigma V_\ell\, d\left(\frac{1}{r}\right) \tag{34}$$

If $V_v \gg V_\ell$, valid far from the critical state, and considering the vapor to approximate ideal gas behavior such that;

$$V_v = \frac{\bar{R}\, T_v}{P_v} \tag{35}$$

Eq. (34) reduces to:

$$\bar{R}\, T_v \frac{dP_v}{P_v} = 2\sigma V_\ell\, d\left(\frac{1}{r}\right) \tag{36}$$

Integrating Eq. (36) between the limits

$$r = \infty\,, \quad P_v = P_s$$

and

$$r = r^*\,, \quad P_v = P_v$$

$$\ln \frac{P_v}{P_s} = \frac{2\sigma V_\ell}{r^* \bar{R}\, T_v} \tag{37}$$

or

$$\frac{P_v}{P_s} = e^{\frac{2\sigma V_\ell}{r^* \bar{R}\, T_v}} \tag{38}$$

This gives the fractional increase in vapor pressure around a liquid drop of radius r*, above its "normal" vapor pressure (for r = ∞). This might be termed the supersaturation pressure ratio. For a liquid-vapor interface other than flat then, thermodynamic equilibrium requires that the vapor be supersaturated, at a pressure greater than the saturation pressure corresponding to the temperature, shown as points A and B, respectively, in Fig. 6. Table II gives values of this pressure increase for water at 68°F for a variety of droplet diameters.

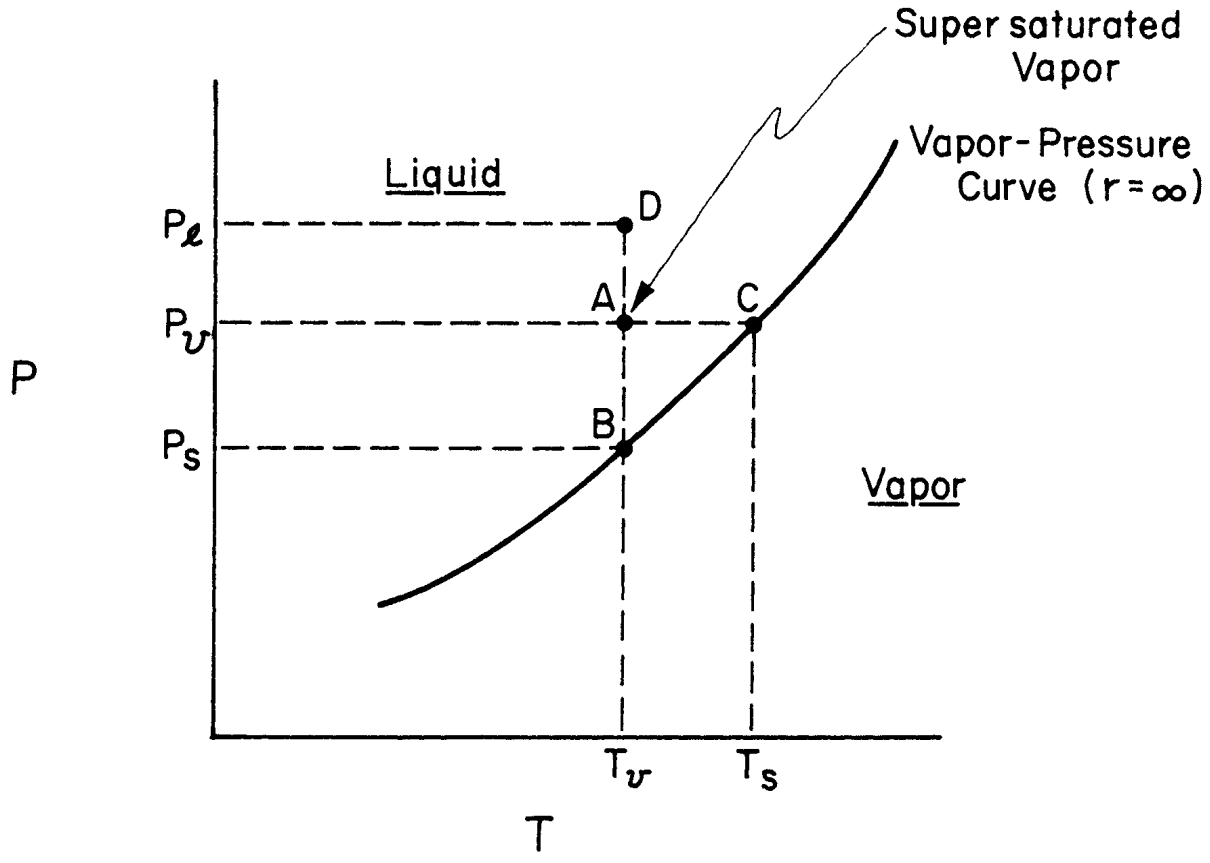

Figure 6. Vapor-Liquid Drop Equilibrium States.

TABLE II. EFFECT OF DIAMETER OF DROP OF WATER ON ITS VAPOR PRESSURE AT 68°F

Diameter-Inches	Approx. No. of Molecules	Supersaturation P_v/P_s
10^{-2}	2.7×10^{17}	1.000009
10^{-4}	2.7×10^{11}	1.00086
10^{-6}	270,000	1.0905
10^{-7}	270	2.38

One notes that the drop diameter must be quite small before the supersaturation pressure ratio becomes of apparent significance. If the supersaturation in a vapor surrounding a drop is less than that given by Eq. (38) for the given drop size, the droplet will evaporate since its effective vapor pressure is higher than that of the surroundings. Conversely, if the supersaturation in a vapor surrounding a drop is greater than that given by Eq. (38), condensation will take place on the drop since its effective vapor pressure is lower than that of the surroundings. A well known example of this effect in operation is that water vapor will not condense in a dust and ion-free atmosphere until its vapor pressure exceeds the saturation point by a considerable amount. From Table II, condensation to a droplet 1.0 micro-inch in diameter requires a 9% increase in vapor pressure. A sphere of this size contains about 270,000 molecules of H_2O, and the probability of so many coming together spontaneously to form a drop of this size is quite small. Therefore, nuclei of some type providing a smaller curvature must be present if condensation is to occur anywhere near the ordinary saturation vapor pressures.

Equation (38) assumes that σ is constant with curvature, but for very small sizes this is no longer valid. Based on arguments from statistical mechanics the following relation between surface tension and droplet radius has been

proposed[11];

$$\sigma(r) = \frac{\sigma_\infty}{1 + \delta/r} \tag{39}$$

where σ_∞ is the surface tension for a flat surface and δ is a length between 0.25 and 0.6 of the molecular or atomic radius in the liquid state.

Equation (38) gives the increase in vapor pressure above the normal saturation pressure necessary for equilibrium between the vapor and a liquid drop of radii r*. It can also be viewed in another way. Solving Eq. (37) for r*;

$$r^* = \frac{2\sigma V_\ell}{RT} \cdot \frac{1}{\ln(P_v/P_s)} \tag{40}$$

For a given vapor temperature T_v (hence a given P_s) and a supersaturated vapor at vapor pressure P_v, a drop of radius r* is in a state of metastable equilibrium. If, due to random fluctuations, the drop becomes slightly greater than r*, condensation will take place on it. If the drop becomes slightly smaller than r* it will evaporate completely. r* can thus be considered as the critical radius which can subsequently serve as a nucleus for condensation. That a drop of radius r* is in a state of metastable equilibrium can be verified as follows:

The total free energy of the system in Fig. 5 was given by Eq. (21). From Eq. (30) it can be shown that

$$n_\ell g_\ell(P_\ell, T) = n_\ell g_\ell(P_v, T) + 4\pi r^2 \sigma \tag{41}$$

The last term of Eq. (41) is the contribution of the surface free energy. Eq. (21) can now be written as

$$G = n_v g_v(P_v, T) + n_\ell g_\ell(P_v, T) + 4\pi r^2 \sigma \tag{42}$$

Let G_o correspond to the state in Fig. 5 where only vapor is present (the drop is completely evaporated). Then

$$G_o = (n_v + n_\ell)\, g_v(P_v, T) \tag{43}$$

The difference between Eq. (42) and Eq. (43) is the free energy change associated with the formation of a drop of radius r, and gives;

$$\Delta G = G - G_o = n_\ell (g_\ell - g_v)(P_v, T) + 4\pi r^2 \sigma \tag{44}$$

At equilibrium, r = r* in Eq. (29), and noting that $n_\ell = 4/3\pi r^3/v_\ell$, Eq. (44) becomes

$$\Delta G = 4\pi\sigma\left(-\frac{2}{3}\frac{r^3}{r^*} + r^2\right) \tag{45}$$

On substituting Eq. (40) into Eq. (45)

$$\Delta G = 4\pi\sigma\left(-\frac{r^3}{3}\frac{\bar{R}T}{\sigma v_\ell}\ln\frac{P_v}{P_s} + r^2\right) \tag{46}$$

Equation (46) is plotted in Fig. 7 as a function of r for the cases where $P_v/P_s \leq 1$ (superheated or saturated), and where $P_v/P_s > 1$ (supersaturated). A maximum in ΔG, designated as ΔG_{max}, occurs only for $P_v/P_s > 1$ at r = r*, and is given by

$$\Delta G_{max} = \frac{4}{3}\pi\sigma(r^*)^2 \tag{47}$$

where r* is given by Eq. (40).

ΔG in Eqs. (45) and (46) is the free energy of formation of a drop of radius r. Since spontaneous porcesses are those associated with a decrease in the free energy, it is obvious from Fig. 7 that droplets will grow spontaneously only in a supersaturated vapor, that droplets of radius $r < r^*$ will not

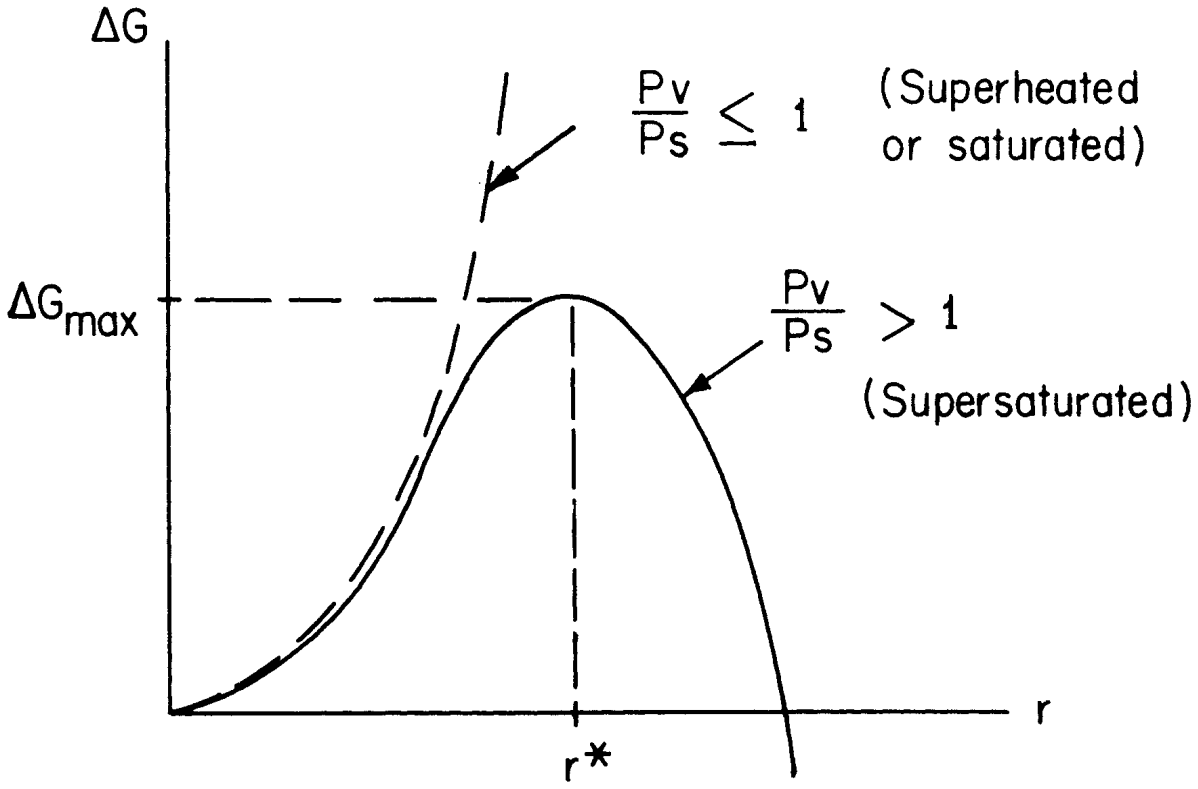

Figure 7. Free Energy of Formation of a Liquid Drop.

grow but will evaporate, and that drops will grow, serving as nuclei for condensation, when $r > r^*$.

Equation (40) holds true only for a pure substance. The presence of a monomolecular surface film of foreign substances (as is always present in the atmosphere) has a considerable influence and requires a more complex analysis[3,4]

A supersaturated vapor, A in Fig. 6, is at a pressure greater than the saturation pressure, P_s, corresponding to the temperature, T_v, at B. It can also be considered as a vapor cooled to a temperature T_v below the saturation temperature T_s corresponding to the vapor pressure P_v, point C in Fig.6. The degree of subcooling $T_s - T_v$, corresponding to equilibrium with a droplet of radius r^*, can be evaluated from Eq. (38) combined with the Clausius-Clapyron equation, which relates the normal saturation temperature and pressure:

$$\frac{dP}{dT} = \frac{h_{fg}}{T v_{fg}} = \frac{h_{fg}}{T(v_v - v_\ell)} \tag{48}$$

For $v_v \gg v_\ell$, and assuming the vapor behaves as an ideal gas, Eq. (35), Eq. (48) becomes;

$$\frac{dP}{P} = \frac{h_{fg}}{\bar{R}} \frac{dT}{T^2} \tag{49}$$

Assuming h_{fg} remains approximately constant over a small interval, Eq. (49) is integrated over the limits

$$P = P_v \,, \; T = T_s \quad (C \text{ in Fig. } 6)$$

and

$$P = P_s \,, \; T = T_v \quad (B \text{ in Fig. } 6)$$

$$\ln \frac{P_v}{P_s} = \frac{h_{fg}}{\bar{R}} \left(\frac{1}{T_v} - \frac{1}{T_s} \right) \tag{50}$$

Equating Eqs. (50) and (37) and rearranging gives;

$$T_s - T_v = \frac{2\sigma v_\ell T_s}{h_{fg} r^*} \tag{51}$$

This gives the subcooling of the vapor below the saturation temperature T_s necessary for equilibrium with a droplet of radius r*. The actual state of the liquid within the droplet is also subcooled, or compressed, as indicated by point D in Fig. 6. From Eqs. (22) and (37)

$$P_\ell = P_s e^{\frac{2\sigma v_\ell}{r^* R T}} + \frac{2\sigma}{r^*} \tag{52}$$

D. Bulk Phase Nucleation

For nucleation occuring in the bulk of a vapor away from solid surfaces two cases can be distinguished; with and without the presence of foreign particles which can themselves act as nuclei. Growth of a drop on a foreign particle also requires a supersaturated vapor condition as specified by Eq. (38), except here the shape of the particle has considerable bearing on r*. The intermolecular forces between the particle and the liquid can be expected to modify the equilibrium conditions.

An important source of condensation nuclei are salt particles from the sea, and considerable effort has been expended to study the significant parameters in the production of these nuclei[2]. The effectivensss of AgI smoke in promoting atmospheric precipitation is believed to be due to its action as initial nucleation centers for ice crystals, which have a lattice spacing very similar to that of AgI[4].

For pure substances in which no detectable foreign nuclei were present, the maximum supersaturation ratio attained experimentally, as defined by the pressure ratio in Eq. (38), was 8 in a non-flow device[12] and up to 100 in a nozzle[13]. Fig. 8 compares the supersaturation limit line attained for

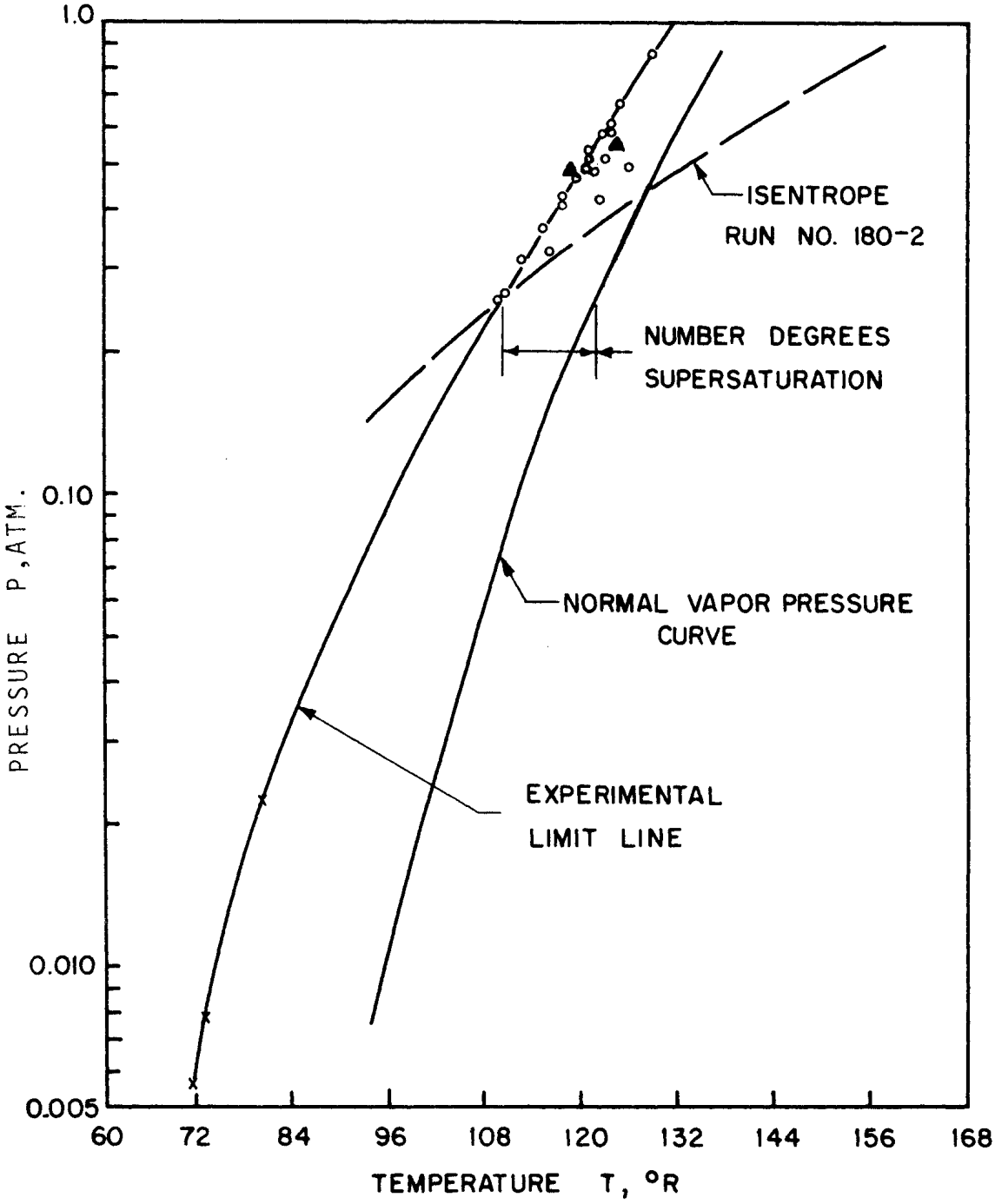

Figure 8. Supersaturation Limit in a Nozzle with Nitrogen. (Ref. 13).

nitrogen vapor with the normal vapor pressure curve, and Fig. 9 shows the variation of supersaturation ratio as a function of the vapor temperature. If foreign nuclei of some unknown but fixed size r* can be considered as present and limiting the degree of supersaturation, then the behavior in Fig. 9 appears to follow the trend predicted by Eq. (38).

For a pure vapor with no foreign nuclei present, condensation nuclei must come from the vapor phase itself. Liquid embryos, or agglomerations of molecules, can form spontaneously even in a thermodynamically stable system owing to local fluctuations. From Eq. (45) these embryos are thus at a higher potential or free energy level, and may reach a level sufficient to become a nucleus for condensation, the maximum point in Fig. 7, if the necessary degree of supersaturation is present. Equation (46) shows that a maximum in ΔG does not exist with a saturated vapor. With a supersaturated vapor, ΔG_{max} can be considered as a potential barrier which plays a role similar to that of the activation energy in chemical reactions[9], and must therefore be a part of any analysis predicting the conditions under which nucleation takes place.

The classical liquid drop model of steady state nucleation of a pure substance is reviewed in Ref. 14. It is based on the description[9] of a supersaturated vapor as a dilute solution of substances (liquid embryos of various size) in a vapor as the solvent. These liquid embryos form as a result of spontaneous and random density fluctuations due to collisions between molecules. With equilibrium the sizes of these embryos is given by a Boltzmann-type distribution, Eq. (53).

$$N_r = C\, e^{-\frac{\Delta G_{max}}{KT}} \tag{53}$$

With supersaturation a quasi-equilibrium condition is assumed to exist, in which embryos reaching the critical size become condensation nuclei and are immediately

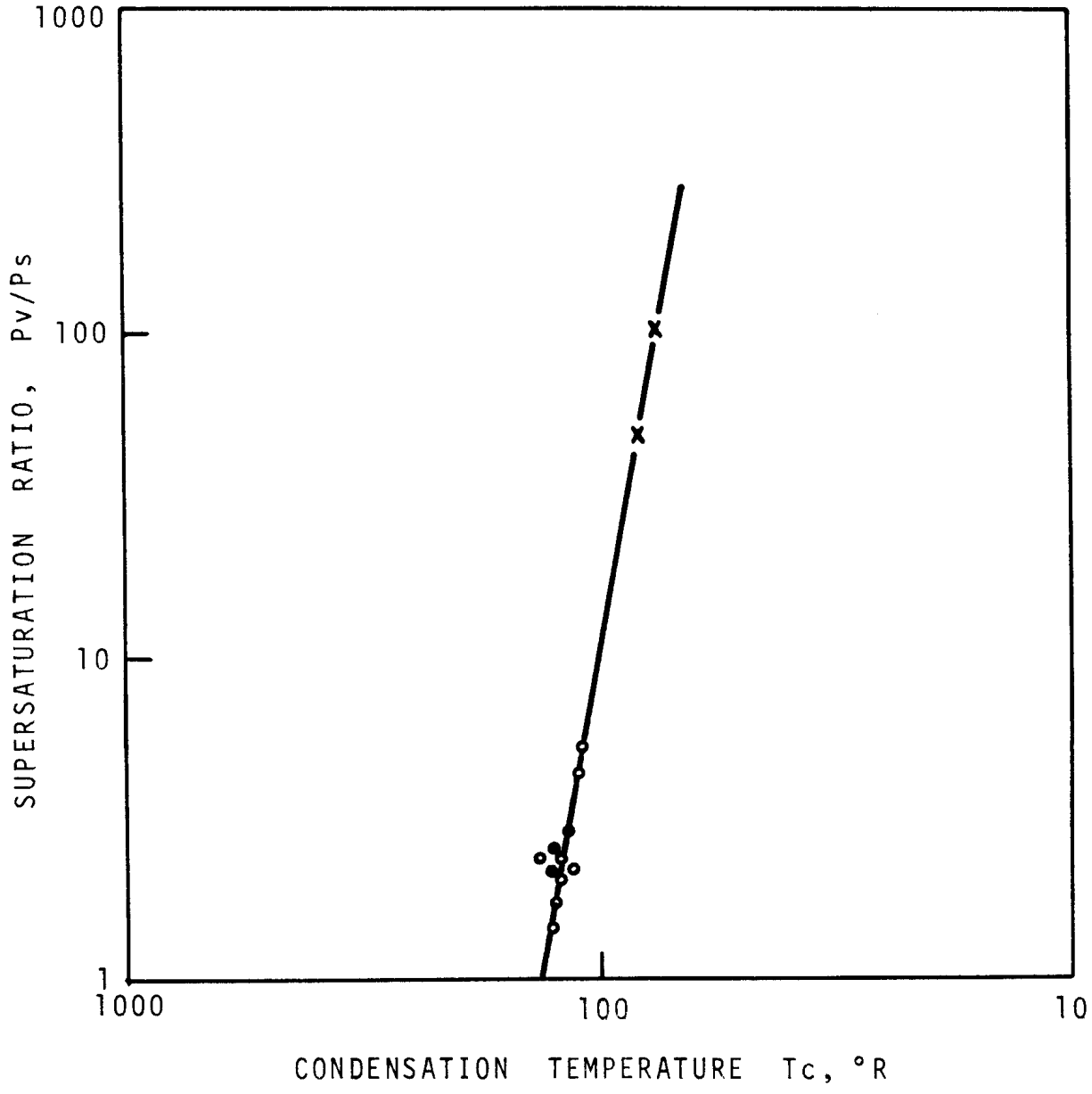

Figure 9. Supersaturation Ratio vs Condensation Temperature with Nitrogen. (Ref. 13)

removed from the distribution. The rate at which these particles are replaced is computed from the rate at which embryos having one molecule less than the critical number gain a single molecule, using results of the kinetic theory. The resulting rate of formation of growing nuclei per unit volume is given as[14];

$$J = \left(\frac{P}{kT}\right)^2 \left(\frac{M}{N_0 \rho_\ell}\right)\left(\frac{2\sigma}{\pi m}\right)^{1/2} e^{-\frac{4\pi\sigma (r^*)^2}{3kT}} \qquad (54)$$

The critical radius r* is related to the supersaturation pressure ratio P_v/P_s by Eq. (40). The larger the supersaturation (with smaller r*) the greater is J in Eq. (54). J is plotted for water vapor in Fig. 10 as a function of the supersaturation pressure ratio. The curve is so steep at low values of J that it is possible to define a critical supersaturation ratio beyond which condensation occurs spontaneously. A number of measurements have been made by observing the condensation upon expansion in a cylinder[15], and these are compared in Table III with the values calculated from Eq. (54).

TABLE III. SUPERSATURATION PRESSURE RATIO (Reference 15)

Vapor	Temp. °K	Measured	Calculated
Water	275.2	4.2 ±0.1	4.2
Water	261.0	5.0	5.0
Methanol	270.0	3.0	1.8
Ethanol	273.0	2.3	2.3
I-Porpanol	270.0	3.0	3.2
Isopropyl Alcohol	265.0	2.8	2.9
n-butyl Alcohol	270.0	4.6	4.5
Nitromethane	252.0	6.0	6.2
Ethyl Acetate	242.0	8.6-12.3	10.4

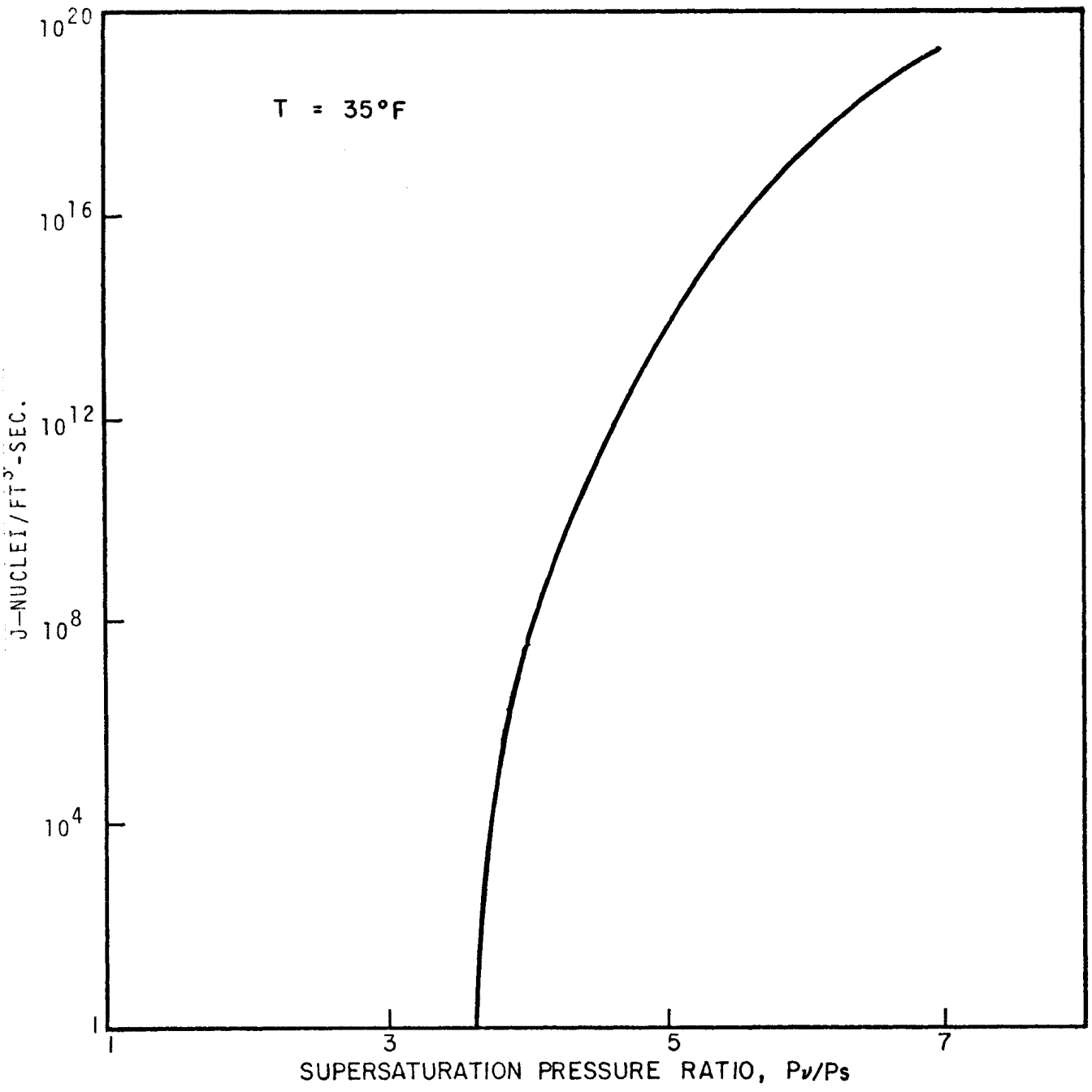

Figure 10. Rate of Formation of Condensation Nuclei in Water Vapor. (Ref. 14)

In nearly all cases the observed ratios agree well with the calculations. Using the limiting supersaturation pressure ratio of 4.2 for water vapor in air at 2.2°C from Table III, the critical radius calculated from Eq. (40) is 6.5 angstroms. The liquid nucleus just large enough to continue to grow thus contains about 40 molecules of water[4] .

Contours of constant nucleation rate are plotted in Fig. 11 for water vapor from Eq. (54). Superimposing the isentropic expansion permits an estimate of whether and how soon condensation may be expected during an expansion in a turbine nozzle. The similarity in form between Fig. 11 and Fig. 8 is interesting, although they apply to different gases. More recent data on nucleation of water vapor in a nozzle follows the prediction of the classical model[16]. However, with NH_3 the nucleation rate follows the Lothe-Pound equation, which predicts nucleation rates higher than the classical model by 10^{12}-10^{18}. The Lothe-Pound equation[17] is based on a quantum-statistical model, and corrects for the effect of size on the surface tension. The classical theory considers that the surface tension is constant. A comprehensive review of nucleation theory is given by Feder et al[18] and presents a new kinetic treatment which accounts for the latent heat. The irreversible thermodynamics of non-isothermal nucleation also is discussed.

E. Nucleation on Solid Phase

Nucleation on a solid surface proceeds to one of two cases; dropwise or film condensation. Nucleation as such does not exist with established film condensation; only a continuous absorption or emission of molecules. This will be considered in the next section.

Dropwise condensation is classified as a nucleation phenomenon[19], where active sites for drop formation are microscopic pits, scratches and solid particles. A discussion of dropwise condensation must include other aspects

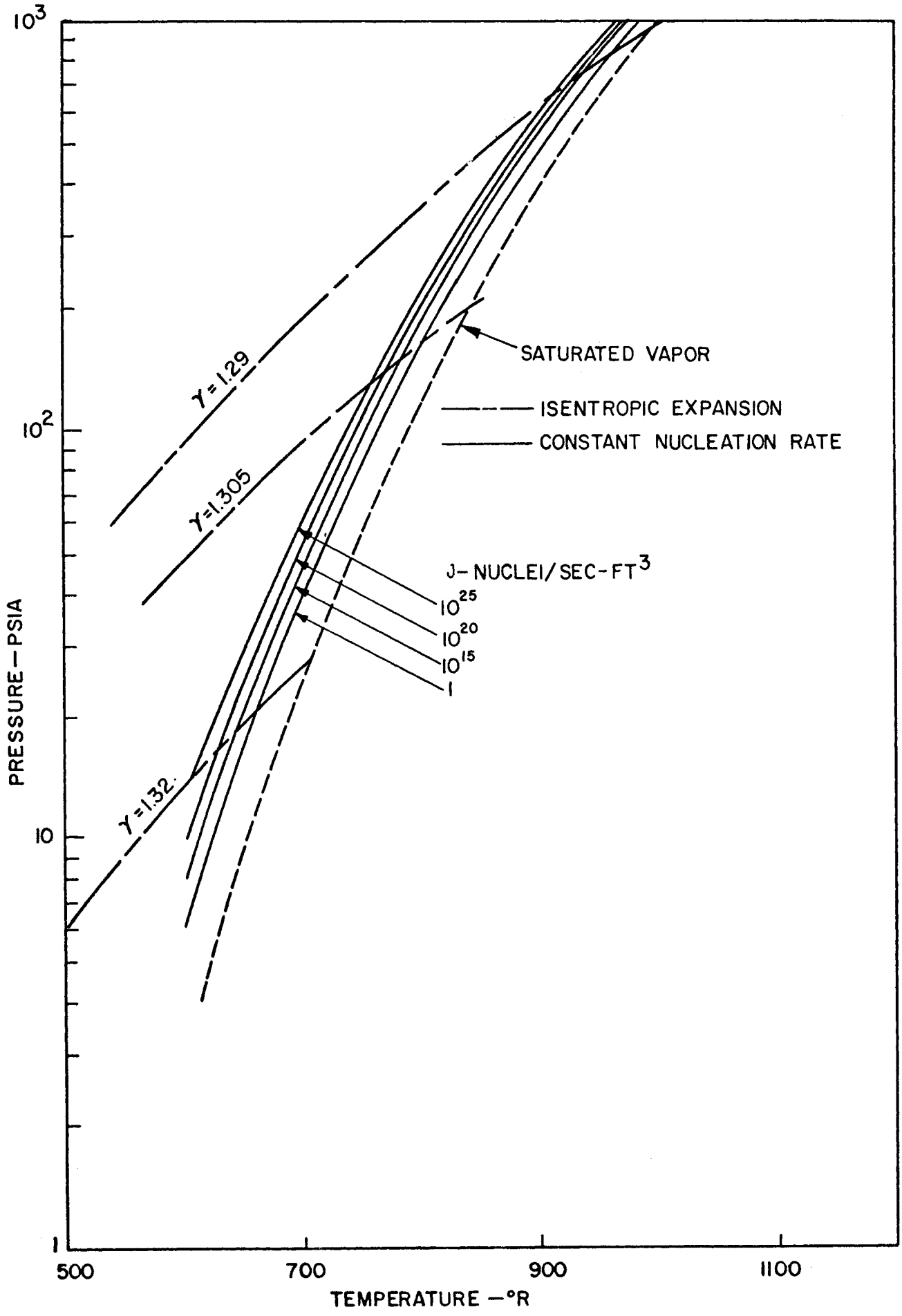

Figure 11. Nucleation Rate for Water Vapor. (Ref. 14)

related to the nucleation phenomena; the droplet population and size distribution, the role of promotors in the regulation of droplet population, and the mechanism of droplet removal. These will be considered below. It has been well established that higher heat transfer rates arise with dropwise condensation than with film condensation, of which Fig. 12 shows one example. A number of different models of the dropwise condensation phenomenon have been proposed to describe and account for the large heat transfer rates. They differ essentially as to the relative importance of condensation directly on the drops and that, if any, on the spaces between the drops. The salient features of several of these models are represented in Fig. 13 and discussed below:

Fatica and Katz (Ref. 21)

This model considers that drop growth occurs primarily by condensation on the drop, with the latent heat transported to the solid surface by conduction through the drop. A two-dimensional flux plot is used to compute the rate of heat transfer. Assuming a uniform drop size and arbitrary fractional coverage of the surface it was possible to compute an average heat flux. Because of the relatively low thermal conductivity of the liquid the heat flux is low except near the intersection of the solid wall and the edge of the drop. It has been suggested[22] that the heat transfer rate through the drop would be enhanced considerably if internal circulation within the drops takes place because of variations in surface tension about the surface with temperature. A detailed finite difference solution of this circulation in a hemispherical drop indicates that the contribution of the circulation is insignificant[23].

Eucken (Ref. 24)

In addition to condensation directly on the drop, it was proposed that a monomolecular layer forms between the drops. Adjacent to the drop this layer is saturated while farther away it is supersaturated. The concentration gradient in the layer associated with the difference in the degree of saturation

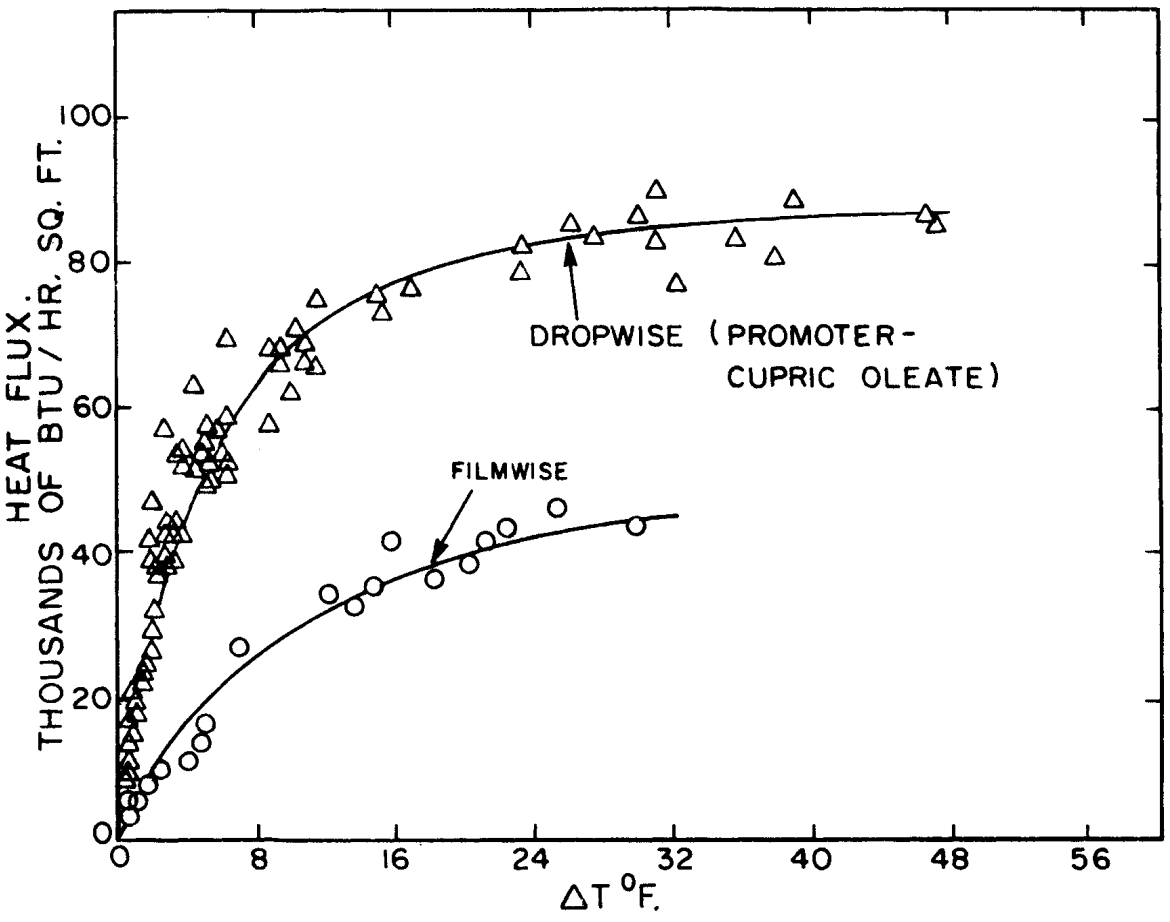

Figure 12. Comparison of Dropwise and Film Condensation of Steam at Atmospheric Pressure on Vertical Copper Surface. (Ref. 20)

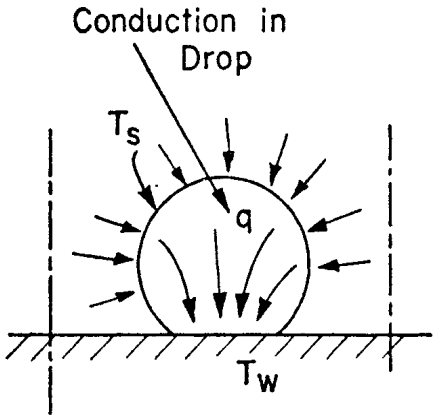

Fatica and Katz (Ref. 21)

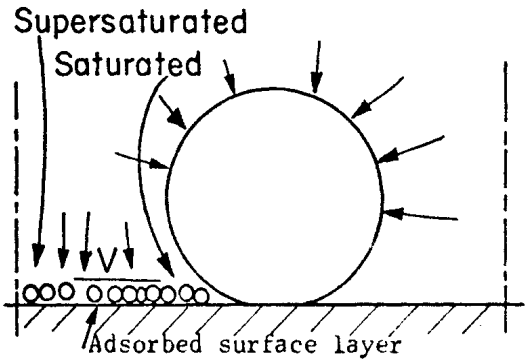

Eucken (Ref. 24)

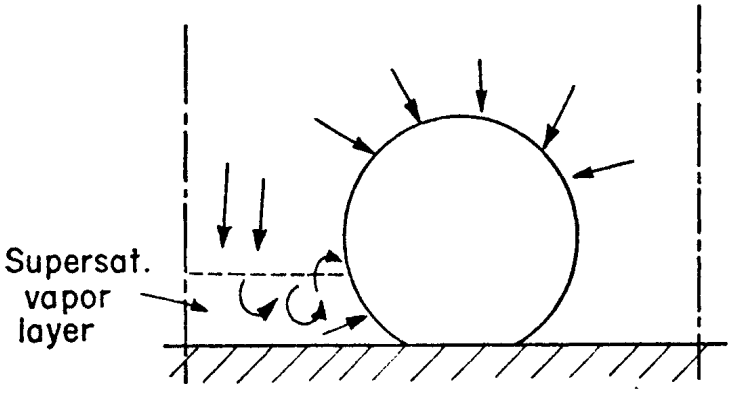

Emmons (Ref. 27)

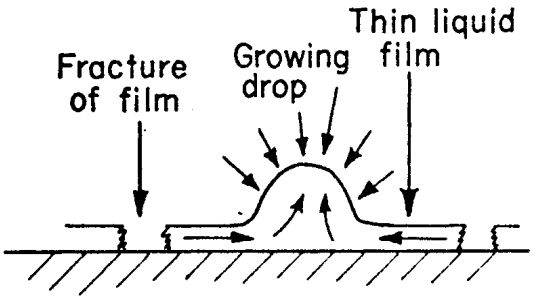

Jakob (Ref. 28)

Figure 13. Several Models for Dropwise Condensation.

serves as the driving force for surface diffusion of the molecules toward the drop.

Eucken[24] also used the kinetic theory of gases to calculate the heat transfer by condensation of steam at atmospheric pressure if all molecules striking the cooling surface were immediately condensed. The results was a flux of $q/A=72 \times 10^6$ BTU/hr. ft^2, about 260 times greater than the maximum observed. According to this only about 0.4% of the vapor molecules striking the solid are retained as liquid.

Emmons (Ref. 27)

This mechanism proposes that the vapor molecules striking the solid bare surfaces are re-evaporated, but at the temperature of the surface and hence subcooled, and then followed by recondensation onto the droplets. The bare cooling surface between drops are thus blanketed by supersaturated vapor. Emmons[27] also considers that the rapid condensation on a bubble causes a local reduction in pressure which sets up violent local eddy currents between drops.

Jakob (Ref. 28)

Jakob [28] suggested that dropwise condensation results from the fracture of a thin film of condensate, which completely covers the solid surface, into drops after the film had grown to some critical thickness, after which the process repeated itself. Observation of dropwise condensation under a microscope appeared to support this[20]. It was noted that drops large enough to be visible (0.01 mm) grew primarily by coalescing with other drops, after which the bare metal beneath is exposed, as noted by a lustrous appearance. The luster disappears very quickly, indicating that the condensation was building up again. It was concluded that heat transfer occurs primarily between the drops, which are "fed" by the fracture of the thin liquid film.

Subsequent works have indicated that the film-fracture mechanism does not take place. Using the optical technique of measuring the change in ellipticity of polarized light upon reflection from a transparent thin film, as manifested by a change in intensity, the thickness of the film can be computed, if one exists[19]. The intensities are recorded against time, as shown in Fig. 14. The upper part of the figure served as a test of the technique. The alcohol was injected on the surface and formed a continuous film on the gold surface. From optical theory the intensity of the reflected elliptically polarized light should increase if a film is present, as is the case toward the right. Each cycle corresponds to a change in thickness of 2500 angstroms. On the lower part of Fig. 14 the heater within the cooled surface was turned off so that condensation could begin. If a thin film formed between drops in well established dropwise condensation, it should also form on a bare surface before drops begin to form. This is seen not to be the case; the intensity did not increase as it would were a film present, but rather decreased because of scattering of the reflected light by the drops. It was concluded that any film, if present, could not be more than one monolayer thick, and therefore no net condensation takes place between the drops.

The conclusion of the above is that condensation occurs only at certain sites on the surface, and dropwise condensation may be classified as a nucleation phenomena in a fashion similar to nucleate boiling. This has been supported by high speed photographs of dropwise condensation taken under very high magnification[29], where it was observed that drops formed repeatedly at fixed sites, both natural and artificial, on the surface. It was postulated that liquid trapped in pits on the surface are the nucleation sites. If this is the case, then the presence of the second phase aids the change of phase process consid-

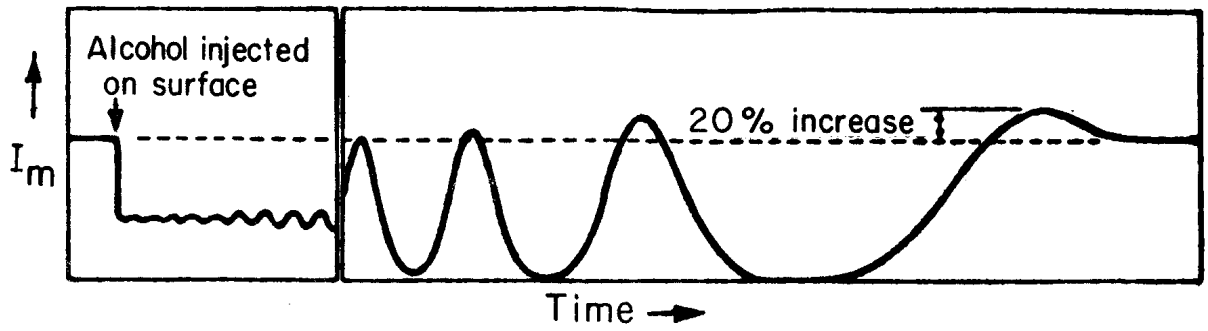

(a) Calibration test. Gold surface with alcohol.

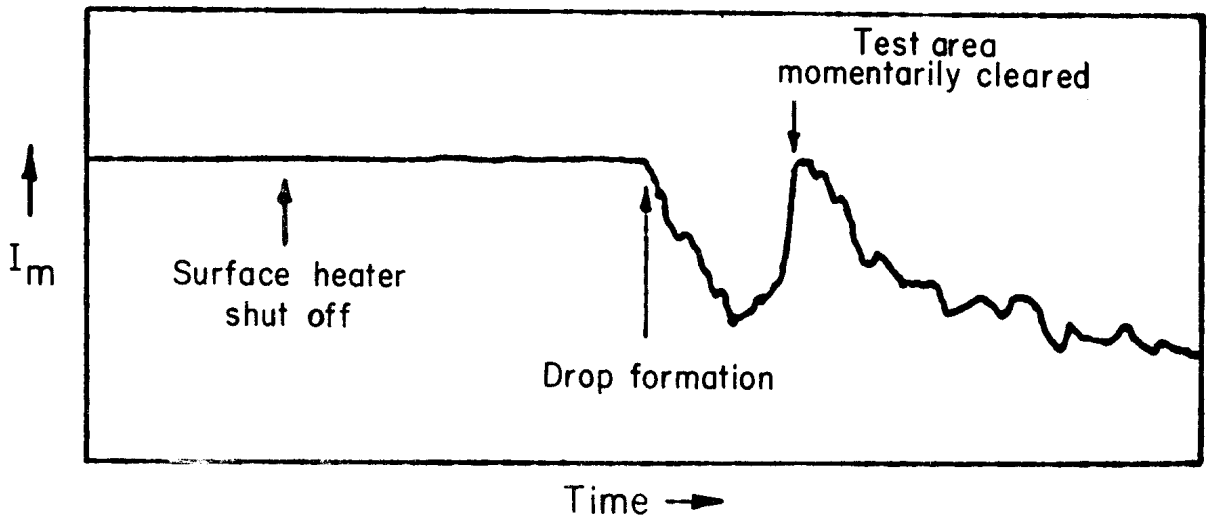

(b) Gold surface with pure steam

Figure 14. Measurements of Intensity of Reflected Polarized Light for Detecting Thin Liquid Film. (Ref. 19)

erably in a fashion similar to nucleation in boiling. It has also been observed that grain boundaries of metals serve as nucleating sites for dropwise condensation[30].

Despite the observations cited above, that no net condensation takes place between drops, more recent studies using an interference microscope[31] indicate the presence of liquid films between drops, which reach a critical thickness of about 0.63 microns before the film fractures into little droplets. It appears that the question as to the existance of thin liquid layers on the surface between the drops is unresolved yet.

The number of nucleating sites has been observed to be very high, up to 7×10^6 sites/in.^{2} with dropwise condensation of ethylene glycol on a vertical surface[32]. The number of coalsecences with other drops was as high as 400,000 as a single drop slid down the surface.

For a given surface-vapor temperature difference the heat flux depends a great deal upon the population density of the nucleating sites. In Fig. 15, heat flux is plotted versus ΔT for various constant values of nucleating site population density, which are noted in the body of the graph, taken from Ref. 33. For a given ΔT, the larger the population density the higher is the resulting heat flux. The effect of variability in population density no doubt accounts for some of the large differences in experimental data in the literature for similar conditions, an example of which is shown in Fig. 16. It is obviously not possible to designate any one result as the "correct" one.

One can surmise from Fig. 15 that there must exist an upper limit on the population density, beyond which complete coalescence would take place between droplets, i.e. the surface would become covered with a film of liquid, called film condensation. It was noted in Fig. 12 that the heat flux decreases with

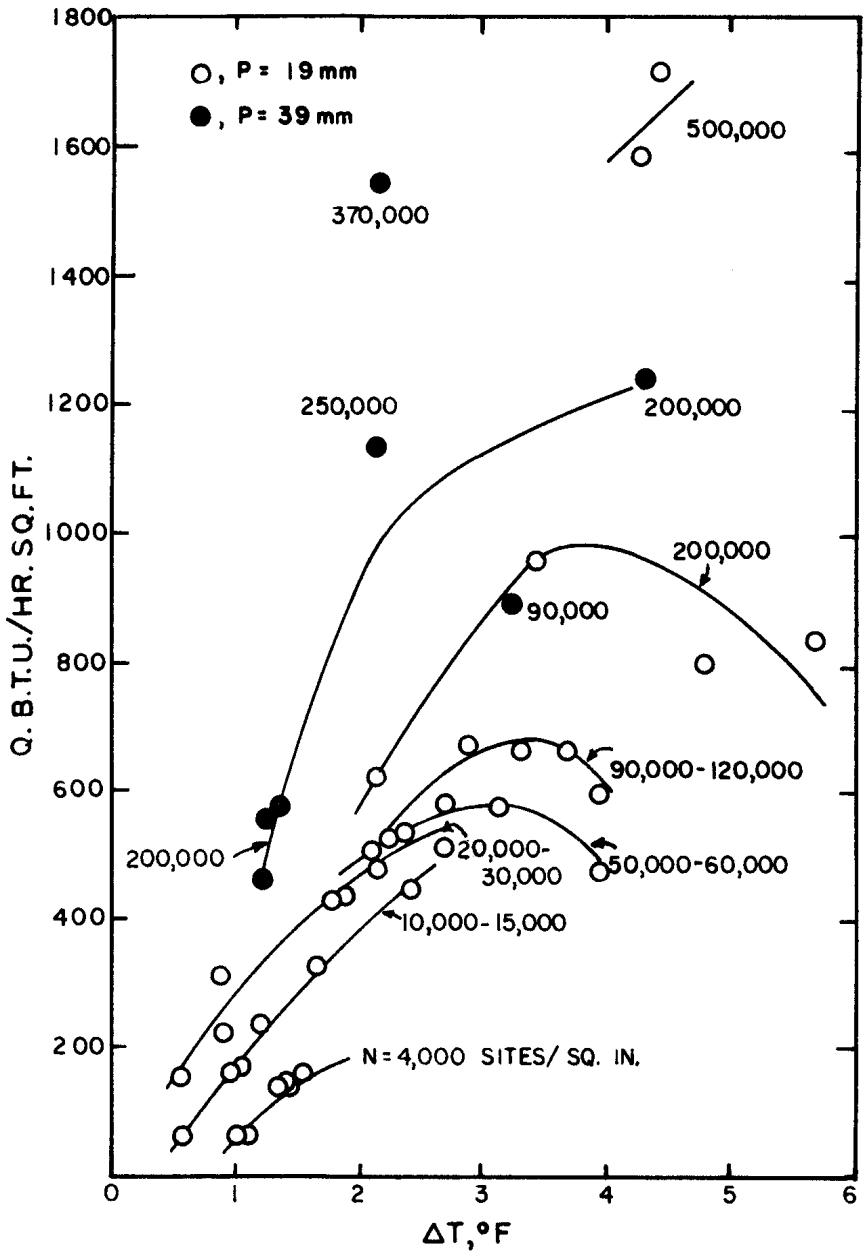

Figure. 15. Heat Flux During Dropwise Condensation of Water on a Horizontal Surface. (Ref. 33)

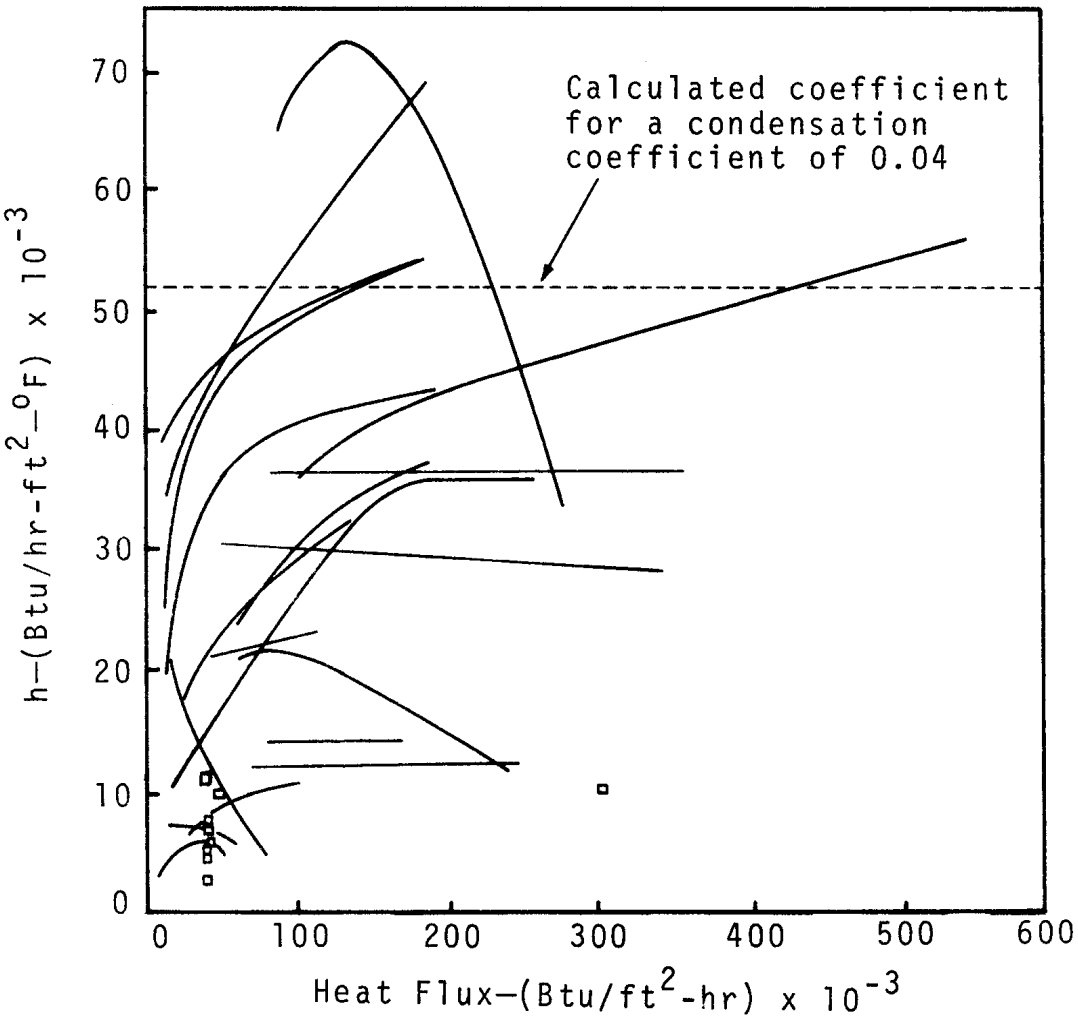

Figure 16. Summary of Published Results of Heat Transfer Coefficient for Dropwise Condensation Nucleation Cavities. (Ref. 48)

film condensation. This is analogous to the upper limit in heat flux with nucleate boiling, called the peak heat flux, beyond which the heat flux decreases as ΔT increases until the surface is blanketed with a vapor film-called film boiling. In both cases it is a cessation of the distinct nucleation process that gives rise to the formation of a film, and the accompanying decrease in performance; in both cases it is the nucleation process that gives rise to the high rates of heat transfer.

From Fig. 15, one can also surmise that for most effective performance it is desirable to maintain as high a population density as possible with dropwise condensation, but not too high, lest film condensation take place. Experimentally it has been found that dropwise condensation of steam on metal (except for the noble metals, c.f. - Ref. 19), occurs only with the use of "promotors". A number of pormotors are listed in Table IV.

TABLE IV. PROMOTORS FOR STEAM

	Ref.
Stearic Acid	34
Montanic Acid	34
Dioctedecyl Disulphide	34, 35, 36
Benzyl Mercaptan	29
Oleic Acid	
Dimethyl-Polysiloxane (Silicon Oil KF-96)	31
Dibenzyl Disulphide	34
Montan Wax	34
Dodecane (Ethanethio) Silane	35, 36

The detailed role that the promotors play has yet to be clarified. They do form a coating on the surface, and it was noted that the effectiveness changed little with variations in thickness of the coating between 0.2 and 11 equivalent monolayers, on a relative scale[34]. Thicknesses less than this did not produce dropwise condensation while those greater seemed to introduce an additional thermal resistance. It was also observed that both abrasion and oxidation of the surface tended to cause the surface to revert to film condensation. These were explained on the basis that gross roughening assists wetting by capillarity,

hence increasing the number of potential nucleating sites. Surfaces with oxide layers required relatively more promotor to make the surfaces hydrophobic (non-wetting). It appears that a promotor tends to eliminate some of the many natural nucleating sites that are present on any real surface by perhaps filling in some of the cavities, or by changing the solid-liquid-vapor surface energy relationships such that a critical size drastically different from that given by Eq. (40) becomes necessary for nucleation to take place. Since filmwise condensation is the more common mode which takes place, to increase heat transfer rates requires the establishment of dropwise condensation on a reliable basis, and hence the reduction in number of nucleating sites such that coalescence does not take place.

Using a variety of particles ranging in size from 1-100 microns (1 micron = 10^{-4} cm = 40 micro inches) and resting on a cooled surface[29], the nucleating ability of these particles were observed on the basis of their composition and size ranges. Table V lists the various materials used in the order of their nucleating ability with water vapor, from the best on down. Also listed is the net heat of adsorption for each substance, and almost a direct relationship exists between nucleating ability and the net heat of adsorption, which is the difference between the heat of adsorption and the latent heat of condensation. Adsorption of vapor on the particle is the first step in the nucleation of drops on the particle and, from Table V, takes place when the heat of adsorption is greater than the latent heat of condensation. The greater the difference, the more easily nucleation takes place.

TABLE V. RELATIVE ORDER OF NUCLEATION ABILITY OF PARTICLES (Ref. 29)

Particle	Particle Size Micron	Nuclation Ability	Net Heat of Adsorption K cal/mole
Sodium Chloride	5-40	Excellent	25.5 (soluble)
Platinum	1-100	Very Good	5.5
Glass	2-40	Very Good	2.7
Aluminum Oxide	2-50	Very Good	1.6
Starch	9-35	Very Good	0.5
Bone Charcoal	3-33	Good	0.5
Silver Iodide	2-24	Poor	0.4
Titanium Dioxide	10-25	Poor	0.03
Graphite	7-44	Very Poor	0.05
Mercury	4-70	Very Poor	0
Teflon	6-43	Very Poor	0
Coconut Charcoal	11-29	None	-0.85
Pyrolytic Graphite	5-50	None	-2.0

Assuming for the moment that the condensation taking place on a surface will be dropwise, it is of interest to predict the wall temperatures at which condensation nucleation may be expected to occur. The analysis is similar to that used to predict the surface superheat for incipient nucleate boiling (30) and assumes that nucleation will begin at a cavity of radius r_c, in Fig. 17. The analysis is also similar to that for predicting the supersaturation necessary for condensation on particles[29]. A cavity of radius r_c exists, Fig. 17, and is considered filled with liquid to give a hemispherical protrusion of height r_c. T_s is the saturation temperature corresponding to the normal vapor pressure, and T_v indicates the vapor temperature profile in contact with a cooled surface at temperatures T_w. As had already been indicated, in order for condensation to occur on a curved interface, the local vapor subcooling must be greater than a minimum amount given by Eq. (51). In order for the cavity of radius r_c in Fig. 17 to act as a nucleating site, i.e. for the drop to grow, the vapor temperature at distance r_c from the wall must have a subcooling greater

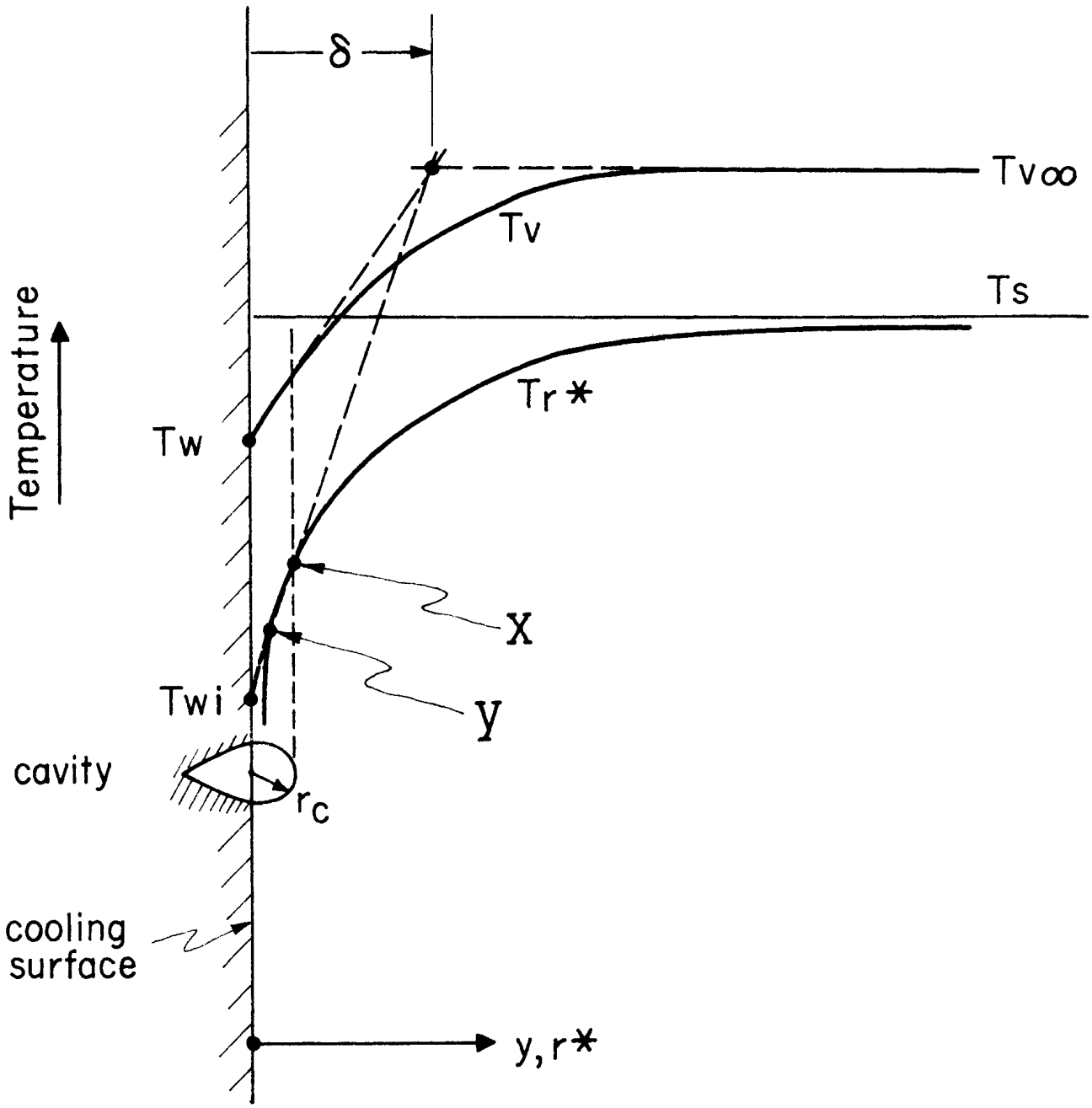

Figure 17. Model for Determining Effective Nucleating Site.

than that given by Eq. (51) for $r^* = r_c$. Letting $T_v = T_{r^*}$, Eq. (51) gives

$$T_{r^*} = T_s \left(1 - \frac{2\sigma v_\ell}{h_{fg} r^*}\right) \tag{55}$$

T_{r^*} is plotted in Fig. 17. The embryo will grow (i.e. nucleation will occur) when the vapor temperature T_v at $y = r_c$ equals T_{r^*} at $r^* = r_c$. Assume that near the wall the vapor profile is linear over a sufficient range, and can be represented in terms of a boundary layer thickness δ, bulk vapor temperature $T_{v\infty}$, and wall temperature T_w by

$$\frac{T_{v\infty} - T_v}{T_{v\infty} - T_w} = 1 - \frac{y}{\delta} \tag{56}$$

If the wall temperature is T_w as indicated in Fig. 17, the cavity cannot serve as a nucleation site, since the temperature T_v at $y = r_c$ is greater than the critical temperature given by T_{r^*} at $r^* = r_c$. If, however, T_w is T_{wi} as indicated in Fig. 17 such that T_v is equal to T_{r^*} (point X), then the site is just at the incipient nucleating point for condensation. To solve for the wall temperature at this state, set T_{r^*} in Eq. (55) for $r^* = r_c$ equal to T_v in Eq. (56) for $y = r_c$. The result is:

$$\Delta T_{wi} = \left(\Delta T_{sup} + \frac{A}{r_c}\right) \frac{\delta}{\delta - r_c} \tag{57}$$

where

$$\Delta T_{wi} = T_{v\infty} - T_{wi}$$

$$\Delta T_{sup} = T_{v\infty} - T_s$$

$$A = \frac{2\sigma v_\ell T_s}{h_{fg}}$$

This gives the minimum value of ΔT_w ($=T_{v\infty} - T_w$) at which the cavity of radius r_c may become an active condensation nucleating site.

Note in Fig. 17 that the boundary layer temperature profile also intersects T_{r^*} at a smaller value of r^*, designated as Y. If ΔT_w is given but the

cavity sizes cover the entire spectrum, the range of cavity sizes which can become active is given by the solution of Eq. (57) for r_c:

$$r_c = \frac{\delta}{2}\left[(1-\theta_s) \pm \sqrt{(\theta_s-1)^2 - \frac{4A}{\delta\,\Delta T_w}}\right] \tag{58}$$

where

$$\theta_s = \frac{T_{v\infty} - T_s}{T_{v\infty} - T_w} = \frac{\Delta T_{sup}}{\Delta T_w}$$

For saturated vapor conditions $\theta_s = 0$. For $T_w = T_{wi}$ in Fig. 17, the two roots of Eq. (58) would correspond to points X and Y, and within this range the local vapor temperature T_v is lower than the critical temperature T_{r*}, hence cavities in this range can become nucleation sites.

If the value of the terms within the square root sign of Eq. (58) is negative, then no site can become active. If a wide range of cavity sizes is present on a surface, then the criteria for incipient condensation is given setting the discriminate of Eq. (58) equal to zero and solving

$$\Delta T_{wi} = \Delta T_{sup} + \frac{2A}{\delta} \pm \left[\frac{2A}{\delta}\left(2\Delta T_{sup} + \frac{2A}{\delta}\right)\right]^{1/2} \tag{59}$$

If the vapor is saturated ($\Delta T_{sup} = 0$), then Eq. (59) reduces to

$$\Delta T_{wi} = \frac{4A}{\delta} \tag{60}$$

Equation (58) is plotted in Fig. 18, along with data for dropwise condensation of water on a horizontal copper surface promoted with benzyl mercaptan[29]. The data points fall within the plotted size range, even though it was difficult to do better than estimate a value for the boundary layer thickness δ in the experiments.

An analysis to determine the critical radius for subsequent growth of the outer surface of a liquid film covering a protrusion on a surface gives the same result as Eq. (51) for homogeneous nucleation[38].

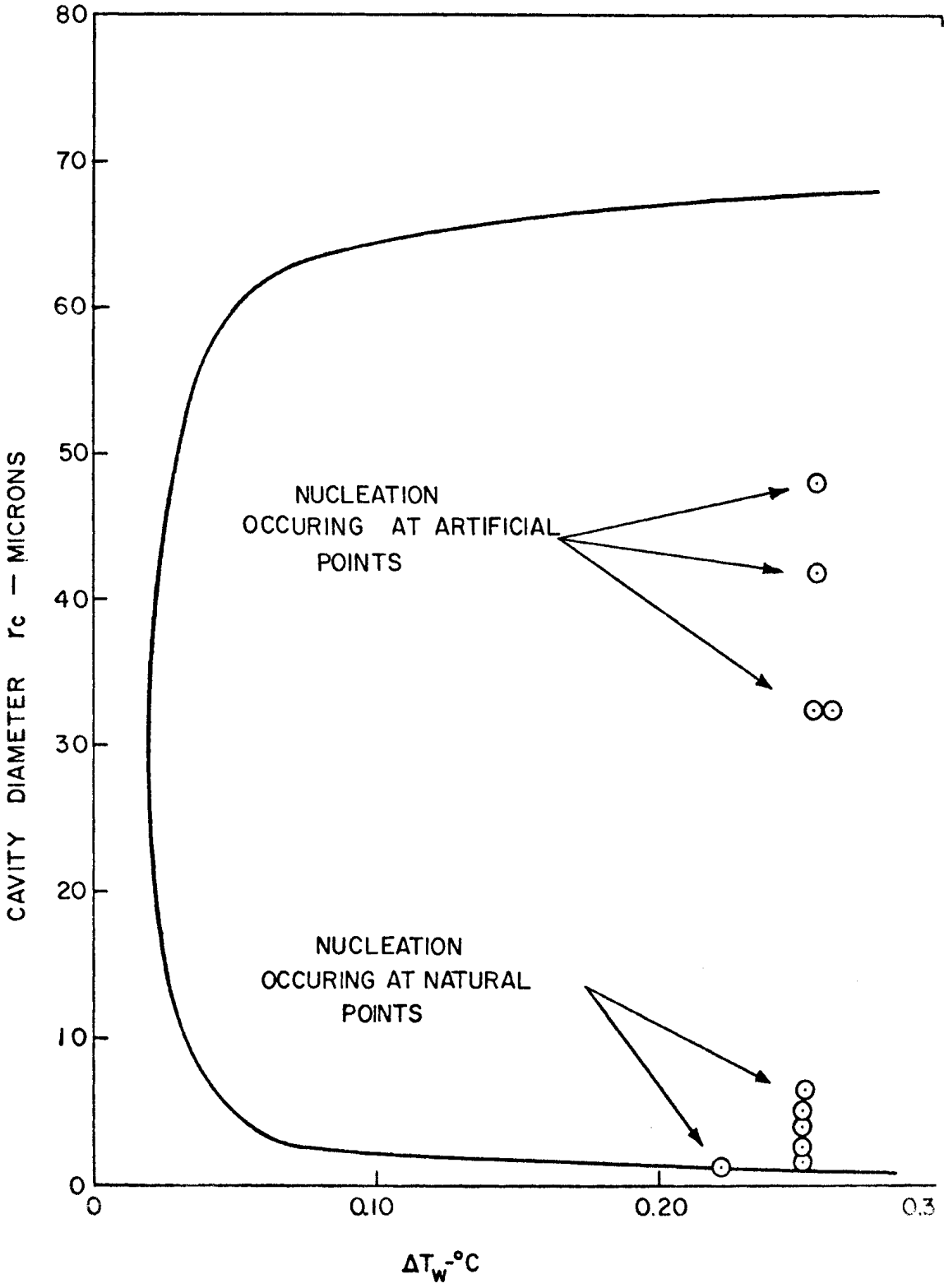

Figure 18. Effective Size Range of Condensation Nucleation Cavities. (Ref. 29)

III. LIQUID-VAPOR INTERFACE PHENOMENA

Once nucleation has taken place (the embryo has become a nucleus and growth begins), subsequent condensation takes place from the vapor onto the liquid. The dynamics of the phenomena at the liquid-vapor interface will now be considered.

The first question raised might be that regarding the nature of the interface-how well defined is it-sharp or diffuse? Strong evidence exists that the change in density from liquid to vapor is very abrupt, the transition layers being only 1-2 molecules thick. This is shown most clearly by the nature of light reflected from the surface. From Fresnel's law of reflection, if the transition between air and a medium of refraction index n is abrupt, the light is plane polarized if the angle of incidence is at the Brewster's angle, or $\tan^{-1} n$. But if the transition is gradual the light will be elliptically polarized[3]. This test is so sensitive it will detect layers of the order of one molecule thick. An experiment by Rayleigh (cited in Ref. 3) with water indicated that a water surface had a transition about one molecule thick.

A related question is the temperature of the interface. If the interface is not sharply defined but consisted of a transition zone, the concept of an interface temperature loses its meaning. However, in light of the results above, it seems reasonable that a temperature can be assigned to each phase at the interface, and the zone of uncertainty is quite small. In fact, the classical concept of temperature itself loses meaning on the molecular scale.

To avoid the complication of a curved interface, consider the condensation of a pure vapor on a plane interface, as represented in Fig. 19. The process is first examined on the basis of a continuum or macroscopic viewpoint. With thermodynamic equilibrium, in the notation on the upper part of Fig. 19,

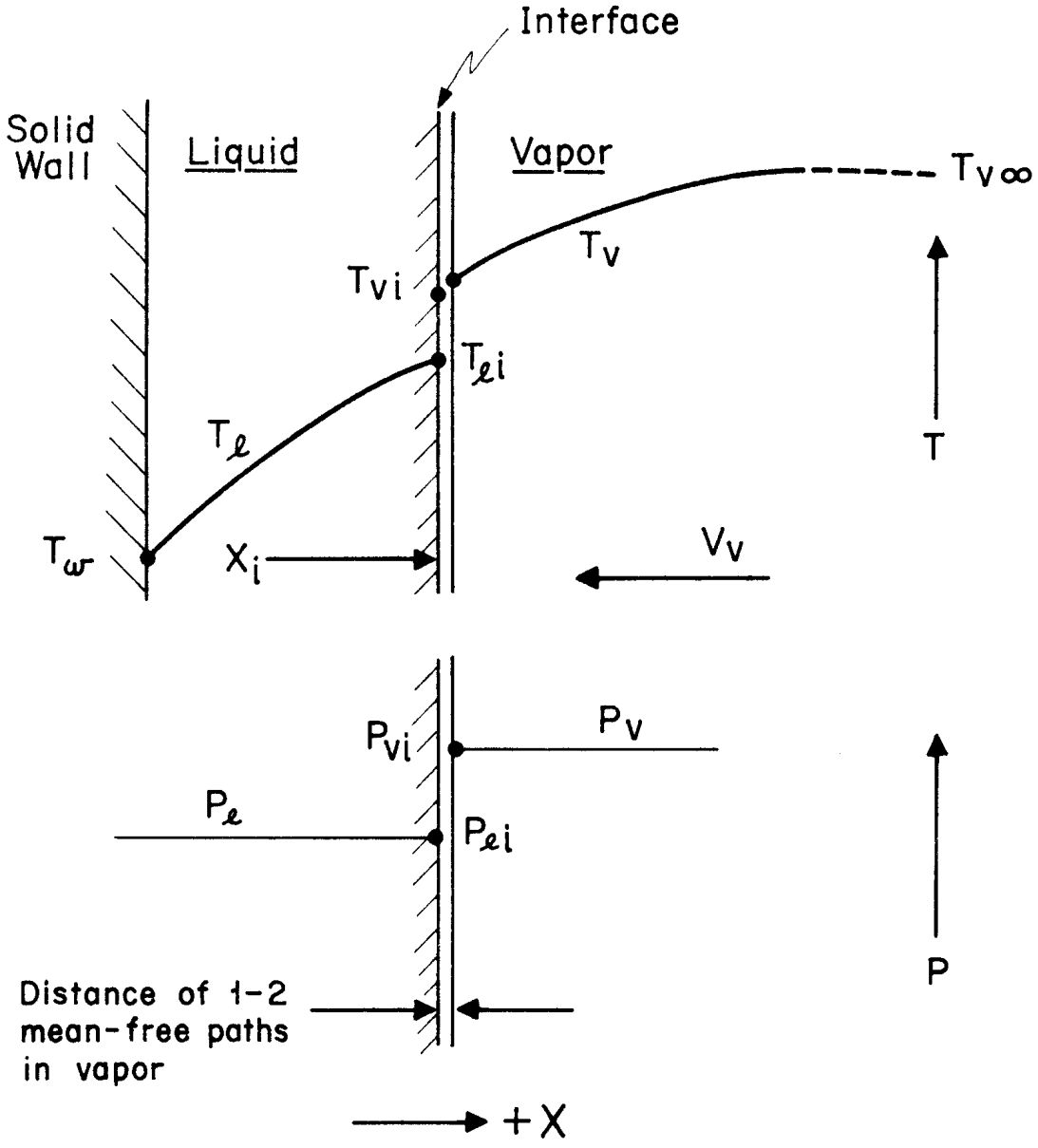

Figure 19. Continuum Representation of Liquid-Vapor Interface.

$$T_\ell = T_{\ell i} = T_{vi} = T_v = T_{v\infty} = T_s \tag{61}$$

and no changes will take place in the absence of any driving forces.

With non-equilibrium, temperature differences will exist in the system, in T_ℓ and T_v. To explore the temperatures at the interface, the temperature of the liquid and the vapor at the interface must be defined. If a sub-miniature temperature measuring device is placed in the liquid, and its temperature distribution explored as close to the interface as possible, the extrapolation of this temperature to the interface is defined as the liquid interfacial temperature, $T_{\ell i}$. In the vapor also, the extrapolation of the vapor temperature to the interface is the vapor interfacial temperature, T_{vi}. This is extrapolated over the distance of one to two mean free paths to avoid the problem of defining temperature in terms of a non-Maxwellian velocity distribution which may exist in the immediate vicinity of the interface[39].

Because of inability to detect the differences between $T_{\ell i}$ and T_{vi}, and in the absence of any known relation between them, non-equilibrium processes treated on a continuum basis consider that

$$T_{\ell i} = T_{vi} = T_s \tag{62}$$

although there exists no "a priori" basis for this. For condensation to take place the latent heat must be removed, by conduction in one or both phases. If the liquid is stationary the interface will move to the right, in Fig. 19. A first law control volume analysis on the interface gives[40]

$$\rho_\ell h_{fg} \frac{dX_i}{dt} = k_\ell \left(\frac{dT_\ell}{dX}\right)_i - k_v \left(\frac{dT_v}{dX}\right)_i \tag{63}$$

The rate of mass transfer between the two phases may be described in terms of dX_i/dT. The first term on the right side of Eq. (63) represents conduction heat

transfer in the liquid phase, and the second term is conduction heat transfer on the vapor side, with the difference being the net energy removal of latent heat- the left side of Eq. (63). With a density difference between the two phases, bulk motion in the vapor takes place, expressed by

$$V_v = \left(\frac{\rho_\ell}{\rho_v} - 1\right) \frac{dX_i}{dt} \tag{64}$$

A driving force is necessary for the vapor motion to take place. With condensation, the vapor concentration at the interface is reduced by the net removal of the vapor, to a value below that for equilibrium conditions. A pressure depression thus exists, as represented on the lower part of Fig. 19;

$$P_{\ell i} < P_{v i}$$

The influence of hydrostatic heads are neglected here. To achieve this reduced pressure requires that the liquid interface temperature $T_{\ell i}$ be below the equilibrium saturation temperature T_s, corresponding to the vapor pressure P_v. The vapor interface temperature T_{v_i} may or may not be the same as T_s. It depends upon the velocity distribution of the vapor molecules at the interface, which consists of molecules coming from the bulk vapor region on the right, molecules reflected from the interface, and molecules emitted from the liquid. If the net sum of these furnishes the same Maxwellian velocity distirhution present at temperature T_s, then

$$T_{v i} = T_s \tag{65}$$

Schrage[39] provides an argument showing that when the entire vapor region is at the saturation temperature (i.e. $T_v = T_s$), then $T_{v_i} = T_s$. However, with superheated bulk vapor, it would be likely that interactions between the three groups of molecules would result in a non-Maxwellian velocity distribution,and one would not expect that Eq. (65) would hold.

The net conclusion of the above discussion is that an interfacial temperature difference ($T_{v_i} - T_{\ell_i}$), sometimes called a "temperature jump", must exist across a liquid vapor interface, even with a continuum treatment of the process. The calculation of the magnitude of this temperature jump, however, requires the introduction of microscopic considerations. One might be tempted to include the temperature difference ($T_{v_i} - T_{\ell i}$) in the marroscopic formulation of the energy interactions at the interface, given as Eq. (63). It would not be correct, however, since the energy transfers in the liquid and vapor are already accounted for in the defined temperature gradients at the interface. The formulation of the problem, however, requires an additional relation between $T_{\ell i}$ and T_{v_i}. In seeking such a relation one might view the difference as a thermal manifestation of a molecular resistance, particularly when dealing with a series of thermal resistances as in film condensation. The difference ($T_{\ell i} - T_{v_i}$) was not detected until much work on condensationof liquid metals had taken place (e.g. see Refs. 41, 42, 43). Its detection depends on the magnitude of the interfacial "resistance" compared to other thermal resistances. If the liquid film in the upper part of Fig. 19 has a relatively high thermal resistance, then

$$(T_{\ell i} - T_w) \gg (T_{vi} - T_{\ell i}) \tag{66}$$

The right hand side might be negligibly small, and no error exists with taking $T_{v_i} \approx T_{\ell i} \approx T_s$. This accounts for the success of the Nusselt theory of film condensation[44] for many fluids like water.

To derive an expression for the interfacial temperature difference it will be assumed that the bulk vapor is at the saturation temperature so that $T_{v_i} = T_s$. The presentation follows that of Schrage[39] and Wilhelm[45].

The interphase mass transfer is viewed as a difference between the rate of arrival of molecules from the vapor space toward the interface and the rate

of departure of molecules from the surface of the liquid into the vapor space. When condensation takes place the arrival rate exceeds the departure rate; with evaporation with opposite occurs; with equilibrium they are equal.

From the kinetic theory of gases, assuming a Maxwellian velocity distribution for the vapor emitted from a liquid surface at $T_{\ell i}$, and considering this vapor to behave as an ideal gas at pressure $P_{\ell i}$, the vapor pressure corresponding to $T_{\ell i}$, the absolute rate of evaporation of a liquid (as into a high vacuum) at $T_{\ell i}$ is given by:

$$\frac{w_{e\,max}}{A} = \sigma_{e\,max} P_{\ell i} \left(\frac{M}{2\pi \bar{R} T_{\ell i}} \right)^{1/2} \tag{67}$$

$\sigma_{e\ max}$ is the maximum value of an evaporation coefficient σ_e, and is attained with the evaporation of a pure liquid into a high vacuum. The evaporation coefficient σ_e corrects the evaporative mass flux for effects associated with polyatomic molecules and the equilibration of their internal degrees of freedom in passing from the initial to the activated states on evaporation. It has been theoretically shown[46] that spherically symmetrical molecules such as CCL_4 and monatomic molecules have values of $\sigma_{e\ max} = 1$, while unsymmetrical ones have values $0 \leq \sigma_{e\ max} \leq 1$. Measured values for liquid metals also give $\sigma_{e\ max} \approx 1$.

When condensation and evaporation occur simultaneously σ_e may be reduced considerably below $\sigma_{e\ max}$ because of interactions between the evaporating flux and the condensing flux. σ_e may be considered as a correction factor for the combined effects mentioned above plus the possible departure of the velocity distribution of evaporating molecules from the equilibrium Maxwellian distribution. Thus;

$$0 \leq \sigma_e \leq \sigma_{e\,max} \tag{68}$$

and the mass flux of evaporating molecules is given by

$$\frac{w_e}{A} = \sigma_e P_{\ell i} \left(\frac{M}{2\pi \bar{R} T_{\ell i}} \right)^{1/2} \tag{69}$$

By a similar analysis, the mass flux of vapor molecules condensing on a liquid surface is given by;

$$\frac{w_c}{A} = \sigma_c \Gamma P_v \left(\frac{M}{2\pi \bar{R} T_v} \right)^{1/2} \tag{70}$$

where σ_c is the fraction of incident molecules that actually condense; the remaining fraction $(1-\sigma_c)$ is reflected and contributes nothing to the net flux. Γ arises from the analysis because of the influence of the bulk vapor velocity V_v moving toward the condensing plane in Fig. 19, and is given by;

$$\Gamma = e^{-\phi^2} + \phi \pi^{1/2} (1 + \text{erf}\, \phi) \tag{71}$$

where

$$\phi = \frac{V_v}{(2\bar{R}T/M)^{1/2}} \tag{72}$$

V_v is given by

$$\frac{w}{A} = \rho_v V_v \tag{73}$$

For w, see Eq. (75) below. σ_c is called the condensation coefficient, and for mathematical simplicity is often taken as

$$\sigma_c = \sigma_e = \sigma \tag{74}$$

although no physical justification exists for this assumption. Each coefficient is associated with a different mechanism; the capture by and escape from a strong intermolecular force[45].

The net mass flux at the interface for a pure substance is then given by the difference between Eqs. (70) and (69);

$$\frac{w}{A} = \left(\frac{M}{2\pi \bar{R}}\right)^{1/2}\left(\sigma_c \Gamma \frac{P_v}{T_v^{1/2}} - \sigma_e \frac{P_{\ell i}}{T_{\ell i}^{1/2}}\right) \tag{75}$$

With thermodynamic equilibrium conditions Eq. (74) is strictly true, and $\Gamma = 0$. Then $P_v = P_{\ell i}$, $T_v = T_{\ell i}$, and $(w/A) = 0$. If Eq. (74) is assumed valid under non-equilibrium conditions, then Eq. (75) becomes;

$$\frac{w}{A} = \sigma \left(\frac{M}{2\pi \bar{R}}\right)^{1/2}\left(\Gamma \frac{P_v}{T_v^{1/2}} - \frac{P_{\ell i}}{T_{\ell i}^{1/2}}\right) \tag{76}$$

This shows that, for any given fluid and mass transfer rate, the interfacial temperature drop $(T_v - T_{\ell i})$ increases as pressure P_v is decreased. Examples of calculations of this are shown in Table VI, taken from Ref. (41), and based on an assumed temperature drop of 5°F across the liquid film.

TABLE VI. TEMPERATURE DROP AT LIQUID-VAPOR INTERFACE. Ref. (41)

Fluid	Assumed Value of σ	$(T_v - T_{\ell i})$ °F, for P_v=			Mass flux-from Nusselt's theory lbm/hr. ft^2
		760mm	100mm	10mm	
Water	1.0	.003	0.01	0.1	7.9
	0.04	0.1	0.7	4.8	
Mercury	1.0	0.3	1.6	10.0	1115
	0.1	5.9	29.6	-	
Sodium	1.0	0.6	2.8	18.0	250

Table VI demonstrates why the presence of this interfacial temperature drop with fluids other than liquid metals has not been observed.

The heat flux corresponding to complete condensation of steam at atmospheric pressure, using the mass flux of steam calculated from Eq. (70) with $\Gamma = 1$ and $\sigma_c = 1$, resulted in $q/A = 72 \times 10^6$ BTU/hr. ft^2 (26). The maximum

heat flux observed with condensation of steam has been about 252,000 BTU/hr.ft^2, so if Eq. (74) is taken as valid, the condensation coefficient is about 0.04, which was stated as agreeing with the values of others[26].

Recent measurements of the condensation coefficient of water with net condensation, using a transient technique, gave values of σ ranging over $0.01 \leq \sigma \leq 0.2$, and with net evaporation in the range $0.02 \leq \sigma \leq 0.8$, which varied with time in a decreasing fashion[47]. An interferometer was used to obtain an approximation of the transient temperature at the liquid-vapor interface. The asymptotic values with net condensation appeared to be 0.01, and with net evaporation was 0.02, in about 0.2 sec. The relationship between these transient measurements and steady ones has not yet been established.

Other recent results with steam at atmospheric pressure indicate that higher values of the condensation coefficient are possible: $\sigma \geq 0.08$, Ref. (48); $\sigma \geq 0.45$, Ref. (49); $\sigma \approx 1.0$, Ref. (50). Table VII, taken from Ref. (49), shows other values for steam.

TABLE VII. PREVIOUS EXPERIMENTAL VALUES FOR THE CONDENSATION COEFFICIENT OF WATER (Ref. (49)).

INVESTIGATION	DATE	TEMPERATURE °C	σ	NATURE OF THE EXPERIMENT
GROUP 1				
Alty	1931	18-60	0·006-0·016	evaporation from a suspended drop
Alty & Nicoll	1931	18-60	0·01-0·02	same
Alty	1933	-8-+4	0·04	same
Alty & Mackay	1935	15	0·036	same
Pruger	1940	100	0·02	evaporation from a horizontal surface
Hammecke & Kappler	1953	20	0·045	same
Hammecke & Kappler	1955	?	0.100	same
Delaney, et al	1964	0-43	0.0415-0.0265	same
GROUP 2				
Hickman	1954	0	0.42	evaporation from a tensimeter jet
Nabavian & Bromley	1963	10-50	0.35 — 1.0	film condensation on a fluted tube
Jamieson	1965	0-70	0.35	condensation on a tensimeter jet
Berman	1961	?	near to 1.0	film condensation on a horizontal cylinder

For both water and liquid metals condensing on a vertical surface, there appears to be considerable evidence that a direct relationship exists between the condensation coefficient and pressure, as shown in Fig. 20. Three different liquid metals as well as water are represented over a wide range of pressures, from 9 independent investigations. The asymptotic value of σ=1.0 for low pressures appears to support the description, made earlier, that the condensation coefficient is a correction factor for interaction between molecules.

An analysis which takes into account the influence of vapor subcooling in a thin zone adjacent to the liquid-vapor interface (on the order of 10 mean-free-paths), results in a calculation of the condensation coefficient σ=1 for much of the data, rather than σ decreasing as pressure increases as in Fig. 20 [51].

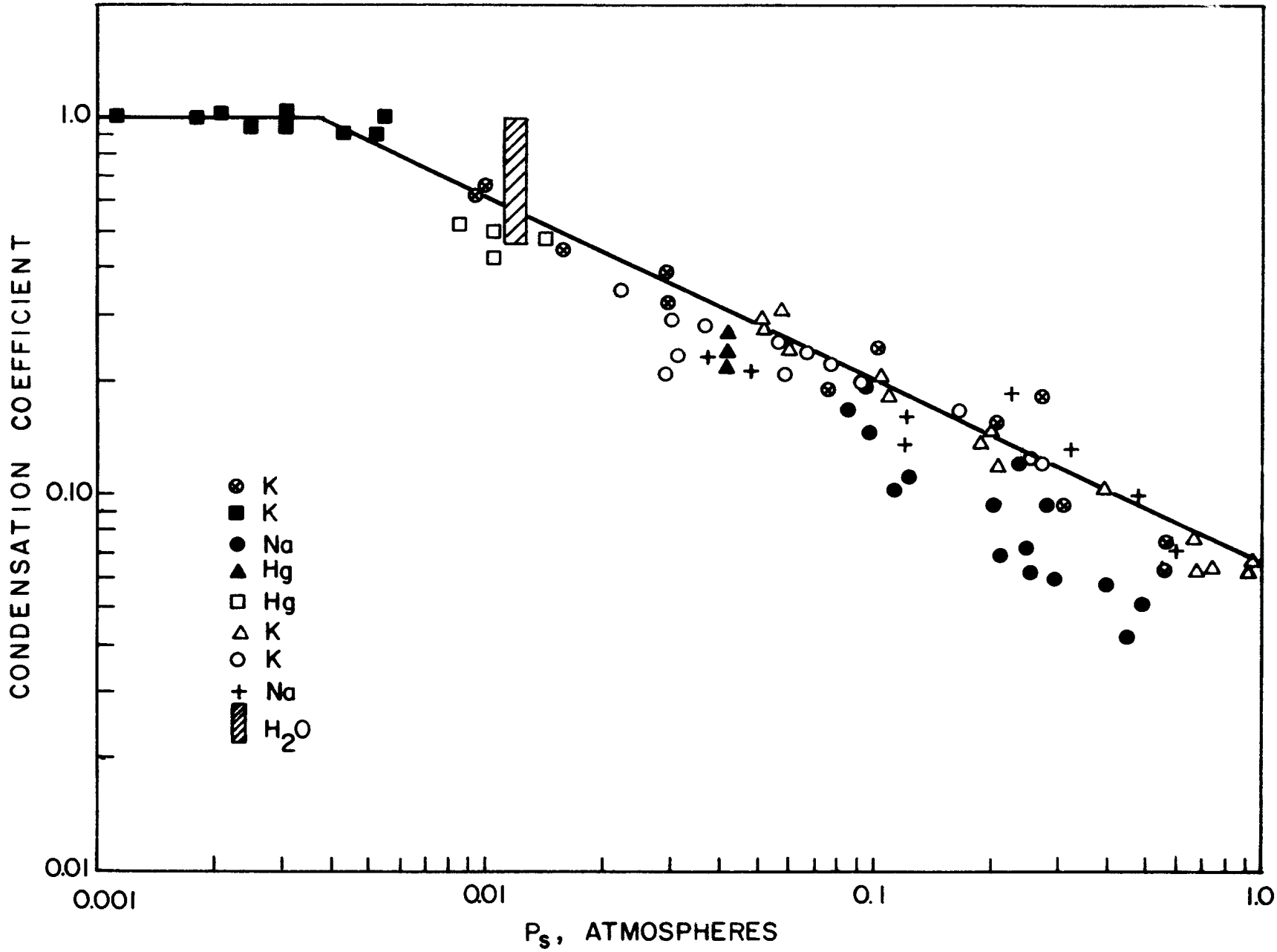

Figure 20. Condensation Coefficient of Potassium vs Saturation Pressure. (Ref. 42)

IV. BULK CONDENSATION RATES

Devices such as steam desuperheaters, spray condensers and direct contact steam-water heaters provide examples where phase changes of pure substances take place in a bulk continuous phase,i.e. away from solid surfaces. The rate at which the phase change takes place is of concern in order to properly design these devices.

The growth of hailstones, rain drops and snow are examples of bulk condensation of mixtures, in which one of the components is relatively inert, or non-condensable. The conditions under which these processes arise and the rate at which they occur are of great interest to meteorologists[52].

Bulk condensation can be classified in two categories, depending on whether the continuous or primary phase is liquid or vapor. Condensation in a supersaturated vapor or on injected subcooled liquid drops would take place as the growth of dispersed liquid drops, while a vapor injected into a subcooled liquid bulk would result in collapse of the vapor bubble, because of condensation. The complete governing equations are identical for both cases, consisting of the equations of conservation of mass, momentum and energy for the region within and outside of the drop or bubble. The growth of the drop is much slower than the collapse of a vapor bubble, for the same initial temperature difference. This, combined with the much lower density of the vapor moving medium for the drop case as compared to the liquid for the collapsing bubble, means that momentum effects can be neglected in the case of the condensation on a drop. These cases are therefore considered independently. Except perhaps for liquid metals, the influence of any interfacial temperature drops can be ignored.

A. Condensation on Drops

Two different cases of condensation on drops will be considered depending

on whether the sink for latent heat removal lies outside of, or within the liquid drop.

1. Supersaturated Vapor

If, as a result of expansion of a pure vapor below the saturation temperature nucleation takes place, and the saturation continues, further growth of the drop occurs by the transfer of heat to the surroundings, and continues as long as the surroundings are supersaturated. It should be recognized that the rate of condensation will depend on the rate at which nuclei are spontaneously formed from the supersaturated vapor as well as the rate of condensation on the nuclei. The rate of formation of nuclei was considered earlier so only the latter process will be considered here. The physical situation is represented in Fig. 21. The ambient temperature $T_{v\infty}(t)$ is related to the pressure $P_v(t)$ in some form such as given in Fig. 11. Also, $T_{v\infty} < T_s$, where T_s is the saturation temperature corresponding to the pressure P_v. The surface temperature is assumed to be at the saturation temperature T_s. This neglects the effect of curvature on the vapor pressure exerted by the liquid, and also assumes that the process is limited by thermal diffusion in the vapor rather than mass diffusion. The transient conduction in the liquid is represented quite simply in differential form[40] and the relation coupling the liquid and vapor region is given by Eq. (63). However, the differential form of the energy equation for the vapor becomes quite complex because of the vapor motion and expansion taking place simultaneously. A simplified solution of this problem has made[53] by considering the adiabatic expansion of a sphere of vapor of radius $R_v(t)$, in Fig. 21, containing a liquid drop at the center, and writing the integral form of the first law of thermodynamics for the entire matter. The assumption is made that the drop is always at a uniform temperature, i.e., the liquid has a large thermal conductivity, and that no relative motion occurs between the drop and its

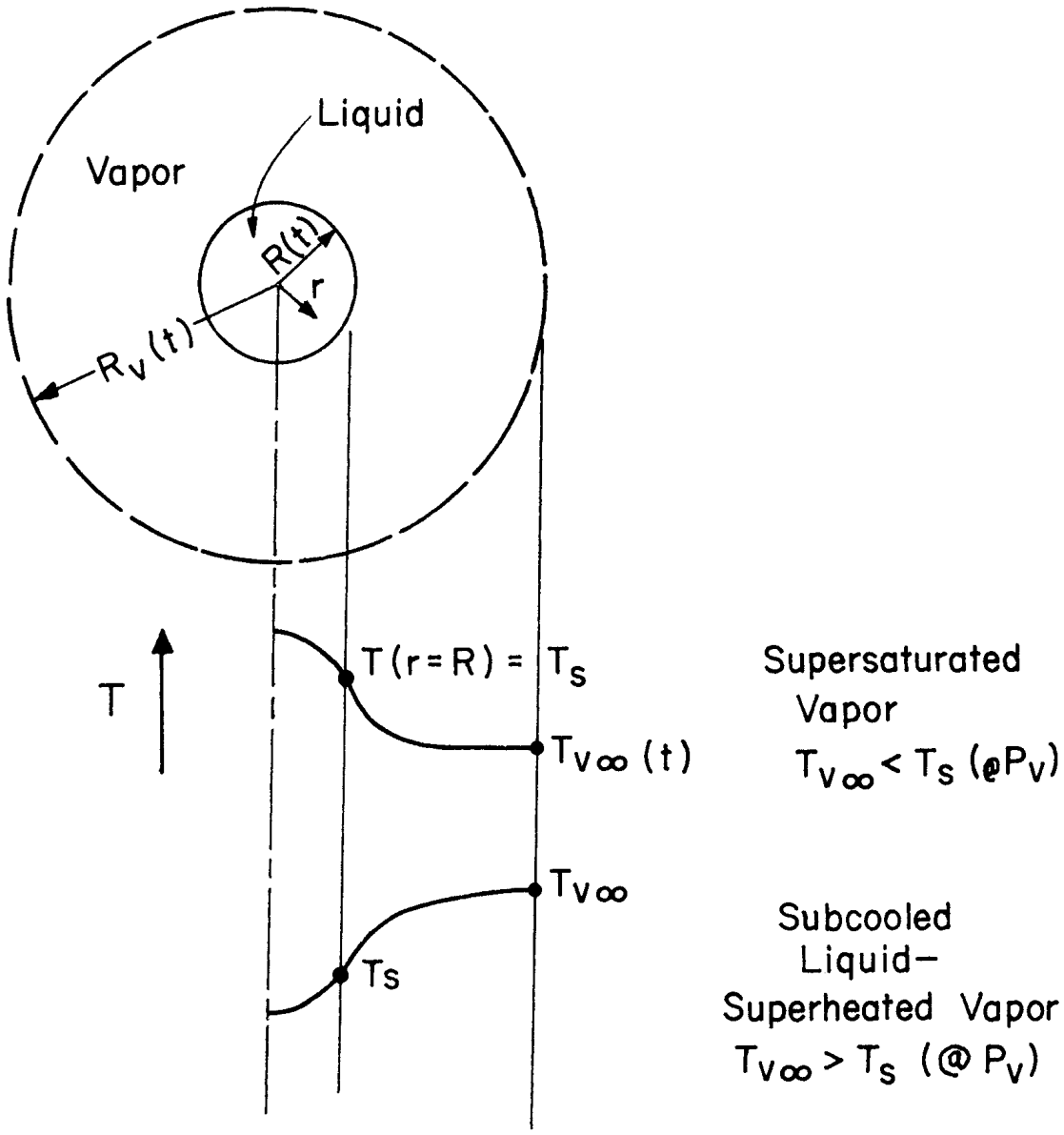

Figure 21. Dropwise Bulk Condensation.

surrounding vapor, i.e., no slip. A perturbation procedure is then used to solve for the drop size as a function of time.

Another theoretical solution to a problem similar to the above has also been made[54]. Measurements of the growth rates of droplets of water, methanol and ethanol from supersaturated vapors were made. By comparing the calculated growth rates with the theoretical ones, the condensation coefficients were computed.

If relative motion exists between the drop and the surrounding vapor, and if the primary resistance is in the continuous phase, provided that the growth rate is not too large, one can use relations for heat and mass transfer obtained for steady conditions for the unsteady processes. This has been done for calculating the growth of spherical hailstones[52], where the relations used were

$$Nu = 2.00 + 0.60\ Pr^{1/3}\ Re^{1/2} \tag{77}$$

for heat transfer, and

$$Sh = 2.00 + 0.60\ Sc^{1/3}\ Re^{1/2} \tag{78}$$

for mass transfer, where Sh is the Sherwood number, giving the mass diffusion coefficient, and Sc is the Schmidt number, giving the ratio of momentum to mass diffusivities.

2. Subcooled Liquid Drop

If subcooled liquid drops are sprayed into a bulk vapor held at a constant pressure P_v, but superheated to temperature $T_{v\infty}$, condensation may or may not initially occur on the surface of the drop, depending on the relative rates of heat transfer in the liquid and in the vapor at the surface of the drop. The physical representation is shown in the lower part of Fig. 21. If the superheat remains constant the drop will obviously evaporate, ultimately. However, if the drop is moving with the vapor in an adiabatic system, then the superheat

will be reduced. Depending on the relative amounts of liquid and vapor present, net condensation may or may not occur. For a constant system pressure the solution of this problem is somewhat simpler than the one described previously, shown in the upper part of Fig. 21, in that the surface temperature of the drop, T_s, is constant.

If the bulk vapor is saturated to begin with, $T_{v\infty} = T_s$, then only the liquid domain of the temperature field remains to be solved. This is given by:

$$\frac{\partial T}{\partial t} = a \frac{1}{r^2} \frac{\partial}{\partial r}\left(r^2 \frac{\partial T}{\partial r}\right) \tag{79}$$

with initial and boundary conditions

$$\begin{aligned} T(r,0) &= T_0 \\ T(0,t) &= \text{Finite} \\ T(R,t) &= T_s \ (> T_0) \end{aligned} \tag{80}$$

The unknowns T(r,t) and R(t) are coupled by the energy equation at the boundary:

$$h_{fg} \frac{dR}{dt} = k_\ell \frac{\partial T(R)}{\partial r} \tag{81}$$

with

$$R(0) = R_0 \tag{82}$$

Even with the many simplifications in this system of equations, a closed form solution is mathematically complex.

A spray-type of condensor, described by Eqs. (79)-(82), has potential in the automotive application of a steam Rankine Cycle in that a small size of condensor is possible. The size of condensors necessary has been a great handicap to the development of a compact closed-water cycle steam power plant. It

is necessary, of course, to have a source of subcooled water available, but this could be achieved with the use of the present heat exchanger (radiator!) on a partial by-pass basis as illustrated in Fig. 22.

B. Condensation in Liquid Bulk

That the process of condensation of vapor injected into a large subcooled bulk of liquid is dynamic is obvious to anyone who has been in the vicinity of steam being bubbled into cold water. Whether a vapor bubble grows or collapses in a bulk liquid depends primarily on whether the liquid is superheated or subcooled with respect to the saturation temperature corresponding to the pressure within the bubble. The literature is quite extensive in the treatment of bubble dynamics arising with boiling and cavitation, and it appears impractical to cover the area here. A comprehensive review covering an earlier period is given in Ref. 55. Florschuetz and Chao[56] have formulated the general problem, and obtained analytic solutions for the inertia dominated and thermal dominated cases, where the energy and momentum equations are respectively neglected. Because of the non-linearity of the general problem it was necessary to solve the intermediate case, where both inertia and thermal effects are present, by numerical means. Good agreement is presented with experiments conducted to eliminate the relative motion induced by buoyant forces. Where buoyant forces were not eliminated, rather severe discrepancies arose[57].

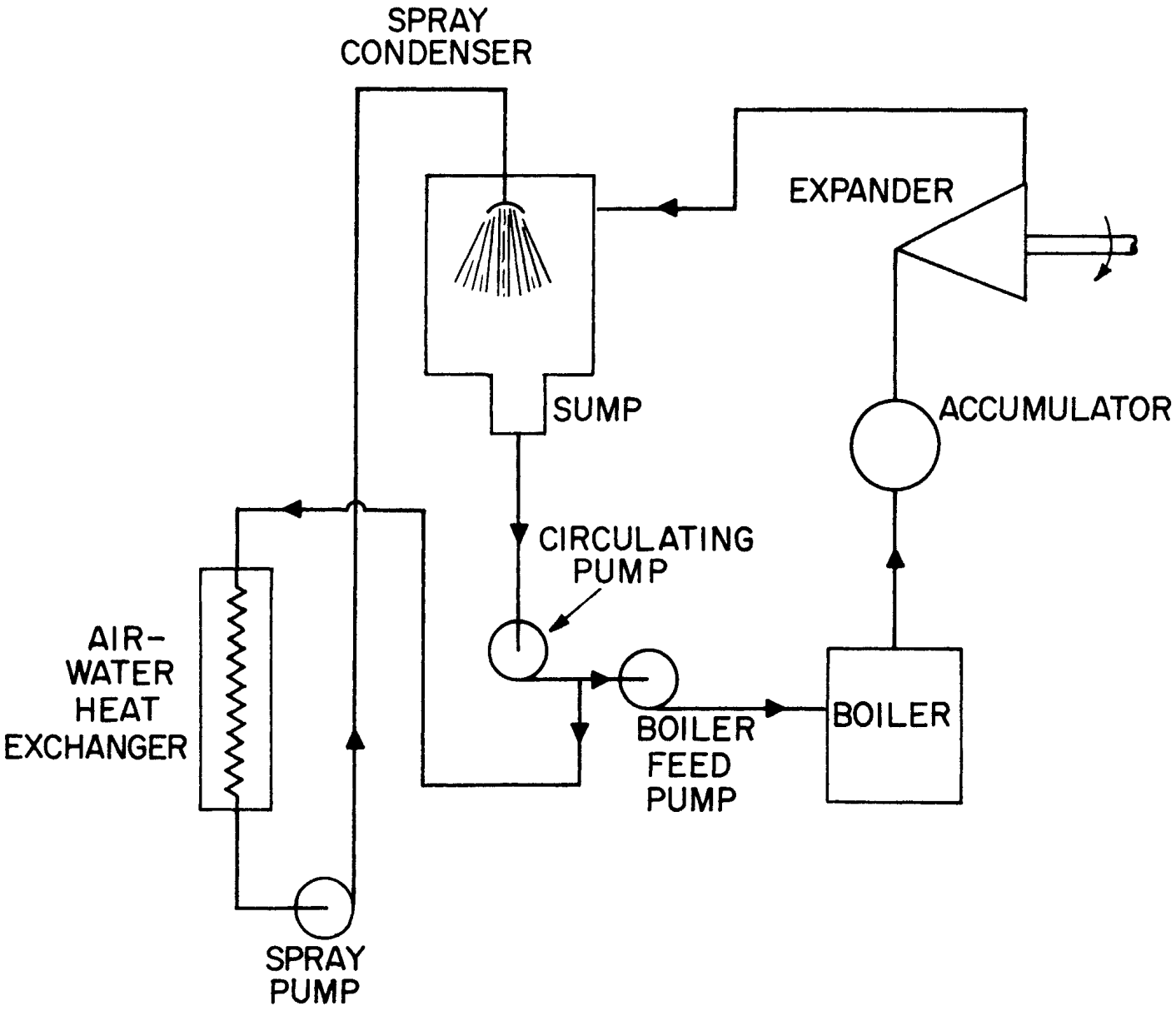

Figure 22. Application of a Spray-Type Condenser to Rankin-Cycle Power Plant.

V. SURFACE CONDENSATION RATES

Prediction of heat transfer rates with film condensation has been quite successful when compared with dropwise condensation. Both will be considered in this section. It would be desirable, however, first to be able to predict "a priori" the prevailing mode of condensation, dropwise or filmwise.

A. Prediction of Mode

As mentioned previously, it has been experimentally observed that steam will condense dropwise on metal surfaces only with the use of promotors, except where noble metals are used. This would seem to indicate that the criteria for the onset of film or dropwise condensation should depend on surface energy relationships. A criteria has been developed [8, 58] based on Eqs. (8) and (11).

Figure 23 (a-c) represents the progressive changes in surface free energy as a solid is brought into contact with a liquid, beginning with a liquid in contact with its saturated vapor and a solid in a vacuum. From Eq. (8), the work of adhesion is given by:

$$W_{\ell c} = \sigma_{\ell v} + \sigma_c - \sigma_{\ell c} \tag{83}$$

The work of adhesion between the solid and the saturated vapor is defined as π_E;

$$W_{vc} = \sigma_c - \sigma_{vc} \equiv \pi_E \tag{84}$$

π_E is sometimes referred to as the equilibrium film pressure [59] or the equilibrium spreading pressure [8]. Substituting σ_c from Eq. (84) into Eq. (83), the work of adhesion becomes:

$$W'_{\ell c} = \sigma_{\ell v} + \sigma_{vc} + \pi_E - \sigma_{\ell c} \tag{85}$$

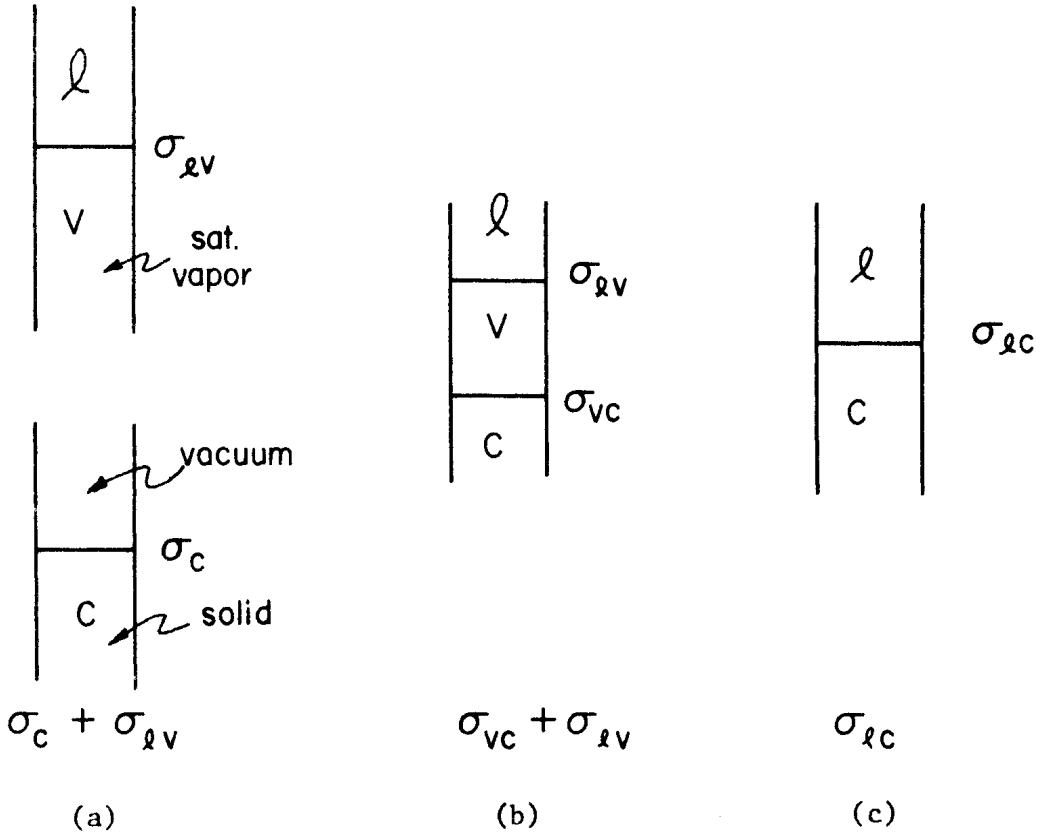

Figure 23. Interface Surface Free Energy.

If, in Eq. (85)

$$\sigma_c = \sigma_{vc} + \pi_E \geq \sigma_{lv} + \sigma_{lc} \tag{86}$$

then the surface free energy in the final state, Fig. 23(c), will be lower than the surface free energy in the initial state, Fig. 23(a), and the liquid will spread spontaneously on the solid. As with Eq. (11), a spreading coefficient is thus defined as

$$S = \sigma_{vc} + \pi_E - (\sigma_{lv} + \sigma_{lc}) \tag{87}$$

Thus, from Eqs. (86) and (87), the criteria for film and dropwise condensation is given by:

$S \geq 0$ spreading-film wise condensation

$S < 0$ non-spreading-dropwise condensation

In order to express the solid surface energies in terms of the contact angle θ, Eq. (12) is rewritten for the drop in Fig. 4 as;

$$\sigma_{vc} = \sigma_{lc} + \sigma_{lv} \cos\theta \tag{88}$$

Substitution of Eq. (88) into Eq. (87) gives

$$S = \pi_E + \sigma_{lv}(\cos\theta - 1) \tag{89}$$

It has been shown that on low energy surfaces such as polytetrafluoroethylene (PTFE), the equilibrium film pressure π_E is negligible (8).. The spreading coefficient S, Eq. (89), then becomes

$$S = \sigma_{lv}(\cos\theta - 1) \tag{90}$$

The spreading coefficient is thus a function of the liquid-vapor surface free energy and the contact angle of the liquid on the particular solid surface.

In principle, dropwise condensation should take place on any low energy surface for which the contact angle is greater than zero, since σ_{sv} in Eq. (90) is a positive quantity, and also would be independent of σ_{lv} (except insofar as it influences the contact angle θ). That this is not a sufficient criteria has been determined experimentally (59). The concept of a critical surface tension σ_{cr} appears to have been successful in describing the spreading behavior of a great variety of liquids on various surfaces (60), and in determining the onset of dropwise condensation on a limited number of surfaces (58, 61).

By measurement of the contact angle of a series of homologous liquids on different surfaces, it was observed that for a given surface, the plot of $\cos\theta$ vs. σ_{lv} yielded an approximately straight line, as with samples shown in Fig. 24 (60). The critical surface tension σ_{cr} for a given solid is then defined as the surface tension at which the liquid completely wets the surface (i.e. $\theta = 0$), and is determined by extropolating the data to $\cos\theta = 1$. The linear relationship was also found to be approximately valid for a variety of non-homologous liquids, although the intercept giving the critical surface tension is less well defined (60). Nevertheless, the critical surface tension is a useful parameter since it is a characteristic of the solid only (which would include a surface layer, if present).

Dropwise condensation (non-spreading) will take place when the liquid-vapor surface tension σ_{lv} is greater than the critical surface tension of the solid (and its surface layer). The critical surface tension of some solids are listed in Table VIII.

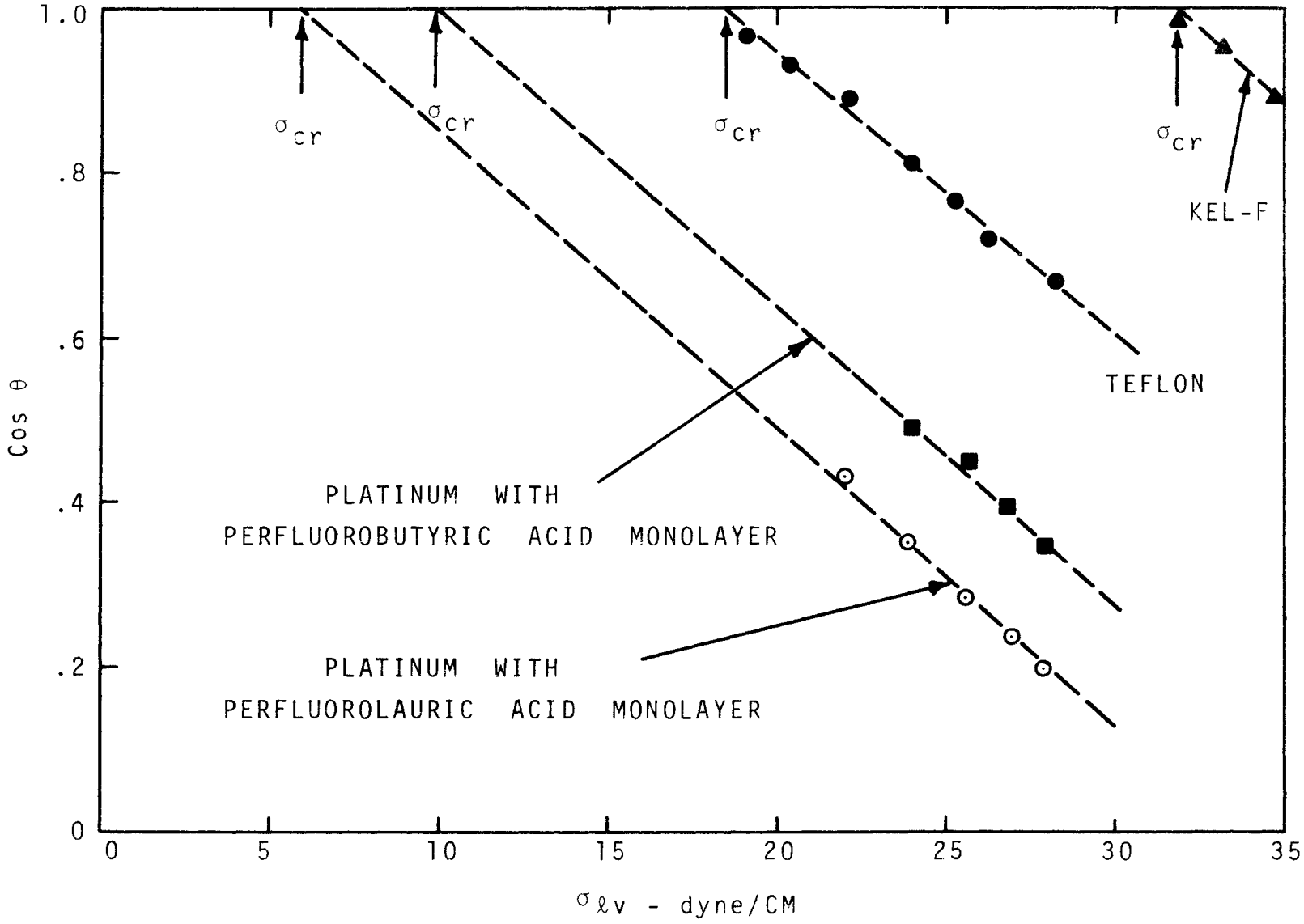

Figure 24. Definition of Critical Surface Tension. (Ref. 60)

TABLE VIII. Critical Surface Tensions of Some Solids (Ref. 60)

Solid	σ_{cr}(dynes/cm)
TFE (teflon)	18
Polyethylene	31
Kel-F	31
Polystyrene	33
Polyvinyl chloride	39
Nylon	46
Platinum with perfluorobutyric acid monolayer	10
Platinum with perfluorolauric acid monolayer	6

Table IX lists the liquid-vapor surface tensions for several different liquids, and the type of condensation taking place on TFE coated surfaces. It is noted that filmwise condensation takes place when the liquid-vapor surface tension is on the order of the critical surface tension for teflon from Table VIII, σ_{cr} = 18 dynes/cm.

TABLE IX. Condensation on Tetrafluoroethylene Surfaces (Ref. 58)

Substance	T-°C	$\sigma_{lv}(T)$	Mode of Condensation
Ethylene Glycol	120	38.1	Dropwise
Nitrobenzene	110	33.3	Dropwise
Aniline	110	33.7	Dropwise
Water	100	60.8	Dropwise
CCL_4	76.8	20.2	Filmwise
Benzene	80	20.5	Filmwise
Methanol	64.7	18.9	Filmwise

Most metallic surfaces are so-called high energy surfaces, but the critical surface tensions of these does not yet appear to have been investigated. Water has one of the highest surface tensions among the more common liquids, and the fact that film condensation occurs with most metals indicates that the critical surface tension of these metals is above the liquid-vapor surface tension of water. The effect of dropwise condensation promotors then is to form a layer which reduces the effective critical surface tension below that of the liquid. Non-spreading of certain liquids on some high energy surfaces such as platinum takes place even with no promotors present, and is attributed to the liquids having the property of being "autophobic", or unable to spread on its own adsorbed film[62].

B. Dropwise Condensation

In attempting to predict or correlate heat transfer rates with dropwise condensation on solid surfaces, or in evaluating experimental results, a number of possible complicating factors should be kept in mind. These include the effects of non-condensable gases, promotor, surface thermal properties, and the droplet removal mechanism. Each will be discussed in turn.

1. Non-condensables

It is important that non-condensables be removed to a high degree for the best performance and reproducibility of condensation[63]. This factor will be dealt with in the discussion on condensation of mixtures.

2. Promotors

The promotors used to produce dropwise condensation can introduce variables. For stable operation the entire system must be saturated with promotor, not just the condensing surface [64]. Cupric oleate in steam in concentrations between 3-50 ppm resulted in good dropwise condensation on copper, stainless steel, inconel, and copper-nickel, and had an effective continuous life

of at least 10,000 hours [20]. However, in a case where the operation was intermittant on a daily basis, with exposure of the surface to air in-between, the effectiveness decreased by 1/2 over a 10 day period.

The type of promotor also can have an influence. Four different promotors were used in one study [36], keeping all other quantities constant. A maximum difference of 50% in the heat transfer coefficient resulted between the various promotors, all with dropwise condensation. It was also observed in this work that if cooling of the surface continued while the surface was exposed to air, such that water vapor in the air would be deposited on the surface, then the promotor remained effective upon starting up again. However, if the surface was permitted to dry up in contact with air, a breakdown in effectiveness of the promotor occured, accompanied by a discoloration of the surface.

In another case[29], the surface was baked for several hours between condensing tests without exposing the surface to air. Upon condensing on the surface afterward, the number of nucleating sites was reduced by one half. The baking process most likely removed liquid that had become trapped in microscopic pits. By flooding the entire surface with liquid before condensing again, the original number of sites was reactivated. One might expect that with continuous operation over a along period of time all potential sites would become activated by a random process of "seeding" from adjacent active sites.

Dropwise condensation was obtained with no promotor by coating the outside of a 3/4" O.D. Admiralty Brass horizontal tube with a 0.0001" film of PTFE (Polytetrafluorethylene)[65] At 7" Hg of steam pressure at q/A=13,000 Btu/hr.-ft^2, the heat transfer coefficient increased from h=2500 BTU/hr.ft^2-°F with film condensation for the uncoated tube to h=6500 BTU/hr. ft^2-°F with dropwise condensation for the coated tube. The latter value includes the

additional thermal resistance of the coating. The advantage of a stable coating over promotors to produce dropwise condensation is obvious: the additional operation of maintaining promotor concentration is eliminated and the vapor is not contaminated.

3. Effect of surface thermal properties

It has been experimentally demonstrated that the thermal properties of the condensing surface exert considerable influence on dropwise condensation (64). Saturated steam at atmospheric pressure was condensed on the underside of a horizontal surface with 3 different metals; stainless steel, zinc, and copper. To eliminate differences due to surface effects, each material was plated with 0.005" thick gold, each promoted by oleic acid. The heat transfer coefficient is defined in the standard way by

$$h = \frac{q/A}{T_v - T_w} \tag{91}$$

It was observed that in all cases the heat transfer coefficient h was independent of the temperature difference $(T_v - T_w)$ and thus also independent of the heat flux. This could be a consequence of the particular character of a gold surface.

The results are tabulated in Table X, with h given in BTU/hr.ft^2°F.

TABLE X. Dropwise Condensation of Steam on Different Materials-Atmospheric Pressure.

Material	K_w BTU/hr. ft°F	h Gold Plated (Ref. 64)	h Bare (Ref. 34)
Stainless Steel	10	2,000	8,000
Zinc	63	4,500	--
Copper	220	10,500	42,000

It is noted that for a 20 fold increase in the thermal conductivity of the substrate material, the condensing coefficient increases 5 fold, both for the gold plated surface[64] and the bare surface[34]. The absolute differences between the plates and bare surfaces are indicative that surface properties as well as substrate thermal properties have an important effect. The effect of substrate thermal properties is postulated as resulting from the temperature variation along the metal surface between the drop center, where the surface is effectively insulated by the drop itself, and the triple interface at the edge of the drop where the majority of heat transfer takes place[64]. This is also implied in models for dropwise condensation proposed much earlier[21,22]. An analytical basis for the influence of the substrate was obtained by solving the two dimensional conduction problem for the substrate, assuming that the drops effectively insulate the surface[66]. It was found that for stainless steel as the condensing surface about 84% of the total resistance was that occuring in the plate itself due to heat flux non-uniformity over the surface, while for copper this was 20%.

4. Droplet removal

It was shown in Fig. 15 that for a given ΔT, the heat flux depended on the population density of the drops. These experiments were conducted at short times after admission of vapor to the test vessel so that the mechanism of drop removal was not a factor, and at low pressure so that the growth rates were low. One might anticipate that as the drops continue to grow in size the population density would change, and would influence the heat flux. That this is indeed the case is shown in Fig. 25, where the effect of nearby drops on the growth rate is presented. The ordinate D^2/t arises from the following:

The relation for spherical phase growth in an infinite medium where the process is governed by heat transfer, due to Scriven[67], as applied to the case of condensation is[33]

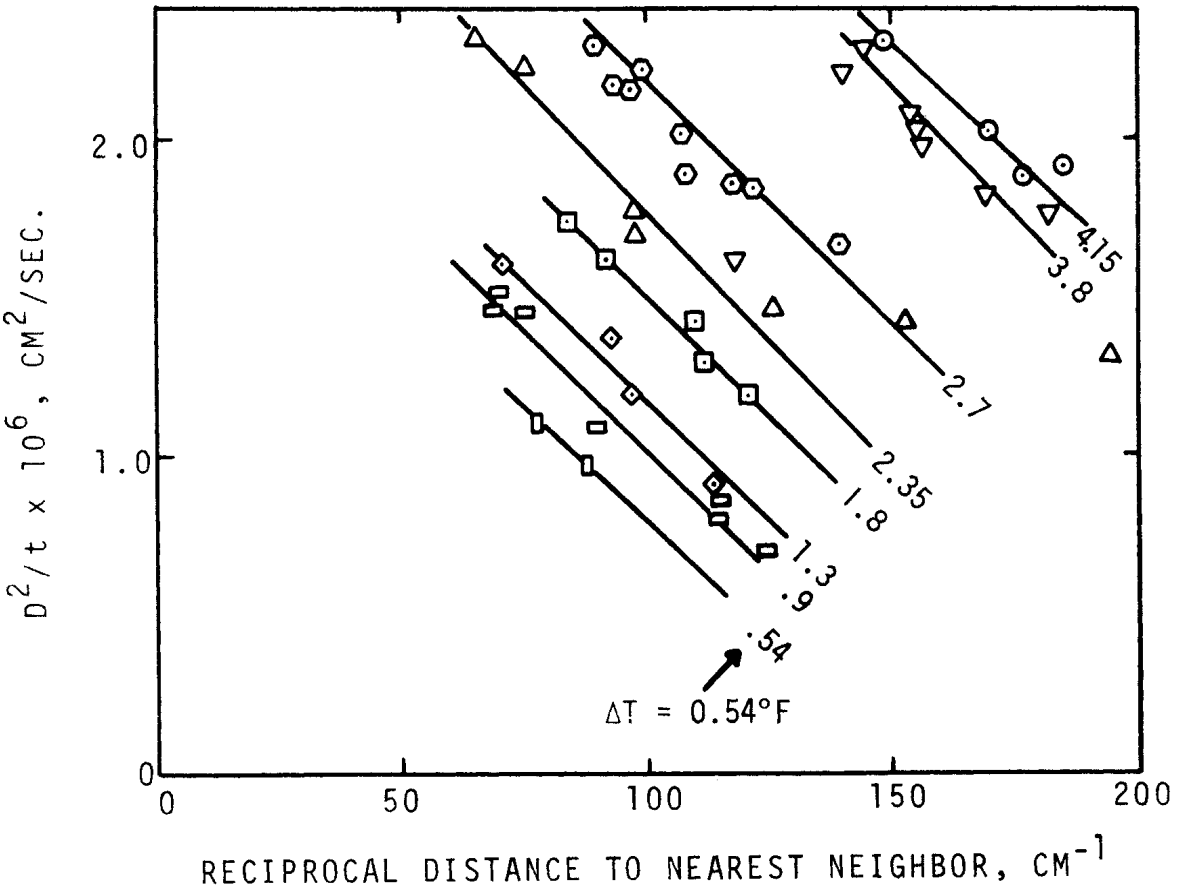

Figure 25. Effect of Nearby Drops on Drop Growth Rate.
P(water vapor) = 19mm Hg. (Ref. 33)

$$\frac{D^2}{t} = \frac{8 k_v}{\rho_\ell h_{fg}} (T_s - T_\infty) \tag{92}$$

where D is the drop diameter, and t is time. For a given subcooling ΔT_s = $(T_s - T_\infty)$ the left side of Eq. (92) should remain constant. This is not the case, as seen in Fig. 25; for a given subcooling the coefficient for the growth equation depends on the nearest neighbor distance, the smaller the spacing the lower is the growth rate. This effect is attributed to competition between drops for the same vapor. All of the results in Fig. 25 plus others at a different pressure were correlated by a single expression, given by (33)

$$G = \frac{D^2}{t} \left[\frac{T_s}{(0.79 + \Delta T)} \right] \frac{\rho_\ell}{\rho_v} \tag{93}$$

where G is a function of nearest neighbor spacing only, and is plotted in Fig. 26. As the spacing between drops decreases the growth rate and hence heat transfer rate associated with each drop decreases. Complicating the process further is the variation in drop sizes and coalescence when contact between adjacent drops occurs.

Figure 27 shows an example of measured drop size distributions for several population densities, and is compared with the maximum theoretical one. Each point represents drops counted in the size range $\pm$20 microns diameter. Note that as population density increases, it is chiefly in the small sizes, because coalescence then takes place with the larger sizes.

Any realistic model for representing dropwise condensation must take into account the population density, size distribution, and the related mechanism for removal of the droplet from the surface, which will influence the maximum possible size. The influence of the size distribution and maximum droplet size was studied theoretically by means of a computer model (68). It is assumed

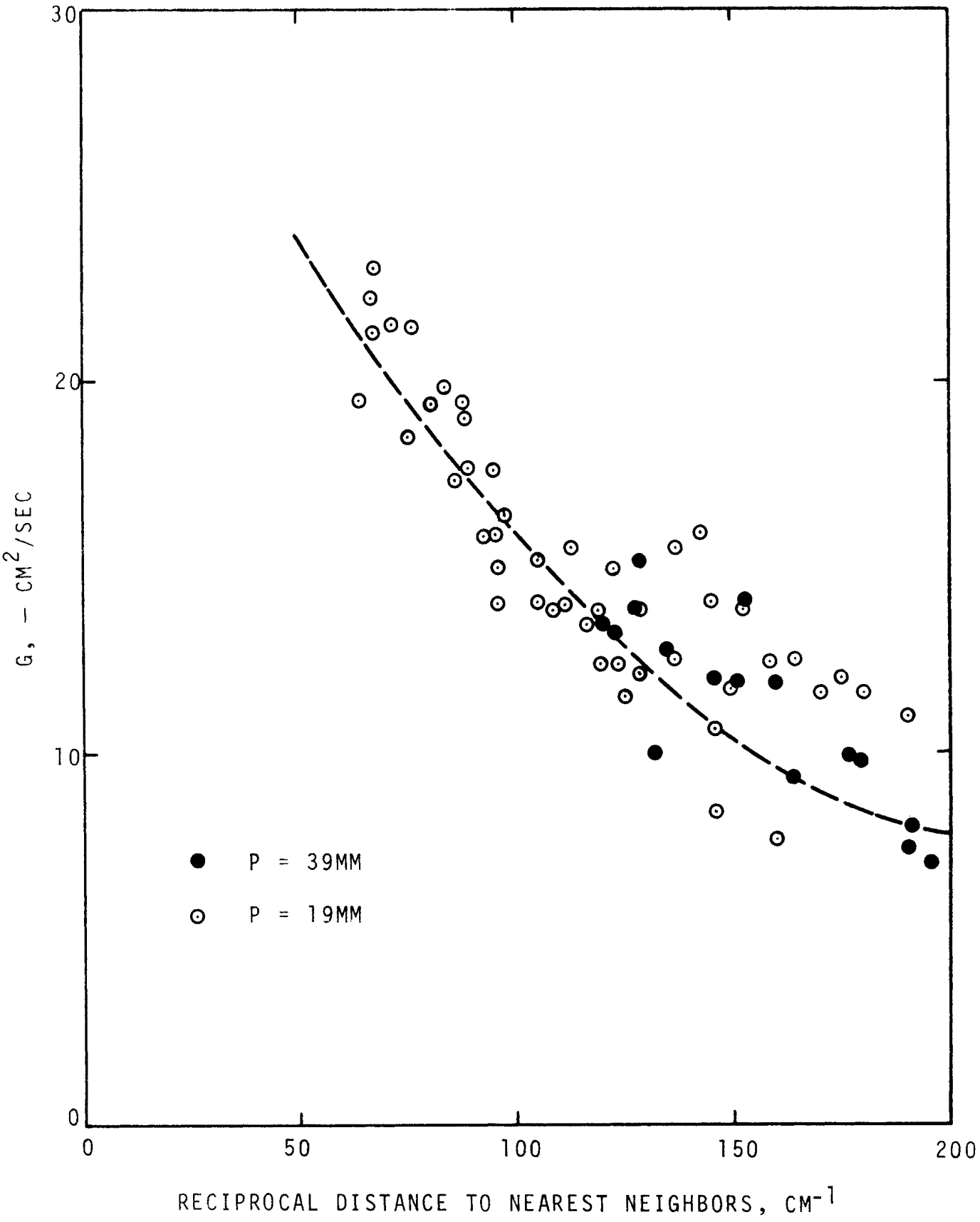

Figure 26. Correlation of Growth Rates of Condensation Water Drops on Copper Promoted by Benzyl Mercaptan. (Ref. 33)

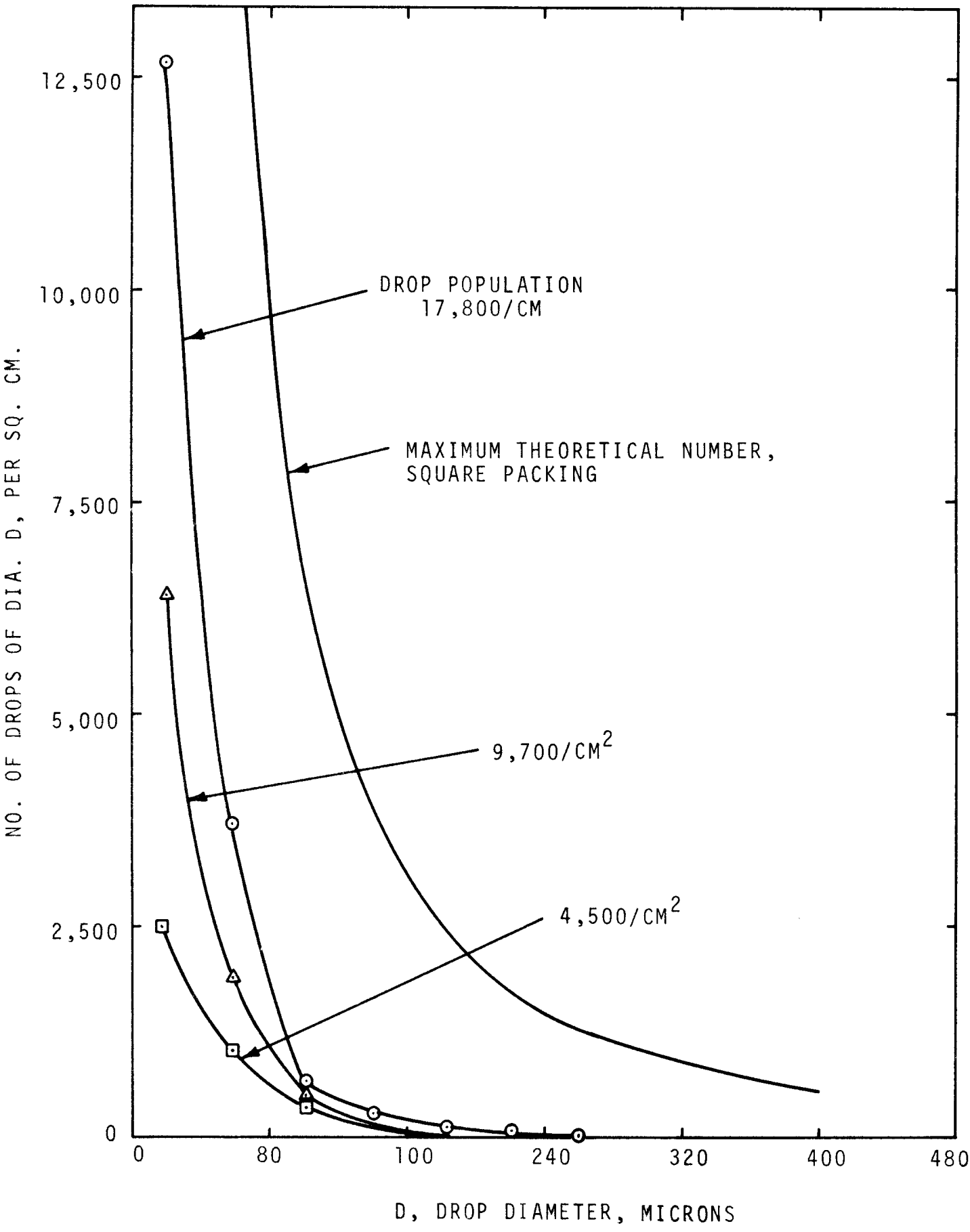

Figure 27. Average Condensation Water Drop Distribution for Maximum Diameters Between 500-3000 Microns. (Ref. 33)

that condensation occurs only on the drops, and the rate is limited by conduction through the drop. It is similar to the work in Ref. 21 except that now a random distribution of sizes and various states of crowding are permitted. The drops grow by condensation and coalescence when contact between adjacent drops occur, and the drops are removed when some arbitrary maximum size is reached. The solution, giving a mean heat transfer coefficient as functions of site population density and maximum drop size, was carried out for the condensation of water vapor at atmospheric pressure, using a digital computer and a Monte Carlo technique. The result is shown in Fig. 28, in which R is the maximum permitted radius of a drop. Included is the range of heat transfer coefficients observed in experiments with steam at atmospheric pressure condensing on vertical surfaces. For large nucleation site densities the heat transfer coefficient is dependent only on the maximum permitted radius. For the small maximum radius (10^{-4}cm) and site densities greater than 10^8 sites/cm^2, the predicted heat transfer coefficients are at least ten times greater than have been actually observed. This implies that extremely large heat-transfer coefficients could be obtained if a mechanism for efficient removal of these drops from a condensor surface could be developed (68). To yield the heat transfer rates obtained in dropwise condensation experiments, Fig. 28 indicates that, according to the model, the nucleation site density must be greater than 5×10^4 sites/cm^2.

5. Correlations

In view of the above complexities it is surprising that any success in correlating experimental data is possible. Care must be exercised in applying particular correlations derived on the basis of experimental work to see that conditions of similarity are met.

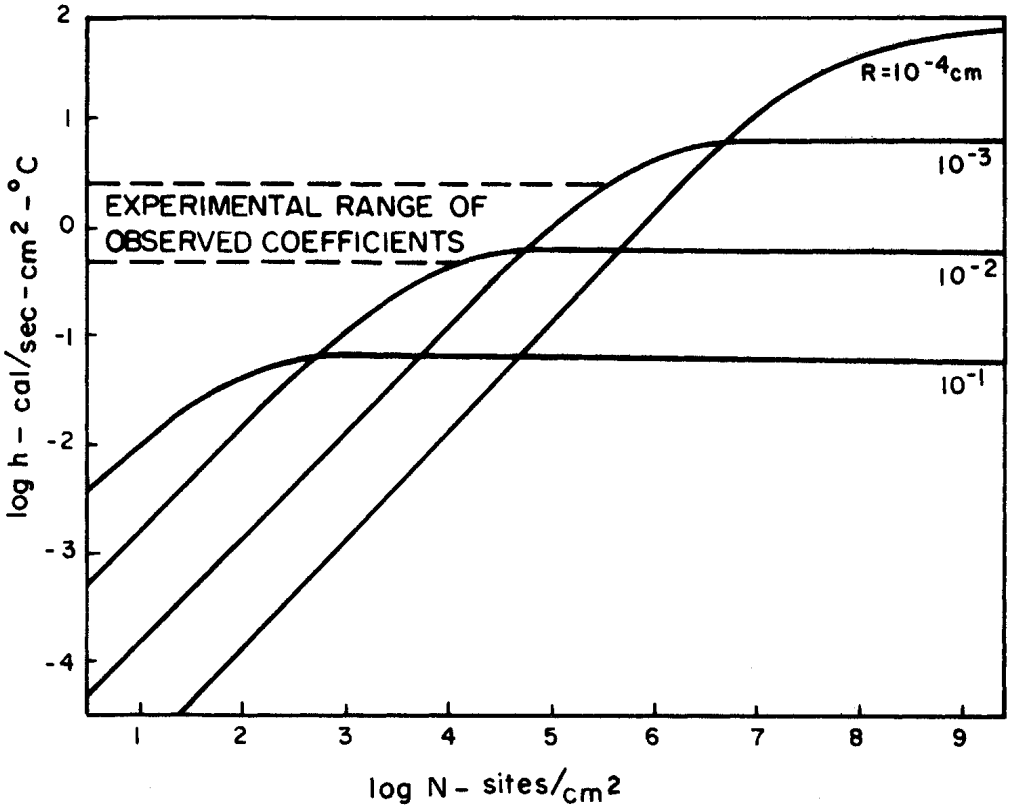

Figure 28. Theoretical Curves from a Computer Model Relating Heat Transfer Coefficient to Nucleation Site Density and Maximum Drop Size. (Ref. 68)

Using dimensional analysis to obtain the dimensionless parameters and experimental data for the functional relationship, the following correlations were obtained describing dropwise condensation of steam on vertical surfaces (69):

$$Nu = 1.6\times10^{-4}(Re)^{-0.84}(Pr)^{1/3}(\Pi_K)^{1.16} \qquad (94)$$

$$\text{for} \quad 8\times10^{-4} < Re < 3.3\times10^{-3}$$

$$Nu = 2.5\times10^{-6}(Re)^{-1.57}(Pr)^{1/3}(\Pi_K)^{1.16} \qquad (95)$$

where $\text{for} \quad 3.3\times10^{-3} < Re < 1.8\times10^{-2}$

$$Nu = \frac{2\sigma T_v h}{h_{fg}\rho_\ell k_\ell \Delta T_w} \quad ; \quad Pr = \left(\frac{\mu C_p}{k}\right)_\ell$$

$$Re = \frac{k_\ell \Delta T_w}{\mu_\ell h_{fg}} \quad ; \quad \Pi_K = \frac{2\sigma\left(\frac{d\sigma}{dT}\right)T_v}{h_{fg}\mu_\ell^2}$$

$$\Delta T_w = T_v - T_w$$

All physical properties are evaluated at the saturation temperature. Equations (94) and (95) are compared with independent data for steam in Fig. 29, with reasonable agreement at higher values of ΔT, corresponding to larger values of Re. These equations are also compared in Fig. 30 with data for dropwise condensation of Ethylene Glycol at various pressures on a copper surface promoted with oleic acid. Because of the deviation at low values of Re, a modification to these equations has been suggested (32) as:

$$Nu = 1.46\times10^{-6}(Re)^{-1.63}(Pr)^{1/2}(\Pi_K)^{1.16} \qquad (96)$$

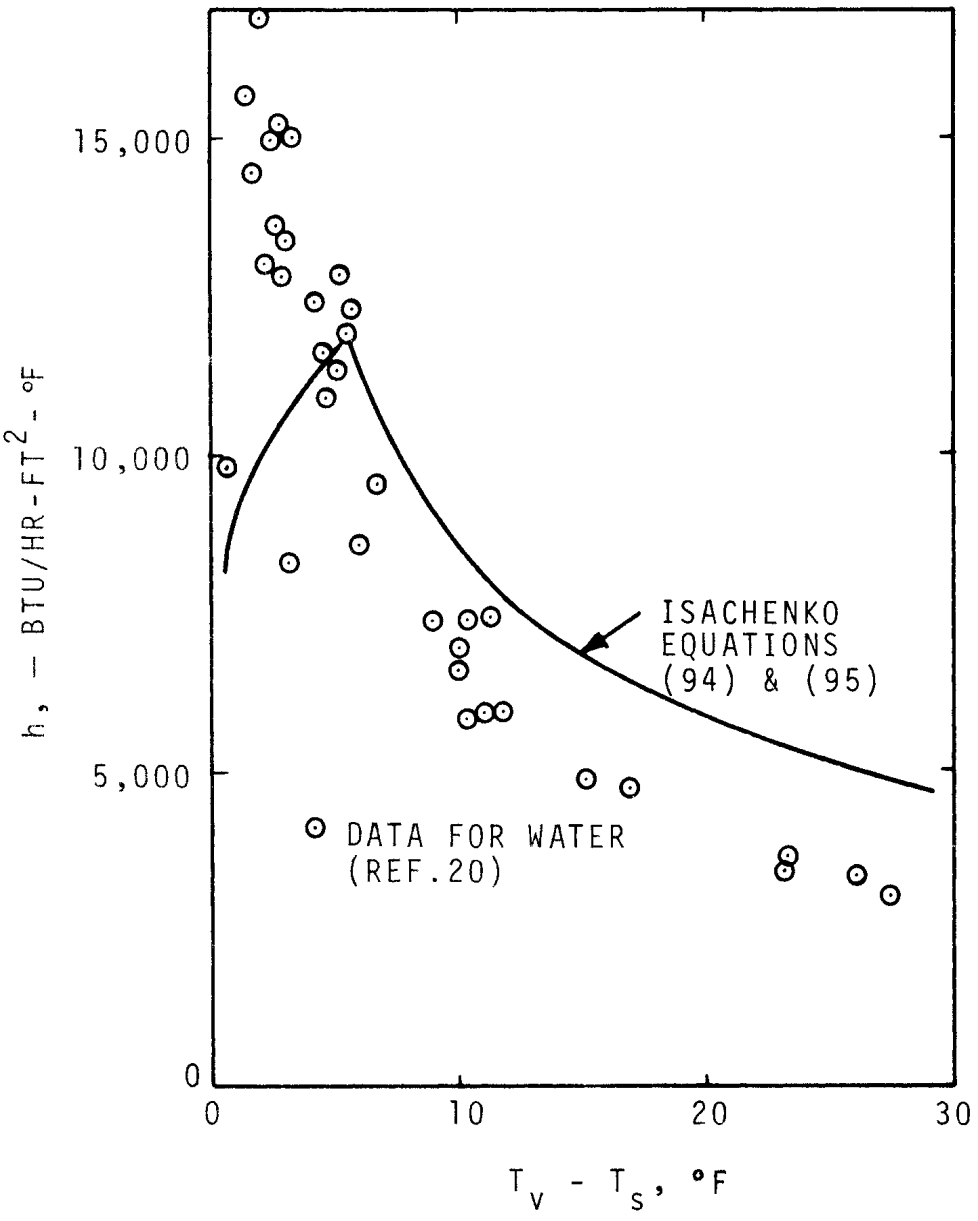

Figure 29. Comparison of Condensation Heat Transfer Coefficients from Correlation with Independent Data for Steam. (Ref. 33)

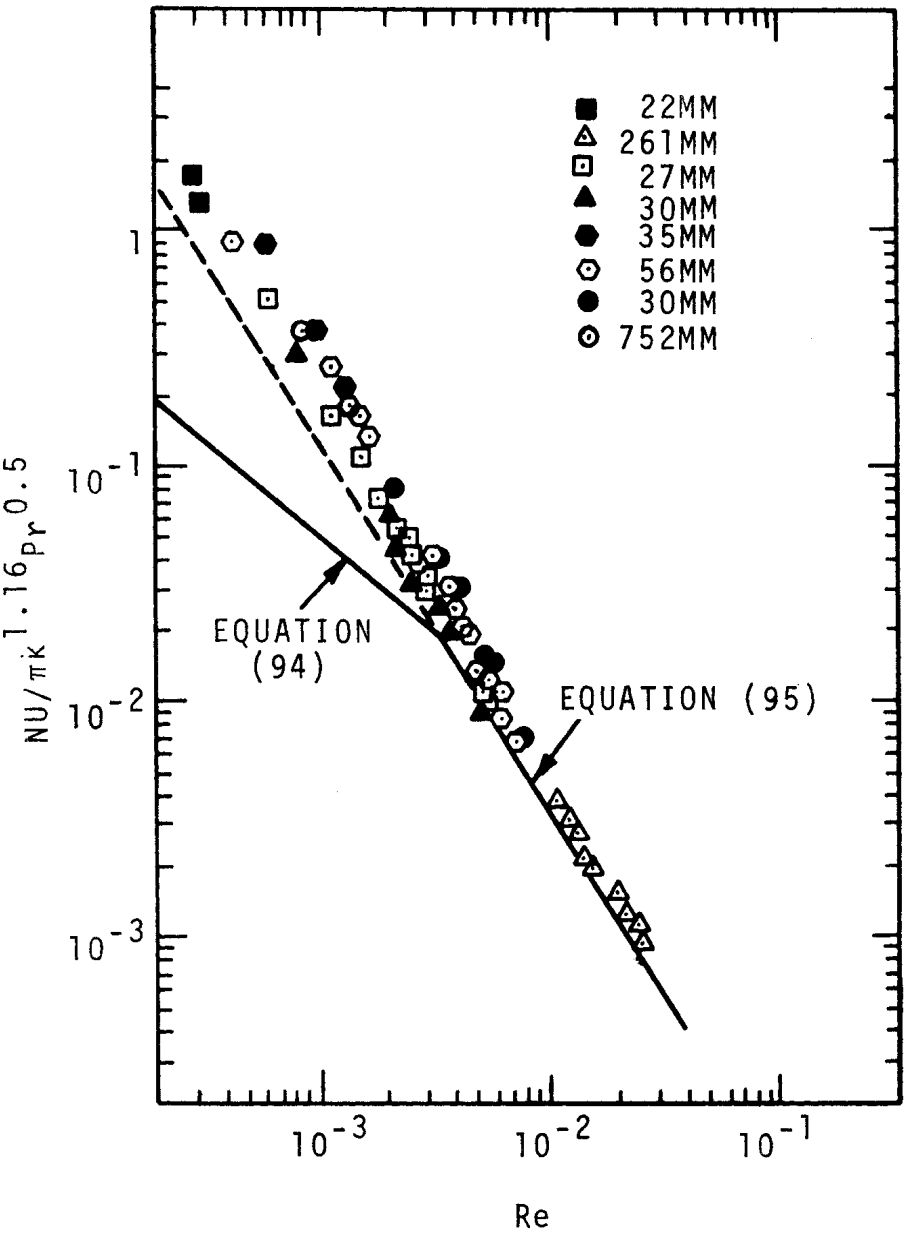

Figure 30. Comparison of Correlation for Dropwise Condensation with Independent Data for Ethylene Glycon. (Ref. 32)

This covers a range of P_r from 1.65 to 23.6, and π_k varies from 7.8×10^{-4} to 2.65×10^{-2}. Equation (96) is plotted in Fig. 31 and compared with data for both steam and ethylene glycol.

Fatica and Katz[21] derived a quantitative expression for the heat transfer coefficient with dropwise condensation based on the heat transfer being conduction limited through the drop, and with uniform drop size and uniform distribution. The application of the equation, however, requires the experimental determination of a number of quantities; the fractional area covered by the drops, the receding, average and advancing contact angles, and the overall heat transfer coefficient through the bare areas between the drops. The necessity for this latter quantity results in limited usefulness of the equation. Another analysis for dropwise condensation had been begun[70] where the heat transfer is also conduction limited by the drop, but it requires additional work.

A further analysis considers the conduction through the drops[35], but takes into account the effect of surface tension on the temperature on either side of the liquid-vapor interface, plus the interfacial temperature difference. A distribution of drop sizes is assumed and adjusted to fit experimental data of heat transfer rates by means of an arbitrary coefficient. Five parameters must be specified, which may make the specific application of the correlation difficult. The various parameters are quite lengthy, and the reader is referred to Ref. 35.

An analysis of dropwise condensation of liquid metals assumes that the unwetted portions of the heat transfer surface do not participate in the heat and mass transfer[71]. The temperature distributions in the drop and wall are calculated with an analog computer, assuming that the heat of condensation is given up at the drop surface. The solution appears to require at least

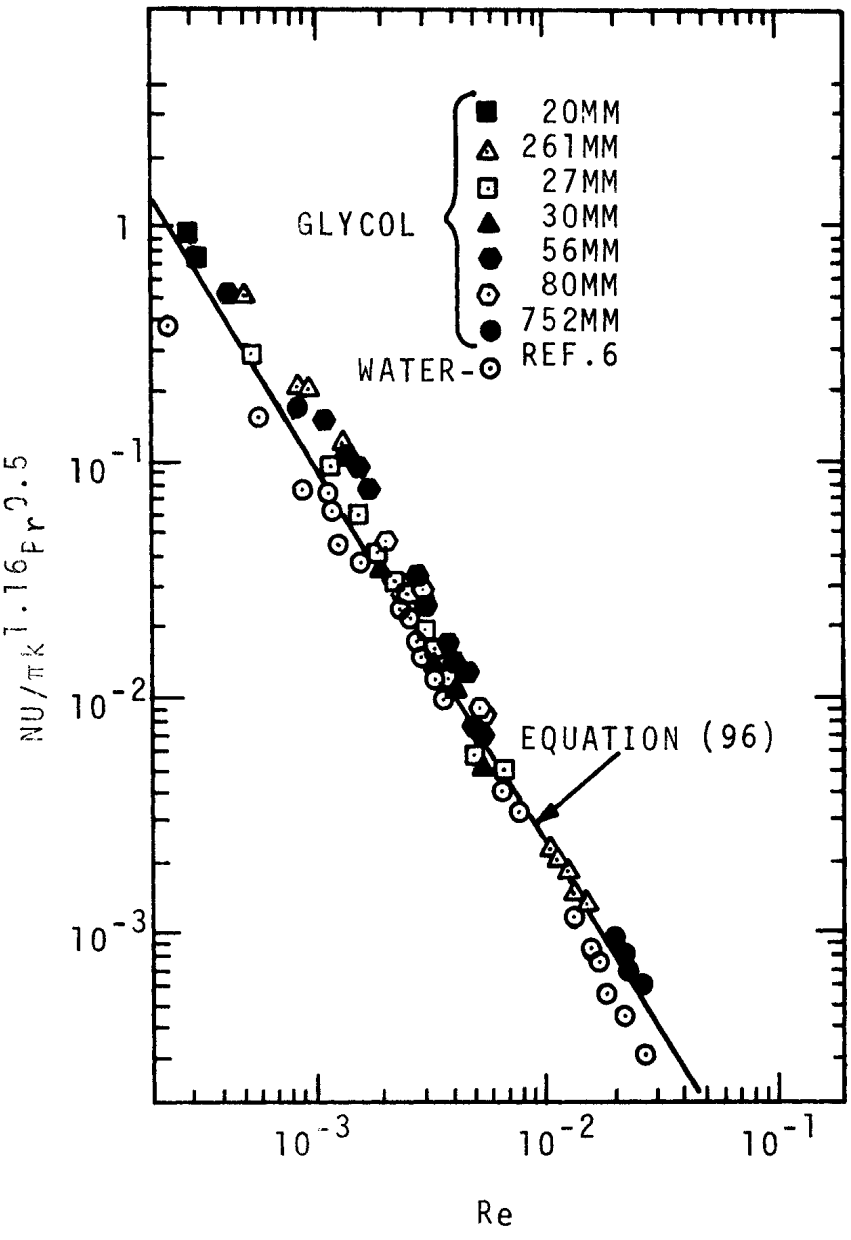

Figure 31. Improved Correlation for Dropwise Condensation on Vertical Surfaces. (Ref. 32)

one empirical constant for a system, and a mean drop diameter and the fractional coverage of the surface by the drops.

The assumption of a quasi-steady temperature distribution in a condensation drop permits an analytic solution for the drop growth rate, given by[19];

$$\frac{dr}{dt} = \frac{k_\ell (T_v - T_s)}{\rho_\ell h_{fg} r} \sum_{\substack{m=1 \\ odd}}^{\infty} \frac{m(2m+1)}{1 + \frac{k_\ell}{h_e r} m} \left[\int_0^1 P_m(x)\, dx \right]^2 \qquad (97)$$

where Pm are Legendre polynomials of the first kind. Comparison with a particular set of experimental data is shown in Fig. 32. The slow rate of growth might be noted, and is a consequence of the very low pressure used; 0.363 lbf/in^2. Whether such good comparison would arise under more dynamic conditions is open to question.

Using Eq. (97) and a model similar to that described in Ref. (71), an expression was derived for the overall heat transfer coefficient with dropwise condensation[66] :

$$\frac{1}{h} = \frac{1}{4\pi k_\ell} \left[\sum_j \left(\frac{r_j}{1 + (2k_\ell / h_i r_j)} \right) \cdot \frac{1}{A} \right]^{-1} + \frac{f^2}{(1-f)^2} \frac{(1 - f^{1/2})^{3/2}}{3.7 k_w} \left[\left(\sum_k r_k \right) \cdot \frac{1}{A} \right]^{-1} \qquad (98)$$

r_j are the radii of the active or growing drops, r_k are the radii of the non-active drops, and h_i is the interfacial heat-transfer coefficient at the surface of the drop.

As a result of their experimental observations Sugawara[31] concludes that the heat transfer in condensation takes place between as well as on the drops, forming a thin film which then fractures to form drops when a critical thickness is reached. To predict the rate of growth of this film, hence the heat transfer rate, requires the solution of two coupled one-dimensional

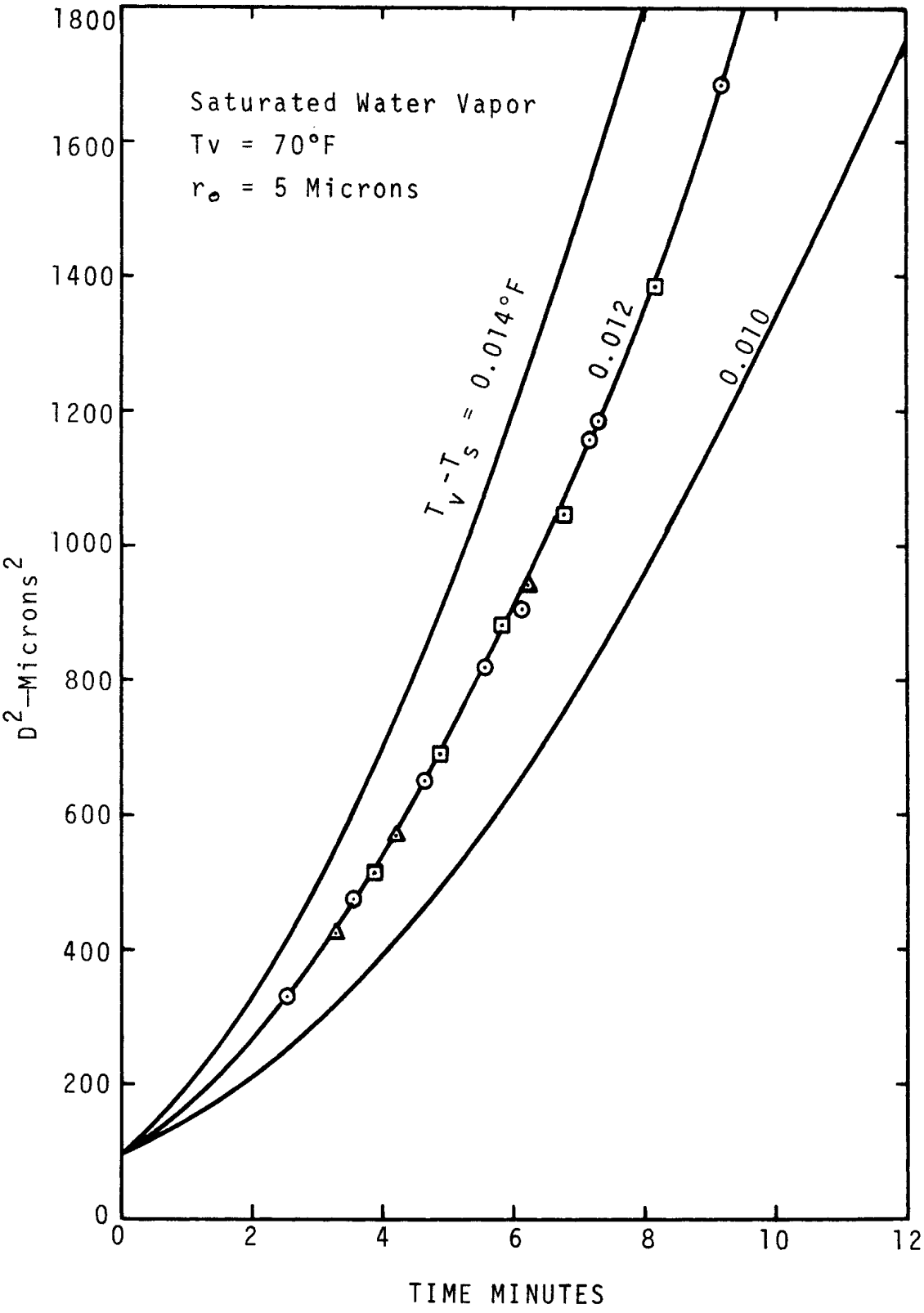

Figure 32. Comparison of Steam Condensation Drop Growth with Quasi-Steady Predictions. (Ref. 19)

transient conduction equations; one for the thin film and the other for the semi-infinite vapor domain. The sample calculations, shown in Fig. 33, appear to consider only the heat transfer between drops. When compared with experiments the ratio of $h_{exp}/h_{computed}$ decreases as ΔT increases, most likely because of the decrease of average area of contact between the vapor and the condensing metal surface, i.e., the bubbles appear to act as thermal insulators in this model. An improvement might be to combine the heat transfer between the drops and the heat transfer through the drops, as in Ref. (21) or (70), and then prorate the contribution of each to the total heat flux on the basis of a fractional coverage of the surface area.

6. Effect of vapor velocity

In one research the velocity of condensing steam, at atmospheric pressure, was varied as it swept past the vertical surface, copper promoted with cupric oleate[72]. The results are shown in Fig. 34, and appear to indicate that there exists some critical velocity. The velocity is the mean between inlet and exit, and varies across the plate because of the condensation taking place. From the behavior of the heat transfer coefficient, decreasing as ΔT_s increases, it appears that non-condensables were present and exerted considerable influence. The non-condensables were measured and given as 0.0036%, a seemingly insignificant amount. However, because of the condensing process, the migration of the vapor molecules toward the condensing surface will "drag" gas molecules along and cause them to become concentrated at the surface, as has been shown experimentally in Ref. 36, resulting in an increased thermal resistance. In another experimental work with a vertical surface[48] it was observed that steam velocity had a marked effect on ΔT at high heat fluxes, but very little effect at low fluxes.

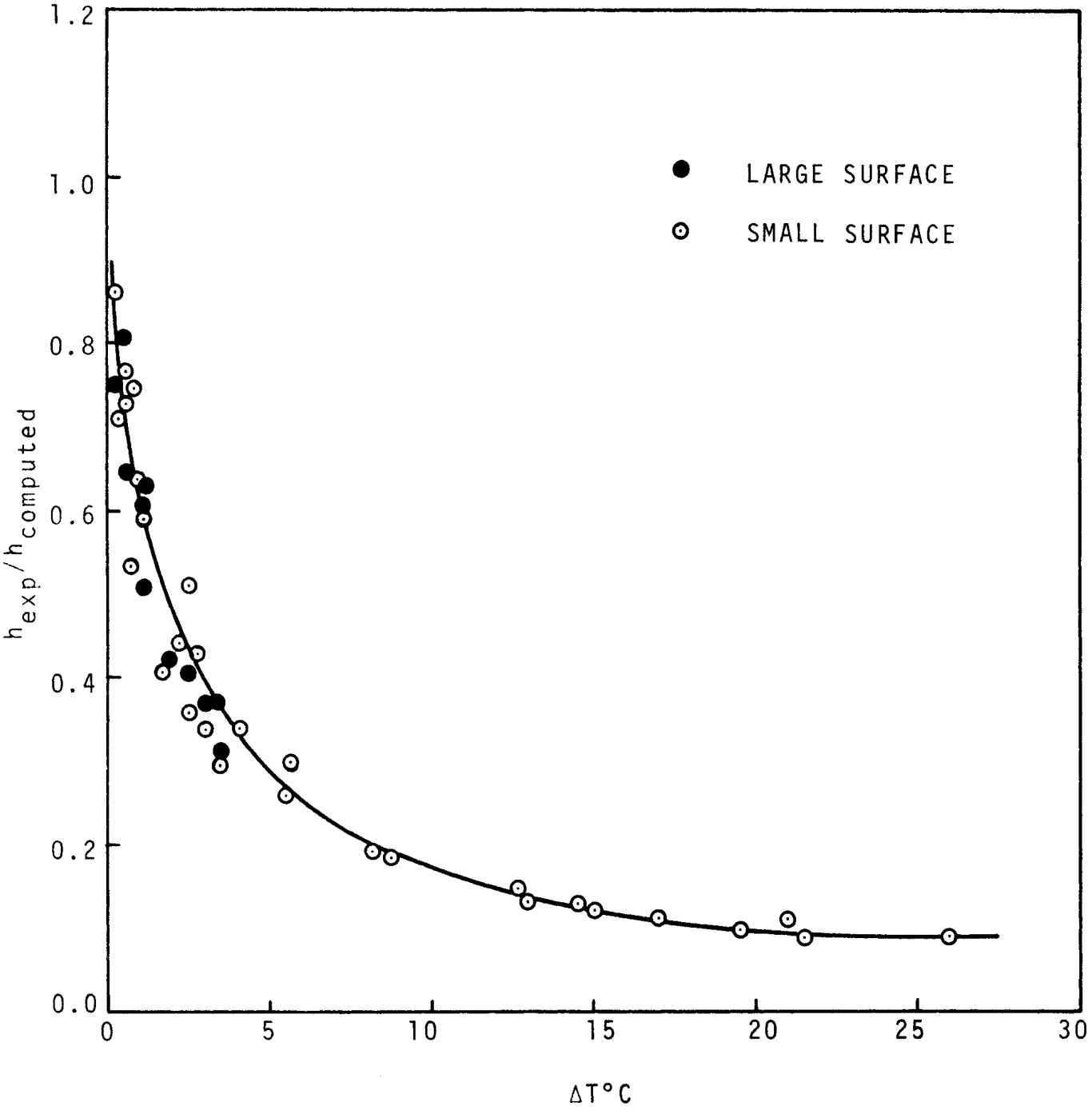

Figure 33. Comparison of Calculated and Experimental Values of Condensation Heat Transfer Coefficient. (Ref. 31)

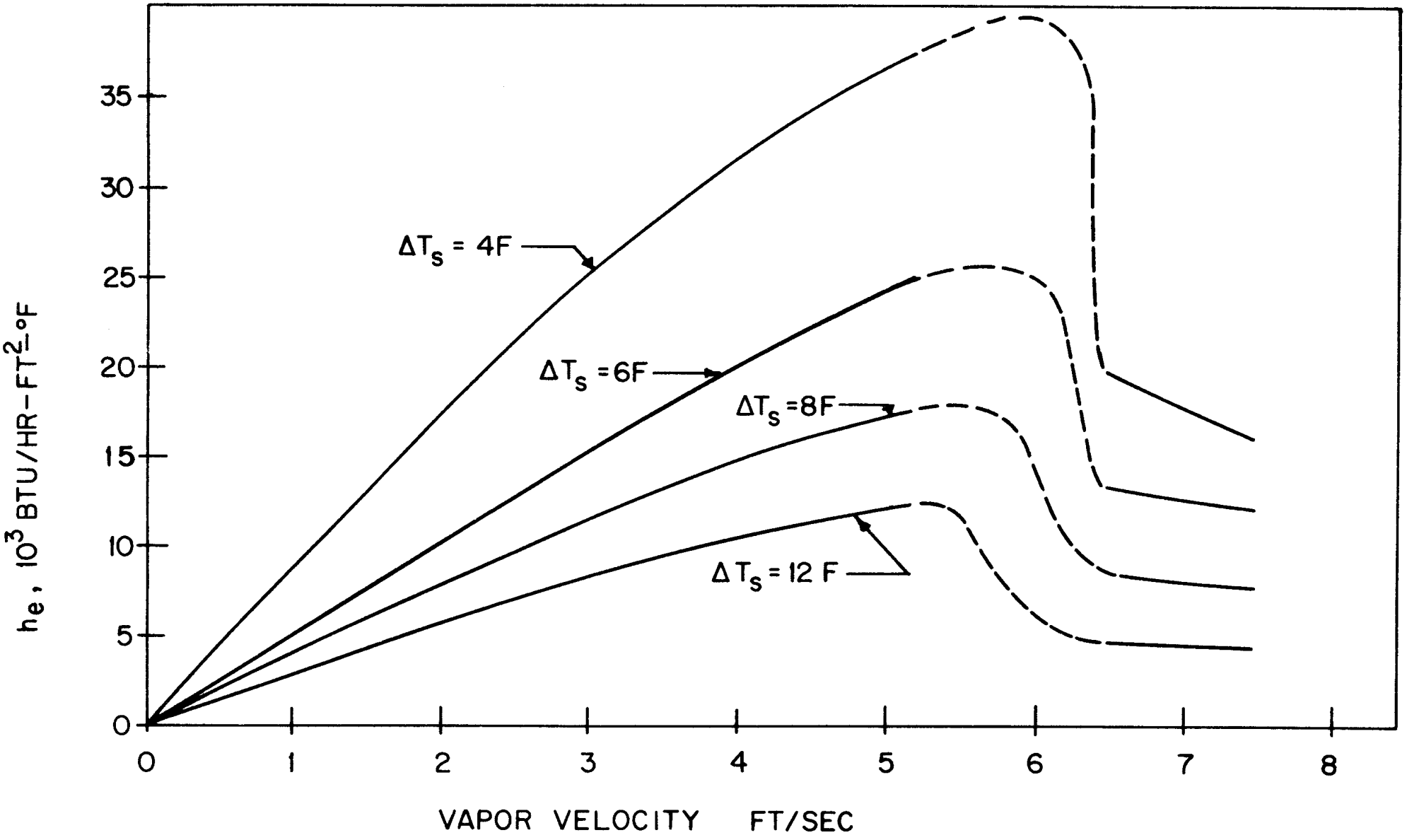

Figure 34. Effect of Mean Vapor Velocity on Dropwise Condensation. (Ref. 72)

An interesting experimental study was conducted to determine the influence of centrifugal acceleration on dropwise condensation[73]. A 6-inch vertical copper cylinder, on which dropwise condensation of steam took place on the outside, was rotated to produce 48 g's. Cooling water was circulated on the inside of the cylinder,and because of instrumentation limitations it was possible to measure only the overall heat transfer coefficient, which decreased as acceleration increased. If the inside single phase coefficient remains constant or increases with acceleration, as appears reasonable, then the outside dropwise condensation coefficient must decrease with increasing acceleration. It is believed that the shearing action of the vapor on the drops inhibited their early removal by centrifugal action and elongated them such as to effectively further insulate the surface.

C. Film Condensation

1. Classical Derivation

The theory of laminar film condensation on vertical and inclined surfaces was first formulated by Nusselt[44]. Improvements have been made over the years, but excepting the behavior with liquid metals, the original theory has been reasonably successful. The formulation of this pioneer work will be reviewed briefly here since it serves as the basis for many subsequent theoretical efforts.

Figure 35 shows the model and notation followed. The downward flow of the film under the action of gravity is laminar, and all fluid properties are considered constant. If the vapor is stagnant or has low velocities, shear stresses at the liquid-vapor interface may be reasonably neglected, and if the film is presumed to be thin then momentum effects in the liquid may also be neglected. Thus, as far as forces are concerned it is necessary only to consider equilibrium between the gravity and viscous forces in the liquid film. Applying the momentum equation to the control volume dx shown shaded in Fig. 35;

$$(\delta - y)(\rho_\ell - \rho_v) g \sin\theta = \mu_\ell \left(\frac{du}{dy}\right)_y \tag{99}$$

Integrating Eq. (99) from y = 0 to y = δ, with boundary conditions u = 0 at y = 0, gives the velocity profile in the film at any position x;

$$u(y) = \frac{g \sin\theta (\rho_\ell - \rho_v)}{\mu_\ell} \left(\delta y - \frac{y^2}{2}\right) \tag{100}$$

u depends on x only insofar as δ depends on x. The mean velocity in the film is given by;

$$\bar{u} = \frac{g \sin\theta (\rho_\ell - \rho_v)}{\mu_\ell} \frac{\delta^2}{3} \tag{101}$$

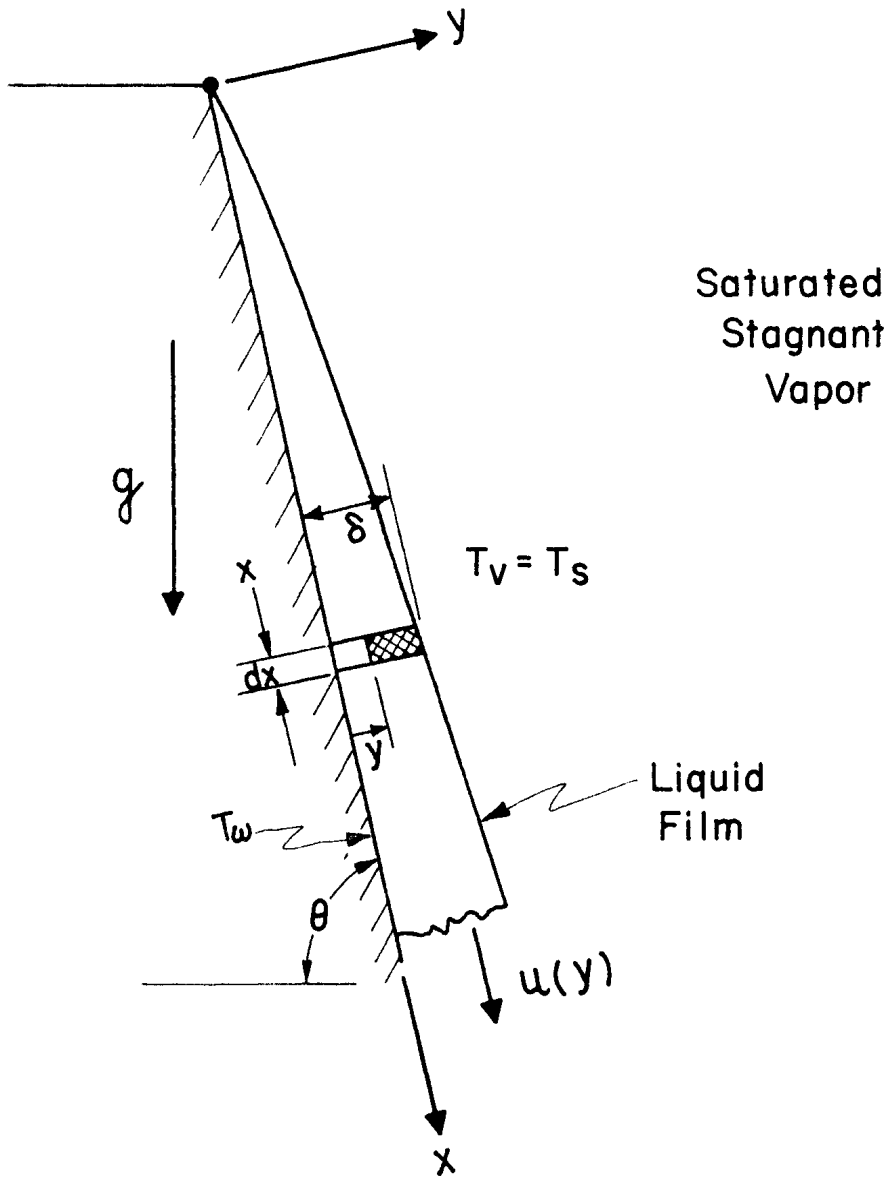

Figure 35. Physical Model for Film Condensation.

and the velocity at the liquid-vapor interface is $u(\delta) = 1.5\ \bar{u}$.

Neglecting the convective heat transfer in the liquid film, which would take place in the x-direction, only conduction in the y direction remains, described by;

$$\frac{d^2T}{dy^2} = 0 \tag{102}$$

with boundary conditions

$$T(y=0) = T_w$$

$$T(y=\delta) = T_s$$

It is here that the interfacial temperature drop is neglected, in considering that $T(y = \delta) = T_s$. Using Fourier's equation which relates the heat flux to the temperature distribution,

$$q/A = -k \frac{dT}{dy} \tag{103}$$

Equation (102) gives a linear temperature distribution which can be put in the form;

$$q/A = \frac{k_\ell (T_s - T_w)}{\delta} \tag{104}$$

The heat transfer coefficient is defined by

$$h = \frac{q/A}{T_s - T_w} = \frac{k_\ell}{\delta} \tag{105}$$

To obtain the as yet unknown thickness $\delta(x)$, the conservation of mass principle is applied, which states that any increase in the mass flow of the film must come from condensation at the liquid-vapor interface, which is related to the heat transfer rate. Let the condensate film flow rate per unit width of the wall be;

$$w = \rho_\ell \bar{u} \delta \tag{106}$$

then, from the energy equation

$$\frac{d w}{d x} = \rho_\ell \frac{d}{dx}(\bar{u}\,\delta) = \frac{q/A}{h_{fg}} = \frac{k_\ell (T_s - T_w)}{\delta\, h_{fg}} \tag{107}$$

Substituting $\bar{u}$ from Eq. (101) into Eq. (107), a differential equation in δ results;

$$\delta^3 d\delta = \frac{k_\ell (T_s - T_w)\,\mu_\ell}{\rho_\ell(\rho_\ell - \rho_v) g \sin\theta\, h_{fg}}\, dx \tag{108}$$

Assuming that condensation begins at x = 0, δ = 0 and Eq. (108) integrates to;

$$\delta(x) = \left[\frac{4 k_\ell (T_s - T_w)\,\mu_\ell\, x}{\rho_\ell(\rho_\ell - \rho_v) g \sin\theta\, h_{fg}}\right]^{1/4} \tag{109}$$

Substituting Eq. (109) into Eq. (105) gives the local heat transfer coefficient;

$$h_x = \left[\frac{k_\ell^3 \rho_\ell(\rho_\ell - \rho_v) g \sin\theta\, h_{fg}}{4 (T_s - T_w)\mu_\ell\, x}\right]^{1/4} \tag{110}$$

One notes that the heat transfer coefficient decreases as x increases, because of thickening of the liquid film. The mean heat transfer coefficient over a length L is obtained by integrating Eq. (110);

$$h_m = \frac{1}{L}\int_0^L h_x\, dx = 0.943\left[\frac{k_\ell^3 \rho_\ell(\rho_\ell - \rho_v) g \sin\theta\, h_{fg}}{(T_s - T_w)\mu_\ell L}\right]^{1/4} \tag{111}$$

Defining a Nusselt number, Eq. (111) is expressed in dimensionless form as;

$$Nu_L = \frac{h_m L}{k_\ell} = 0.943\left[\frac{\rho_\ell(\rho_\ell - \rho_v) g \sin\theta\, h_{fg} L^3}{(T_s - T_w)\mu_\ell k_\ell}\right]^{1/4} \tag{112}$$

Defining a Reynolds number of the liquid film by

$$Re_L = \frac{4 w_L}{\mu_\ell} \tag{113}$$

where w_L is given by Eq. (106) at length x = L. Neglecting the subcooling in the liquid film, the energy equation gives, from Eqs. (105) and (107);

$$w_L h_{fg} = h_m (T_s - T_w) L \tag{114}$$

Substituting Eq. (114) into Eq. (113) for w_L, and then Eq. (111) into Eq. (113) for h_m, taking $\theta = 90°$, and for the state far removed from the critical point of the fluid such that $\rho_\ell \gg \rho_v$, we obtain for a vertical plate;

$$\frac{h_m}{k_\ell}\left(\frac{\nu_\ell^2}{g}\right)^{1/3} = 1.47\, Re_L^{-1/3} \tag{115}$$

where ν is the kinematic viscosity. Since $(\nu_\ell^2/g)^{1/3}$ has units of length, the left hand side of Eq. (115) could be interpreted as a Nusselt number.

2. Laminar Film Condensation

The accomplishments in laminar film condensation since the work of Nusselt will be subdivided into four groups, depending on the mechanism by which the liquid condensate film is set in motion and removed. The thickness of the film governs the heat transfer rate and this is in turn dependent on the driving force for liquid motion. The four driving forces are; gravity body forces, forced convection or vapor shearing action, rotational or centrifugal forces, and miscellaneous (magnetic, electrostatic, capillary) forces.

a. Gravity body force

The first modification to the Nusselt theory was to apply a correction to take into account the heat capacity of the liquid film[74]. The heat transfer at the wall is greater than the energy from the latent heat by the sub-cooling of the liquid film that takes place, it being saturated only at the liquid vapor interface. An approximation for the correction was developed and consists of replacing h_{fg} in Eqs. (107)-(112) by h'_{fg} as follows:

$$h'_{fg} = h_{fg}\left(1 + 0.4\,\frac{(T_s - T_w)\,C_p}{h_{fg}}\right) \tag{116}$$

This form of the correction applies for values of $(C_p \Delta T/h_{fg})$ up to about 3. This same form has been applied to account for superheating effects in film boiling[74].

An approximate analysis using an integral procedure, removing the restriction of neglecting the convection heat transfer[75], resulted in h_{fg} in Eqs. (107)-(112) being replaced by:

$$h''_{fg} = h_{fg}\left(1 + 0.68\,\frac{(T_s - T_w)C_p}{h_{fg}}\right) \qquad (117)$$

This is listed as being valid for $(C_p\ \Delta T/h_{fg})$ up to one.

The problem of film condensation on a vertical surface was formulated in terms of the boundary layer theory, and includes the influence of both convection and momentum in the liquid, but still neglects shear at the liquid-vapor interface[76]. The results are presented in Fig. 36, which show that for Pr $>$10 liquid momentum (acceleration terms) can be neglected. The momentum effects arise because of the necessity for accelerating the vapor in a direction parallel to the wall as it changes phase to liquid. Even for Pr=1, Fig. 36 indicates that the error due to neglecting acceleration will be less than 5%. For small Pr numbers, such as with liquid metals, the momentum of the vapor becomes important, as noted in Fig. 37. Also included is Nusselt's theory (neglecting momentum of the liquid film) in which the ordinate has a value of one, the dimensionless form of Eq. (110).

In a further work involving a boundary layer-type solution to the same problem, the shear forces at the liquid-vapor interface are taken into full account[77]. These result in induced motion in the vapor, which must come at the expense of momentum in the liquid. The liquid thus has a lower velocity when shear is acting, and the heat transfer coefficient should be somewhat smaller. That this indeed is the case for Pr=1 is seen in the solu-

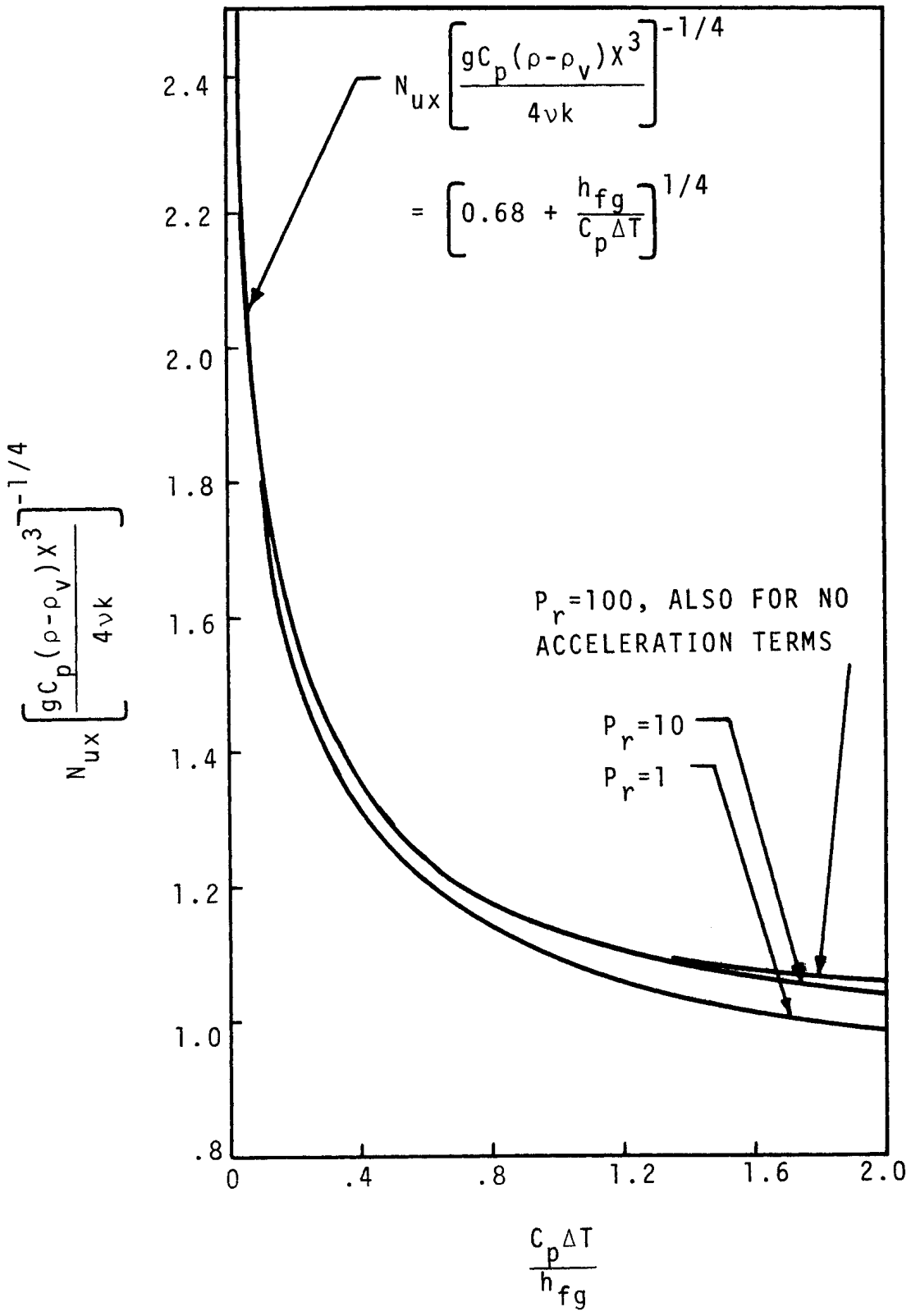

Figure 36. Local Heat Transfer from Solution of Complete Boundary Layer Equation. (Ref. 76)

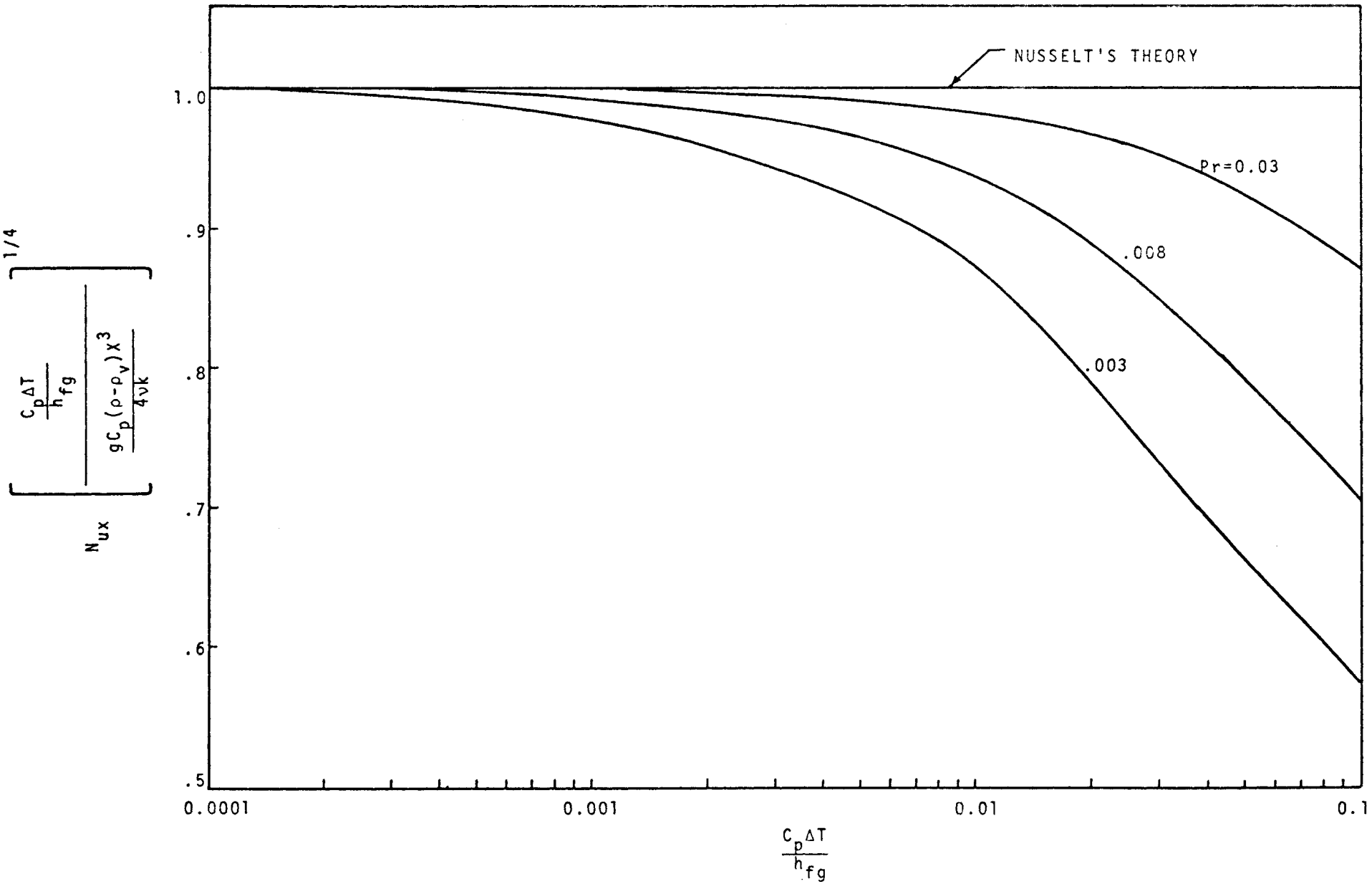

Figure 37. Local Heat Transfer for Low Pr Numbers from Solution of Complete Boundary Layer Equation. (Ref. 76)

tions plotted in Fig. 38, and in Fig. 39 for all of the low Pr number cases. For Pr $>$10 interfacial shear can be neglected, and even for Pr = 1, the effect is small. The dashed lines in both Figs. 38 and 39 correspond to the same results seen in Figs. 36 and 37, respectively. The ordinate = 1 in Fig. 39 again corresponds to the Nusselt theory, so considerable error would arise in applying it to liquid metals.

An independent solution was obtained for this same case, where momentum, convection and interfacial shear effects are retained, but using a perturbation scheme on a modified integral boundary layer equation[78]. The results appear similar to those in Ref. 77, except are presented as average values. Figure 40 presents results from Ref. 78, and for the ordinate value of one is the same as Eq. (112). In Fig. 41 comparison is made with the theoretical results neglecting interfacial shear[76] and with experimental data for condensing mercury[79]. It appears that further work, experimental as well as analytical, is needed to eliminate discrepancies. It is possible that thermal interfacial resistances are in part responsible for these discrepancies. An approximate working equation, valid within 1% for the results plotted in Fig. 40, is given as[78];

$$\frac{h_m}{h_{Nusselt}} = \left(\frac{1 + 0.68\beta + 0.02\,\beta\gamma}{1 + 0.85\beta - 0.15\,\beta\gamma}\right)^{1/4} \qquad (118)$$

where h_m is the mean heat transfer coefficient, and $h_{Nusselt}$ is the mean heat transfer coefficient as computed from the simple Nusselt theory Eq. (111), and

$$\beta = \left(\frac{c_p \Delta T}{h_{fg}}\right) \; ; \quad \gamma = \left(\frac{k_\ell \Delta T}{\mu_\ell h_{fg}}\right) \qquad (119)$$

The ranges of applicability of Eq. (118) are given by $\beta \leq 2$, $\gamma \leq 20$, and for liquids with Pr $>$ 1 or Pr $<$ 0.05.

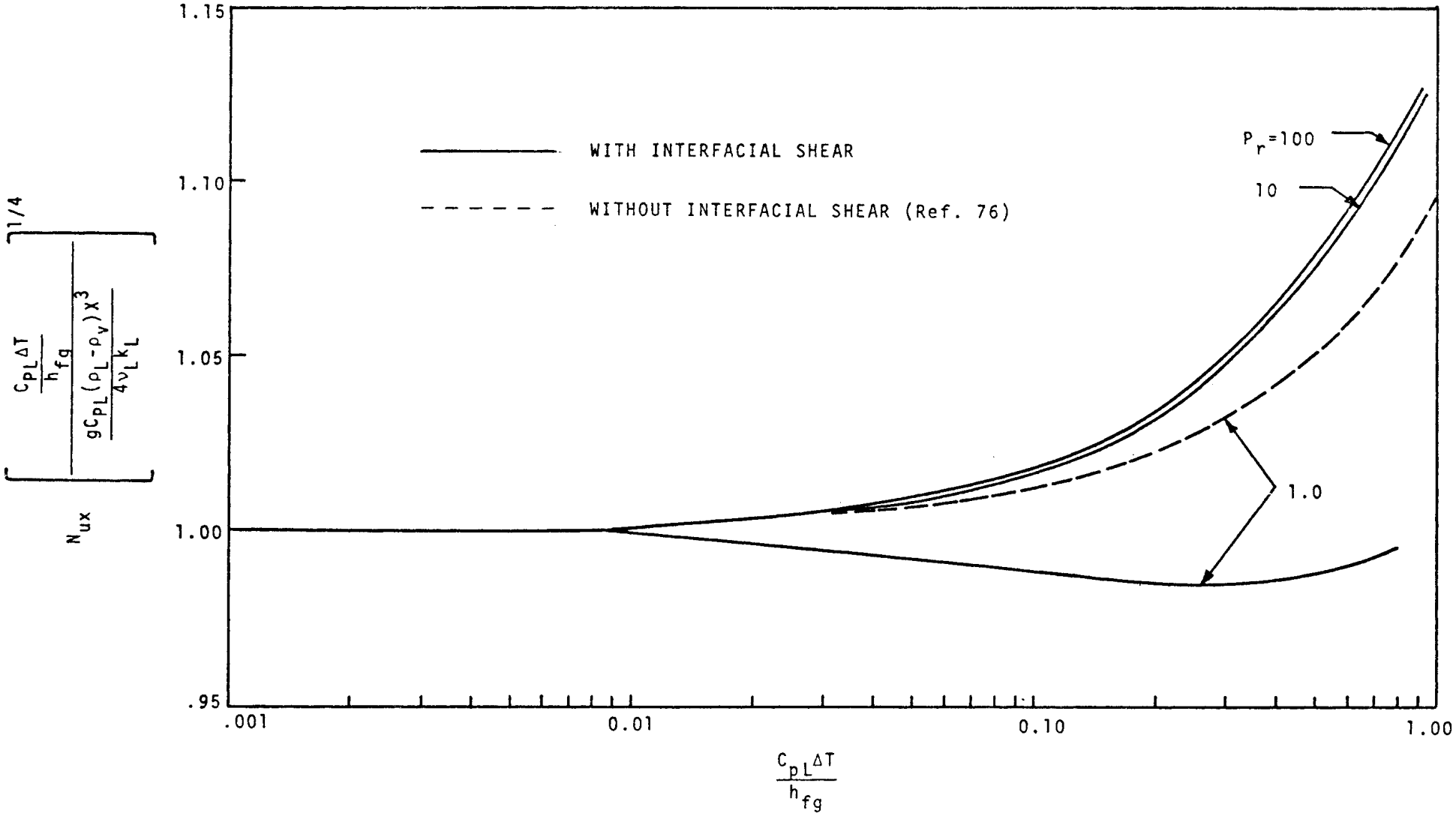

Figure 38. The Effect of Interfacial Shear Stress on Heat Transfer, Pr > 1. Laminar Film Condensation on Vertical Surface. (Ref. 77)

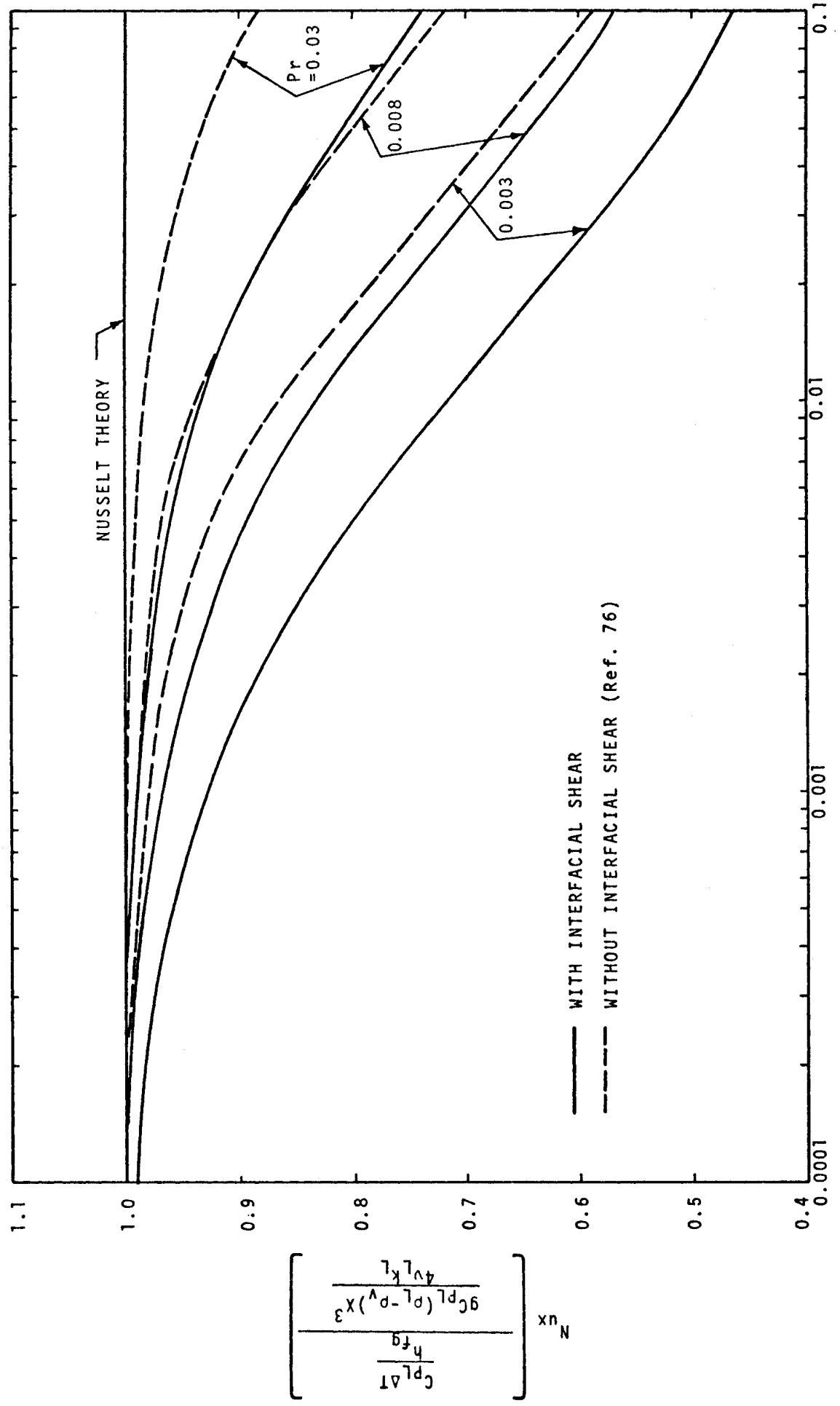

Figure 39. Effect of Interfacial Shear Stress on Heat Transfer, Liquid Metal Range. (Ref. 77)

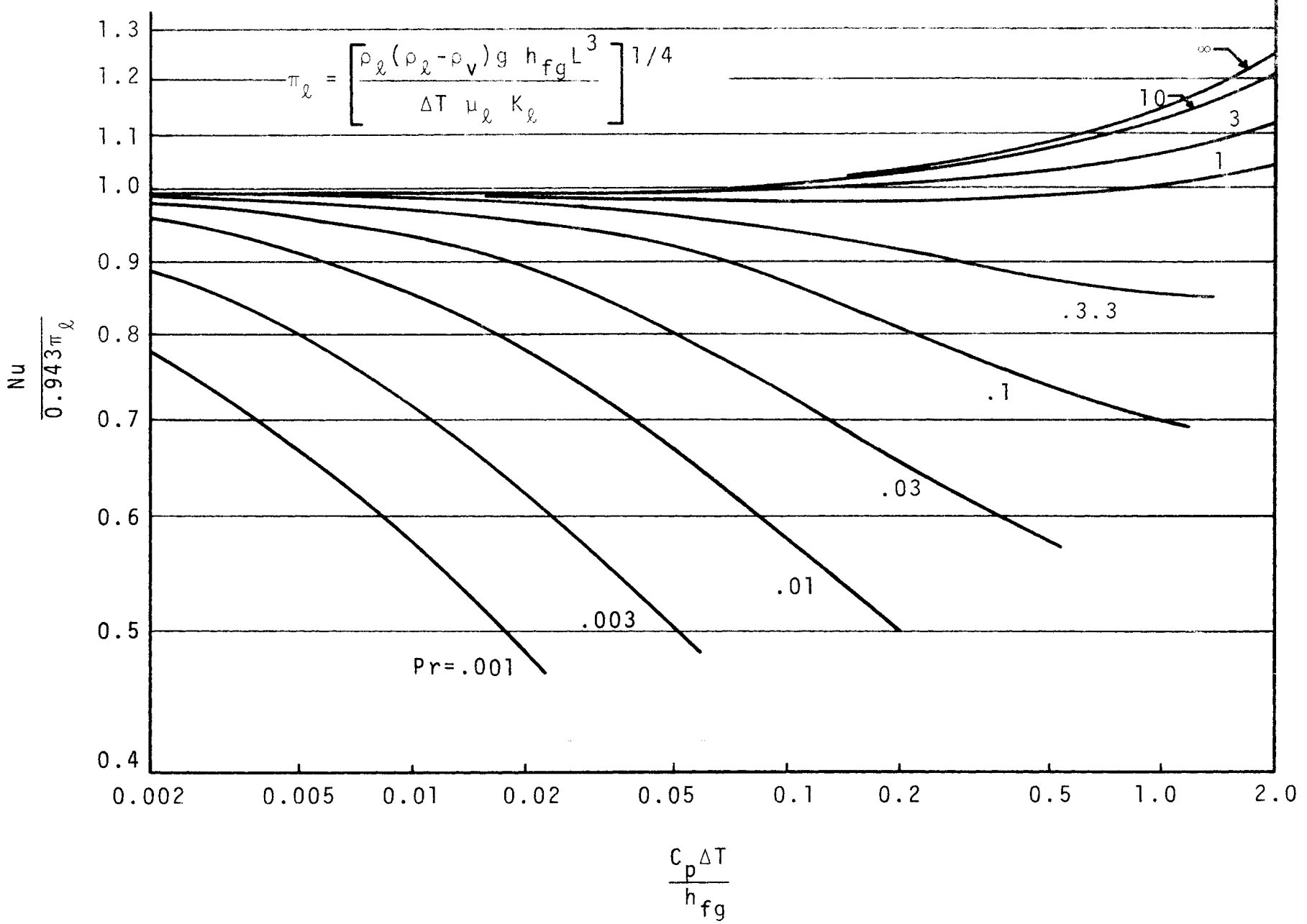

Figure 40. Theoretical Heat Transfer - Laminar Film Condensation on a Vertical Surface. (Ref. 78)

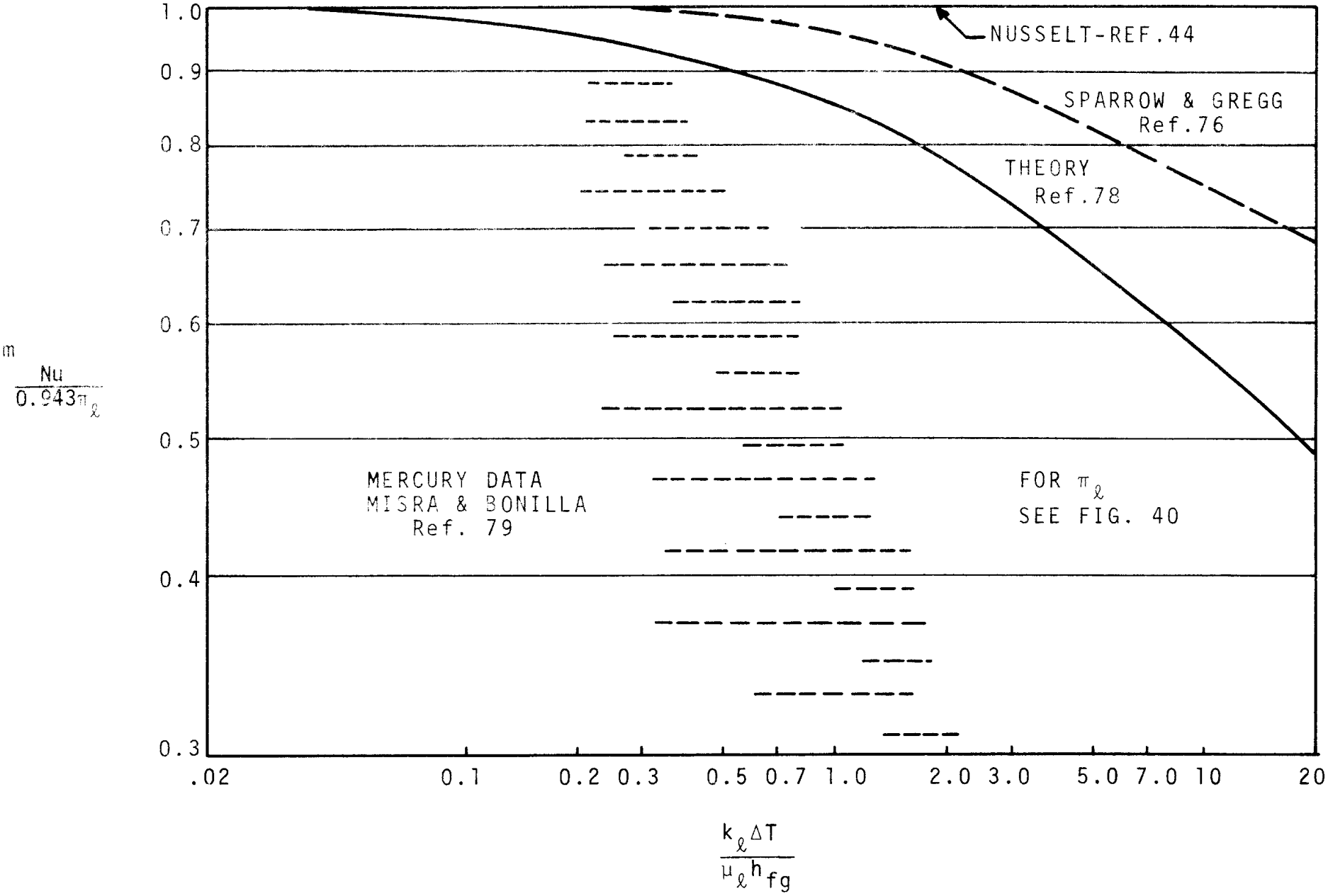

Figure 41. Comparison with Data and Theories for Liquid Metals. (Ref. 78)

Boundary layer-type analyses were also applied to film condensation on vertical surfaces to solve the problem for variable physical properties of the condensate, notably viscosity[80], and for the case where the plate is non-isothermal[81]. A similarity solution also was obtained for film condensation on a flat plate where the gravity field varied in a direction parallel to the plate[82]. Interfacial shear is neglected, and the gravity field must vary in a special way, given by:

$$g(x) = C_1 X^{C_2} \tag{120}$$

where C_1 and C_2 are constants. Another solution was obtained where the gravity field varied linearly[83].

Although experimental data for film condensation on horizontal tubes is quite extensive, that for vertical surfaces is relatively scarce. Four different sources reporting data obtained with steam are mentioned in Ref. 84, and which give heat transfer coefficients varying from 22 to 53% above that predicted by the Nusselt equation. More recent results with steam, both saturated and superheated[84], are plotted in Fig. 42. The fraction of coverage of the filled-in points indicates the fraction of superheat between 0-100°F. These results are considerably below that predicted by the Nusselt relation, and a distinct change in some mechanism occurs, as manifested by a knee in the data. Perhaps a departure something like a transition to turbulence occurs. Also interesting is the fact that at low Reynolds number the heat transfer coefficient remains constant.

The heat flux measured with film condensation of saturated n-Butyl alcohol vapor on a vertical surface[85] is plotted against the condensate film temperature drop in Fig. 43, and compares well with the Nusselt theory. A number of different computed curves are included which take into account

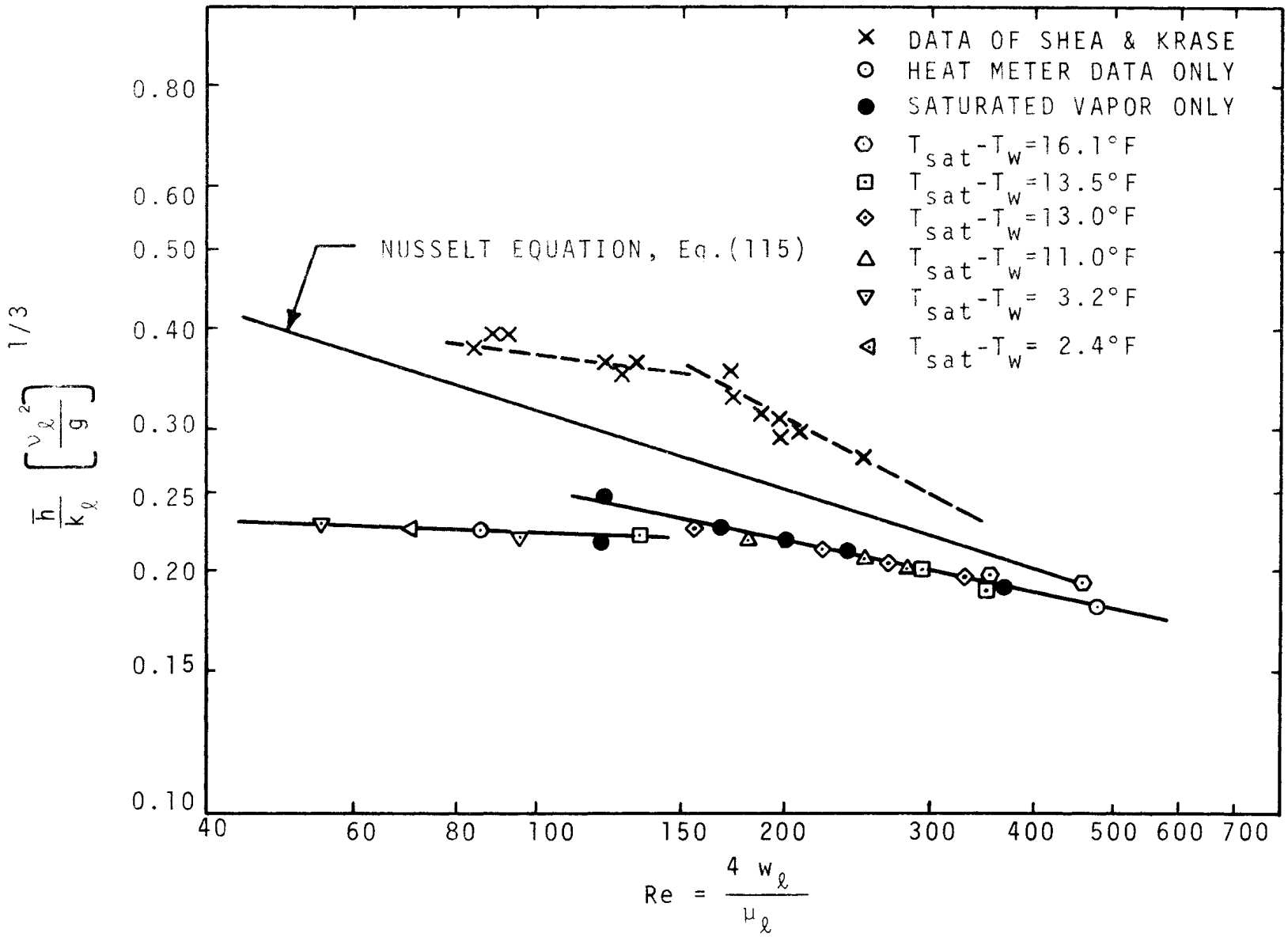

Figure 42. Experimental Data for Condensation of Saturated and Superheated Steam on a Vertical Surface. (Ref. 84)

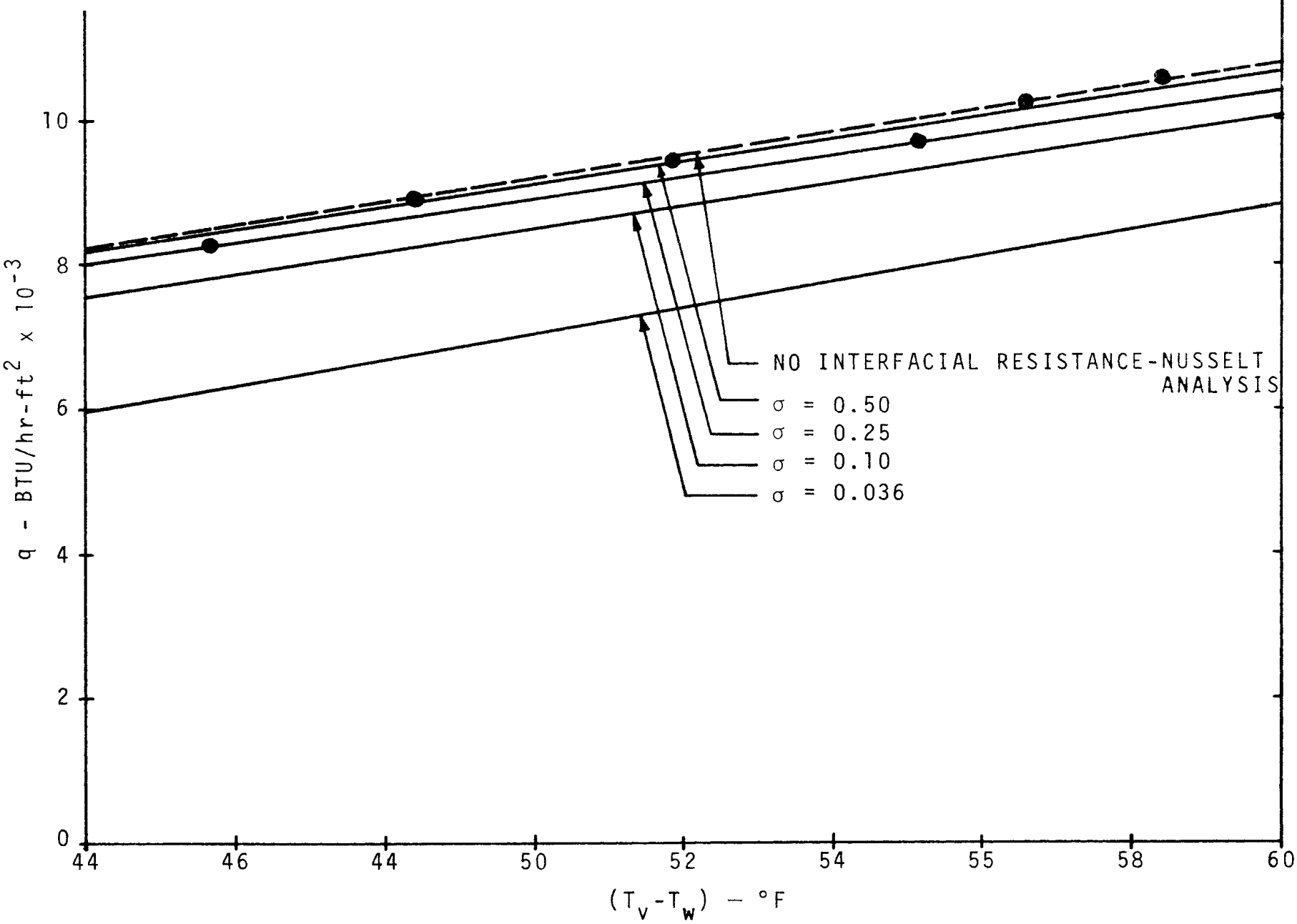

Figure 43. Heat Flux vs Temperature Difference for Film Condensation of Saturated n-Butyl Alcohol on a Vertical Surface. (Ref. 85)

different interfacial resistances associated with various values of the condensation coefficient. One can conclude from Fig. 43 only that the condensation coefficient lies in the range $0.25 < \sigma < 1.00$. It was found in this same research[85] that non-condensables were being created continuously and it was felt that some of the low values of condensation coefficients reported earlier for this class of material may be due to the presence of non-condensable gases.

Data obtained with film condensation of saturated potassium vapor on a vertical surface[42] was used, in conjunction with the Nusselt Eq. (111) for determining the liquid film temperature drop, to compute condensation coefficients from Eq. (76). These were shown earlier in Fig. 20 and compared well with the data of others. In another study of film condensation of liquid metals, the condensation heat transfer coefficient is computed from the kinetic theory, assuming $\sigma = 1$ and neglecting the thermal resistance of the liquid film[71]. Reasonably good comparison is shown with experimental data obtained for lithium, sodium, potassium and mercury.

Experimental data for vertical tubes, which should be similar in behavior to vertical flat plates if the tube diameter is much larger than the film thickness, is shown in Fig. 44 and compared with the Nusselt Eq. (115). The comparison is better if the coefficient is changed from 1.47 to 1.88 as recommended in Ref. 1.

Laminar film condensation on the underside of horizontal and inclined surfaces is treated analytically and experimentally in Ref. 86, and an approximate solution is given for film condensation on top of a horizontal cooled surface of finite width in terms of the liquid film thickness at the edge[87]. This is similar, phenomenologically, to film boiling on the underside of a horizontal surface of finite width, treated in Ref. 88.

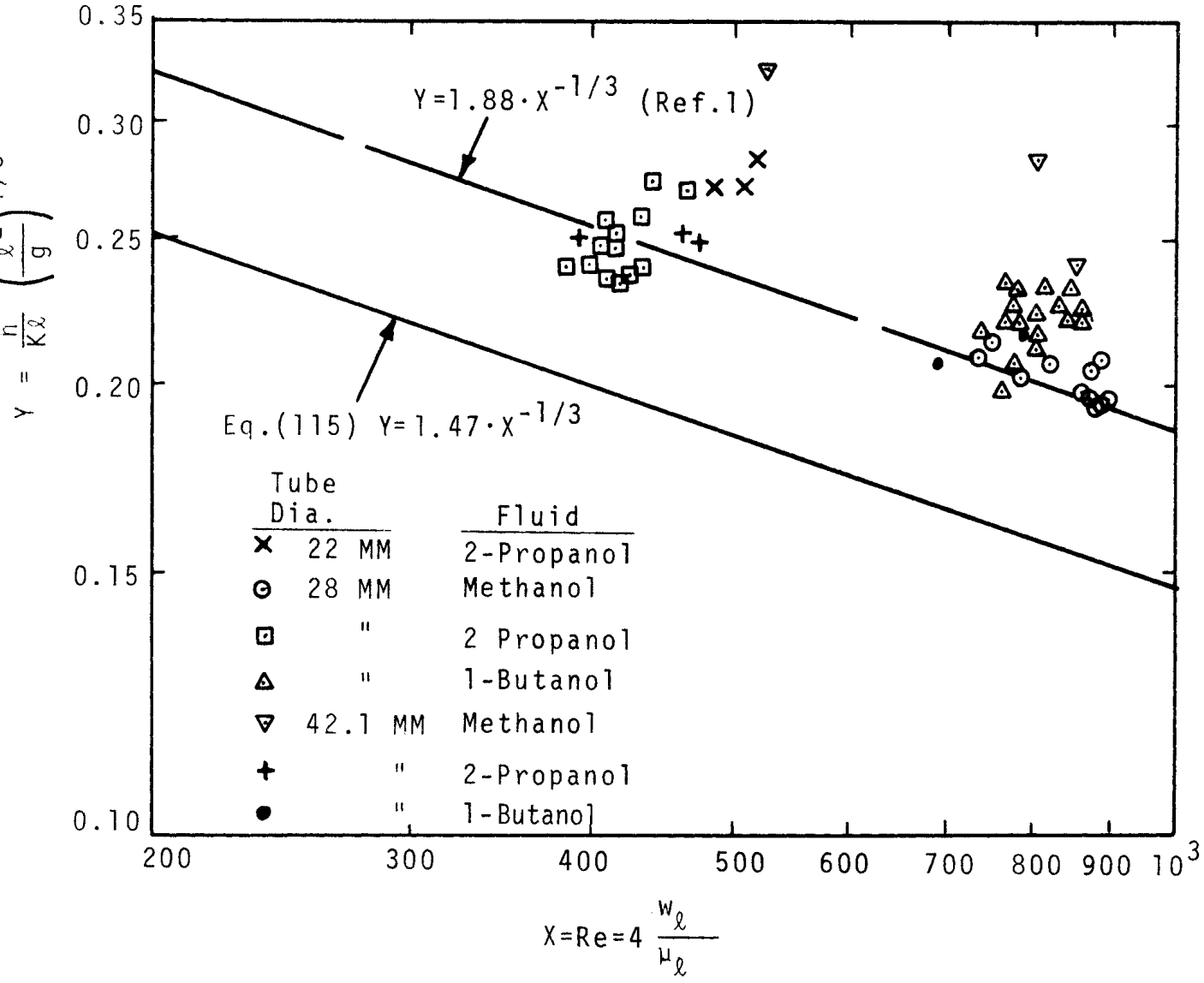

Figure 44. Variation of Condensing Film Coefficient with Re for Vertical Tubes. (Ref. 148)

Analyses of transient laminar film condensation on vertical surfaces have been made[89,90] for the case where momentum effects and interfacial drag are neglected. In one case[89] the transient arises by suddenly decreasing the wall temperature below the saturation temperature, while in the other, transients in both wall temperature and in the gravity field are considered.

Nusselt[44] obtained an average film condensation coefficient for the outside of a horizontal pipe by integrating Eq. (110) about the periphery of the tube. The result is, for $\rho_\ell \gg \rho_v$

$$h_m = 0.725 \left[\frac{k_\ell^3 \rho_\ell^2 g h_{fg}}{\Delta T \mu_\ell D_o} \right]^{1/4} \tag{121}$$

where D_o is the outer diameter of the tube and $\Delta T = T_s - T_w$, the temperature drop across the liquid film. Placing Eq. (121) in dimensionless form gives, for horizontal tubes;

$$\frac{h_m}{k_\ell} \left(\frac{\nu_\ell^2}{g} \right)^{1/3} = 1.51 \, Re_L^{-1/3} \tag{122}$$

where the Reynolds number is given by Eq. (113), in which the mass flow rate of condensate per unit length is used.

Experimental data for the horizontal tube are compared with Eq. (122) in Fig. 45. It is noted that the data are correlated better if the coefficient in Eq. (122) is changed from 1.51 to 1.27.

Film condensation on the outside of inclined tubes is predicted reasonably well if the body force in Eq. (121) is multiplied by $\cos \alpha$, where α is the angle of the tube to the horizontal[91];

$$h_m = 0.725 \left[\frac{k_\ell^3 \rho_\ell^2 h_{fg} g \cos\alpha}{\Delta T \mu_\ell D_o} \right]^{1/4} \tag{123}$$

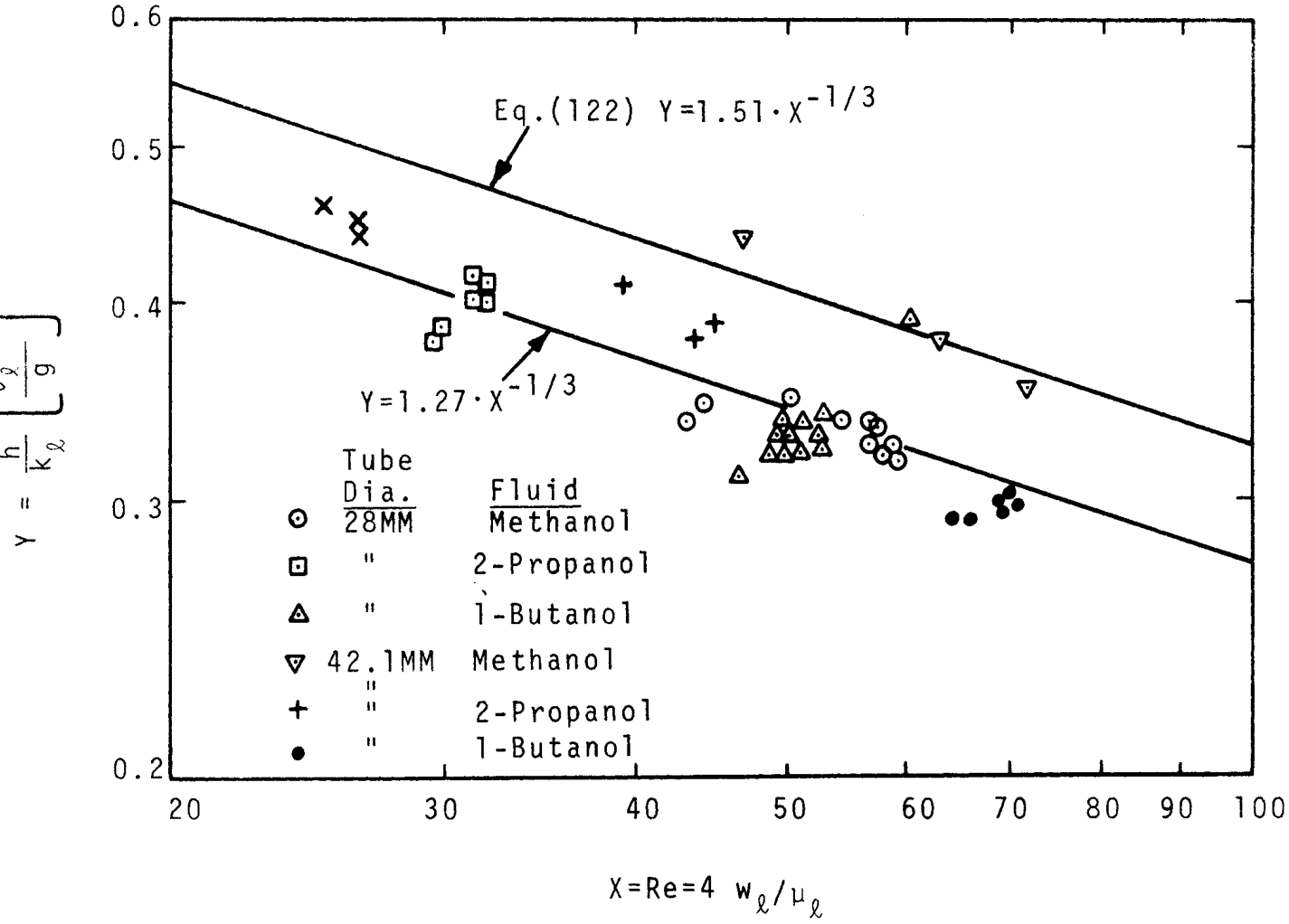

Figure 45. Condensing Heat Transfer Data with Horizontal Tubes Compared. (Ref. 148)

Eq. (123) is compared with experimental data in Fig. 46. A more realistic model for film condensation on inclined tubes is claimed by considering two zones[92] ; the upper portion of the tube, which may be treated with the Nusselt-type model and where surface tension effects are neglected, and the bottom part of the tube, where the flow is affected by surface tension and may be laminar or turbulent.

Boundary layer-type equations for laminar film condensation on single and vertical banks of horizontal tubes have been solved and are reported in Ref. 93.

b. Forced convection

In cases considered now, it is the shear stresses at the liquid-vapor interface that causes the liquid film flow to take place.

A study of forced convection condensation over a flat plate using a boundary layer type of analysis takes into account the presence of non-condensable gases and interfacial thermal resistance[94]. A related work considers the additional effect of superheating the vapor[95]. In both of these a liquid and a vapor gas boundary layer are used, with continuity of shear at the interface serving as the liquid driving force, neglecting the momentum transfer associated with the condensing vapor. The combination of body force and vapor forced-convection induced motion of the liquid film over a flat plate is treated approximately by an integral method[96]. An analytical and experimental study was made of film condensation of a saturated vapor moving parallel to a subcooled liquid film with no heat transfer to the solid surface[97] . Thus, once the liquid has reached saturation no further condensation will take place. The analysis accounts for turbulence in the liquid film,interfacial shear stresses, and assumes that the interface is smooth although experiments show this not to be the case. Comparison of the measure-

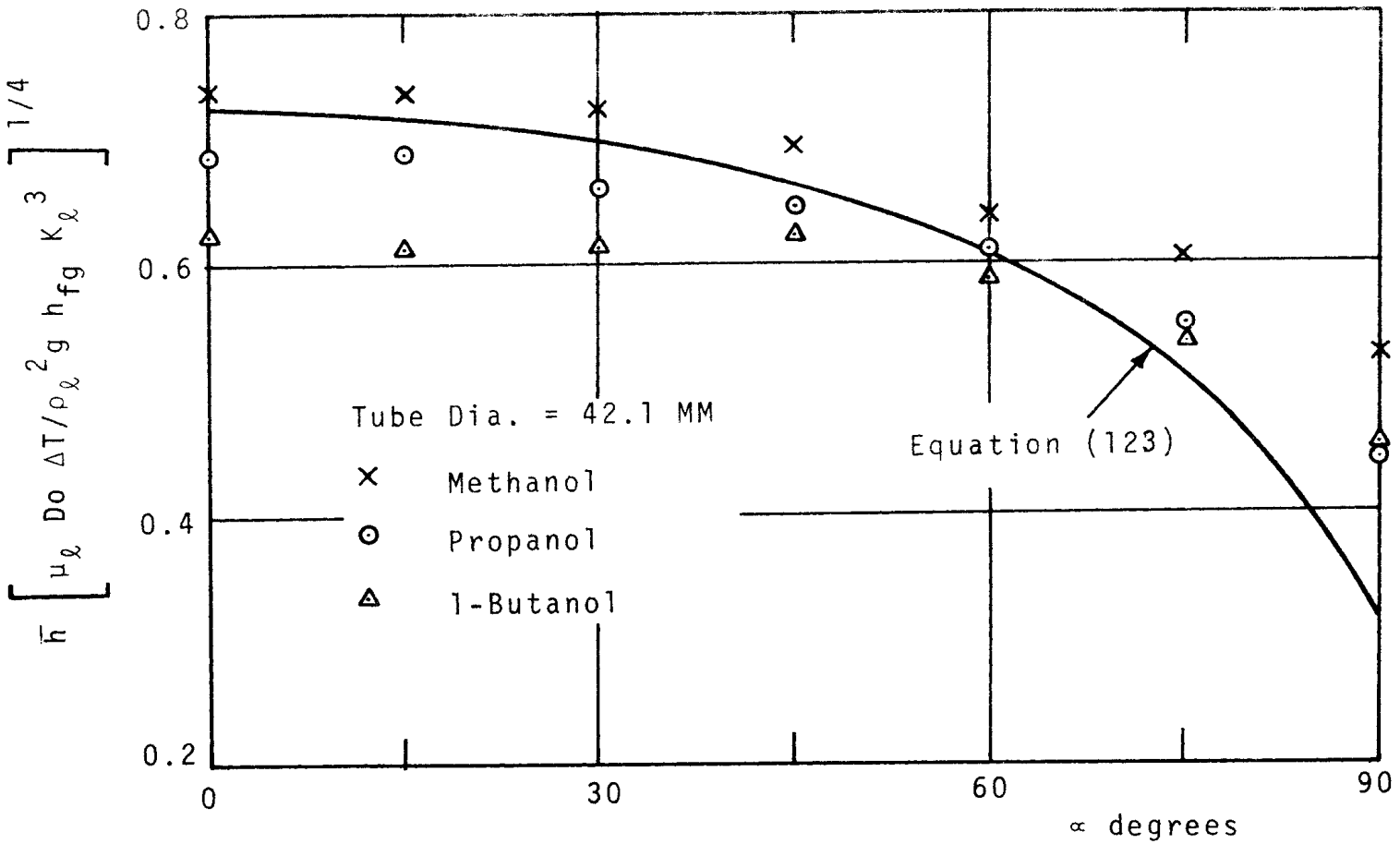

Figure 46. Variation of Condensing Film Coefficient with Tube Inclination. (Ref. 148)

ments with the computed wall temperatures and film thicknesses appear reasonably good. An analytic solution, based on the Nusselt assumptions, has been obtained for laminar film condensation of a vapor flowing perpendicular to a horizontal cylinder[98].

Nusselt[44] solved the problem of forced convection condensation flow up and down the inside of vertical tubes, using shear stresses at the liquid-vapor interface computed from normal pressure drop data for tubes. This assumes that the film thickness is small compared to the tube diameter. The use of the usual friction factor in determining interfacial shear with forced convection condensation has been under discussion[99].

Condensation inside horizontal tubes is somewhat more complicated than that inside vertical tubes because of the tendency of the condensate to fill the bottom of the tube at the lower flow rates. According to Jakob[26], if this effect is neglected Nusselt's theory of condensation on the outside of horizontal tubes should apply. A recent work presented a method for computing the local heat transfer coefficient about the tube[100]. Near the top the coefficient is independent of the amount of liquid and Nusselt's theory applies. Near the bottom the analogy between heat and momentum transfer is used to determine the heat transfer coefficient as with a single phase.

Pressure drop in a tube with condensation is treated as pressure drop due to the uncondensed vapor[101]. As velocity increases, some recovery of pressure from the axial momentum of the vapor should occur, and is taken into consideration in Refs. 102 and 103. Vapor momentum becomes an important means for obtaining liquid film driving forces in zero gravity, and studies have presented the criteria necessary for stable operation[104]. An experiment with non-wetting mercury condensing in a tapered horizontal tube at standard and short time zero gravity showed that the effect of gravity was negligible[105].

Many correlations of non-dimensional types with empirical coefficients have been proposed for condensation in horizontal tubes. Data have been correlated by a single-phase type flow equation of the form[106].

$$Nu\, Pr^{-m} = C\, Re^{n} \tag{124}$$

where the Reynolds number is based on the liquid mass velocity equivalent of the mixture of vapor and liquid.

Data of condensing methanol and Freon-12 were correlated by the following[107], giving the axial local values of the heat transfer coefficient;

For

$$1{,}000 < \left(\frac{DG_v}{\mu_\ell}\right)\left(\frac{\rho_\ell}{\rho_v}\right)^{1/2} < 20{,}000$$

$$\frac{h_x D}{k_\ell} = 1.38\,(Pr_\ell)^{1/3}\left(\frac{h_{fg}}{C_{p\ell}\,\Delta T}\right)^{1/6}\left[\left(\frac{DG_v}{\mu_\ell}\right)\left(\frac{\rho_\ell}{\rho_v}\right)^{1/2}\right]^{0.2} \tag{125}$$

and for

$$20{,}000 < \left(\frac{DG_v}{\mu_\ell}\right)\left(\frac{\rho_\ell}{\rho_v}\right)^{1/2} < 100{,}000$$

$$\frac{h_x D}{k_\ell} = 0.1\,(Pr_\ell)^{1/3}\left(\frac{h_{fg}}{C_{p\ell}\,\Delta T}\right)^{1/6}\left[\left(\frac{DG_v}{\mu_\ell}\right)\left(\frac{\rho_\ell}{\rho_v}\right)^{1/2}\right]^{2/3} \tag{126}$$

where $G_v = \rho_v V_v$, the mass velocity of the vapor. Equations (125) and (126) are plotted in Fig. 47, along with other recent data[108].

Reynolds analogy between heat and momentum transfer was applied to the condensation of saturated vapor in a horizontal tube[109]. The result is an expression for the local heat transfer coefficient given by:

$$\frac{h_x}{h_L} = \left(\frac{\rho_L}{\rho_x}\right)^{1/2} \tag{127}$$

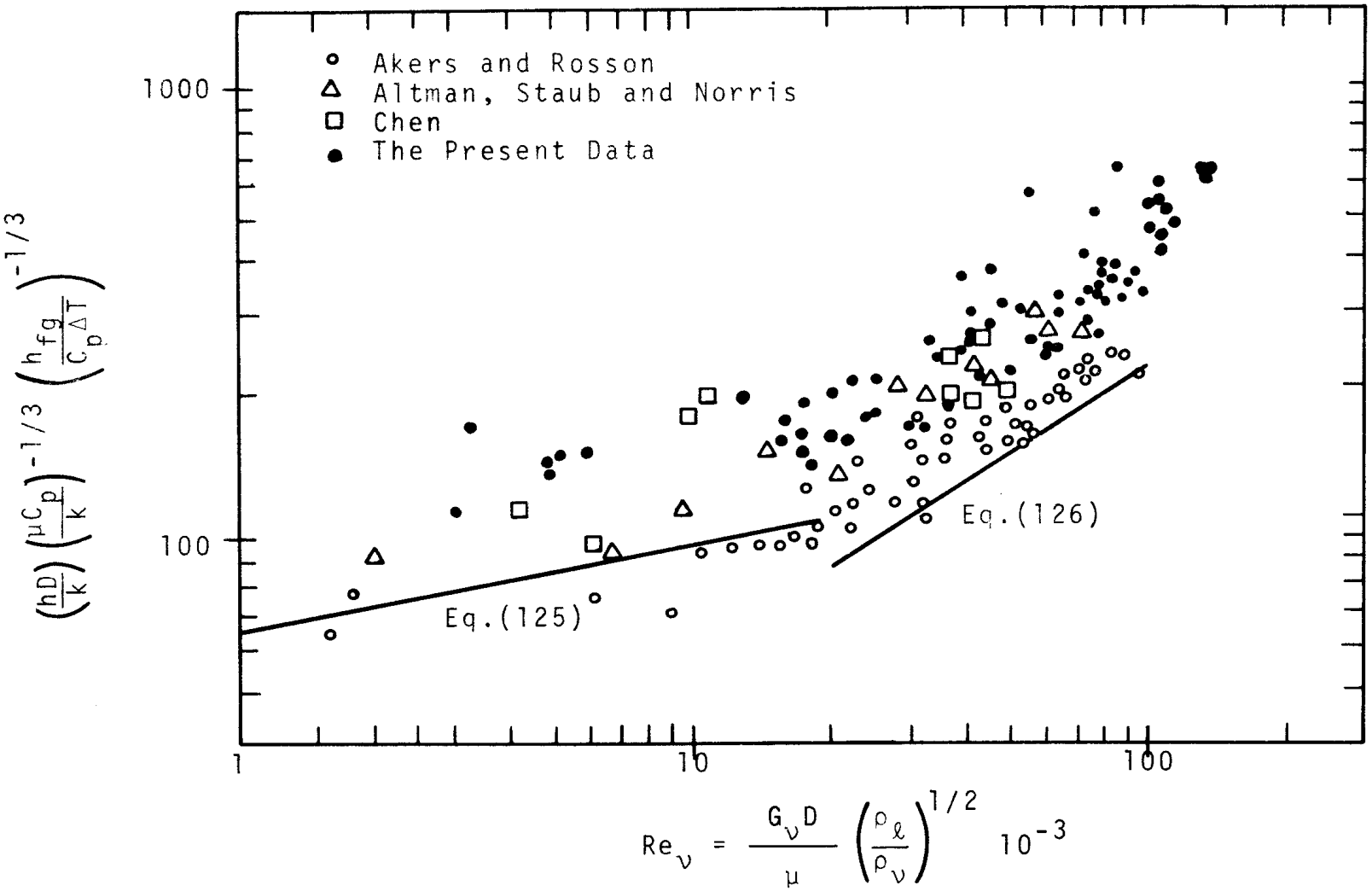

Figure 47. Correlation of Condensation with Forced Convection in Horizontal Tubes. (Ref. 108)

where ρ_x is the average density of the local liquid-vapor mixture and ρ_L is the liquid density. The single phase exit heat transfer coefficient h_L is computed from a general turbulent correlation, given as:

$$Nu = 0.021\, Re^{0.8} Pr^{0.4} \left(\frac{Pr_\ell}{Pr_w}\right)^{1/4} \tag{128}$$

Comparison of Eq. (127) with experiments for steam are shown in Fig. 48.

An emperical correlation which was successful in drawing together within ±15% the experimental data for the condensation of refrigerants R-11, 12, 21, 22, 113, 114 obtained in 4 different laboratories, in both vertical and horizontal orientations, is given as[110]:

$$\overline{Nu} = 0.05\, \overline{Re}_{eq.}^{0.8}\, \overline{Pr}_\ell^{0.33} \tag{129}$$

where

$$Re_{eq.} = Re_v \left(\frac{\mu_v}{\mu_\ell}\right)\left(\frac{\rho_\ell}{\rho_v}\right)^{0.5} + Re_\ell \tag{130}$$

The Nusselt and equivalent Reynolds numbers are the mean between inlet and outlet, while the Re_v and Re_ℓ used to compute the equivalent Reynolds number are determined as if the vapor and liquid each respectively occupied the tube alone. Further experimental correlations and analytical work dealing with condensation within horizontal tubes are presented in Refs. 111, 112, and 113.

c. Rotating condensation

By replacing the gravity body force by centrifugal acceleration it is possible to increase the condensation heat transfer coefficient significantly, since the liquid film thickness can be decreased. It also provides a mechanism for obtaining liquid film motion under zero gravity. The theoretical prediction for condensation on a rotating disc[114] shows that the condensate film thickness is uniform over the entire disc and inversely proportional to

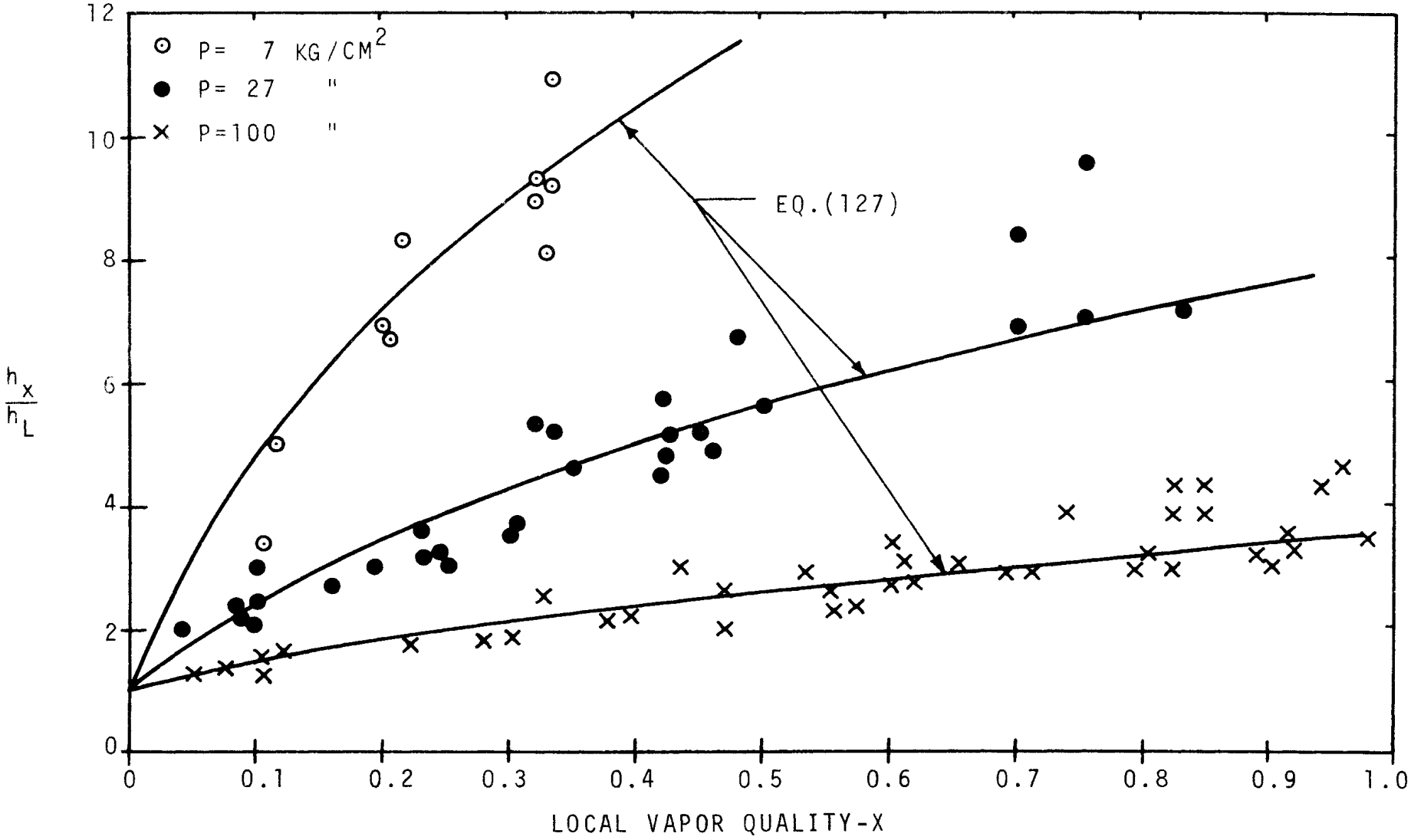

Figure 48. Local Heat Transfer Coefficient with Condensation of Steam. (Ref. 109)

the square root of the rotational speed. Experimental results[115] fall about 25% below the predicted values.

With film condensation on the outside of a horizontal tube rotating about its own axis, the heat transfer coefficient first increased with rotation, then decreased[116]. The initial increase occured because of the net thinning of the liquid film, referred to above, owing to centrifugal forces. The decrease occurs approximately when the axisymmetric waves in the condensate film degenerate into drops. Interfacial drag on the drops then tends to retard their removal from the surface, resulting in a decrease in the heat transfer coefficient. In two other experimental works, with rotating vertical cylinders, the film condensation coefficients increased with rotation[73,117]. Other works involving condensation on rotating systems are found in Refs. 118, 119.

d. Miscellaneous liquid film removal

Means other than gravity and centrifugal acceleration for removal of the liquid film in condensation have been considered in order to either improve the performance of film condensation, or to provide for its steady operation in zero gravity.

In Ref.120 an electromagnetic field replaces the gravity body forces, but can be used only with liquid metals. For non-conducting fluids, electrostatic fields have been successful in improving performance. Increases in the heat transfer coefficient by up to threefold were obtained with a D.C. field[121], and up to tenfold with an alternating electric field[122]. Another method for condensed liquid film removal is by suction through a porous cooled plate[123,124]. Surface tension or capillary forces can also be effective for liquid removal under zero gravity[103] by placing a wicking material in the vicinity of the cooling surface.

An attempt to improve film condensation on the outside of a vertical tube was made by the use of transverse vibrations of the tube[125]. Previous experiments show that beyond a critical condition, below which the effect of vibration is negligible, the condensation heat transfer coefficient increases continually to about 55% above the stationary value. Observation of the condensate film on the tube showed that the liquid was not thrown from the tube, by the vibration, as might be expected, but rather moved from one side of the tube to the other. It was believed that this motion contributed to greater mixing in the film, and hence the improved heat transfer.

3. Turbulent Film Condensation

The laminar character of the condensate film constitutes one of the most basic assumptions of Nusselt's theory. Since the mass flow rate increases with x on a vertical surface, one might expect that at a given Reynolds number the film becomes turbulent and Eqs. (110) and (112) no longer apply.

The Prandtl analogy for pipe flow was used to compute the heat transfer with a turbulent condensate film[126]. Based on this a mean empirical equation is suggested for turbulent condensation on a vertical plate;

$$Re'_L = 0.30\times10^{-2}\left[\frac{h_{\ell}\rho_{\ell}^{2/3} g^{1/3}(T_s - T_w) L}{\mu_{\ell}^{5/3} h_{fg}}\right]^{3/2} \qquad (131)$$

The Re'_L is defined differently here than by Eq. (113), as

$$Re'_L = \frac{W_L}{\mu_{\ell}} = \frac{h_m(T_s - T_w) L}{\mu_{\ell} h_{fg}} \qquad (132)$$

Equation (131) is plotted in Fig. 49, taken from Ref. 126, along with the Nusselt equation, and includes a wide variety of data. The critical transition between laminar and turbulent film flow takes place at $Re'_L = 350$.

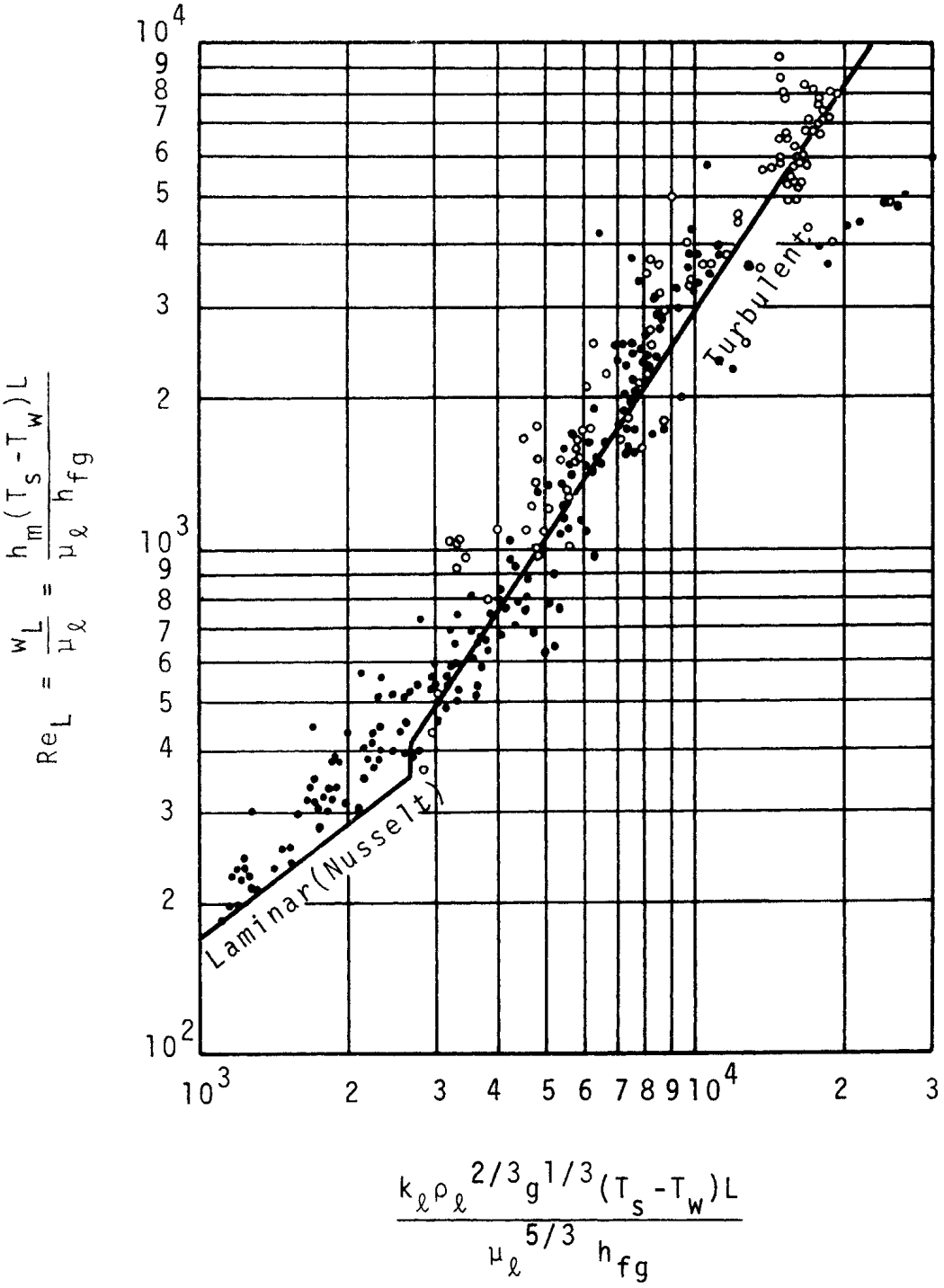

Figure 49. Heat Transfer with Condensation on a Vertical Surface. (Ref. 126)

An analysis similar to the above was conducted to cover wider ranges of Prandtl numbers[127,128]. The results are compared with liquid metals in Fig. 50.

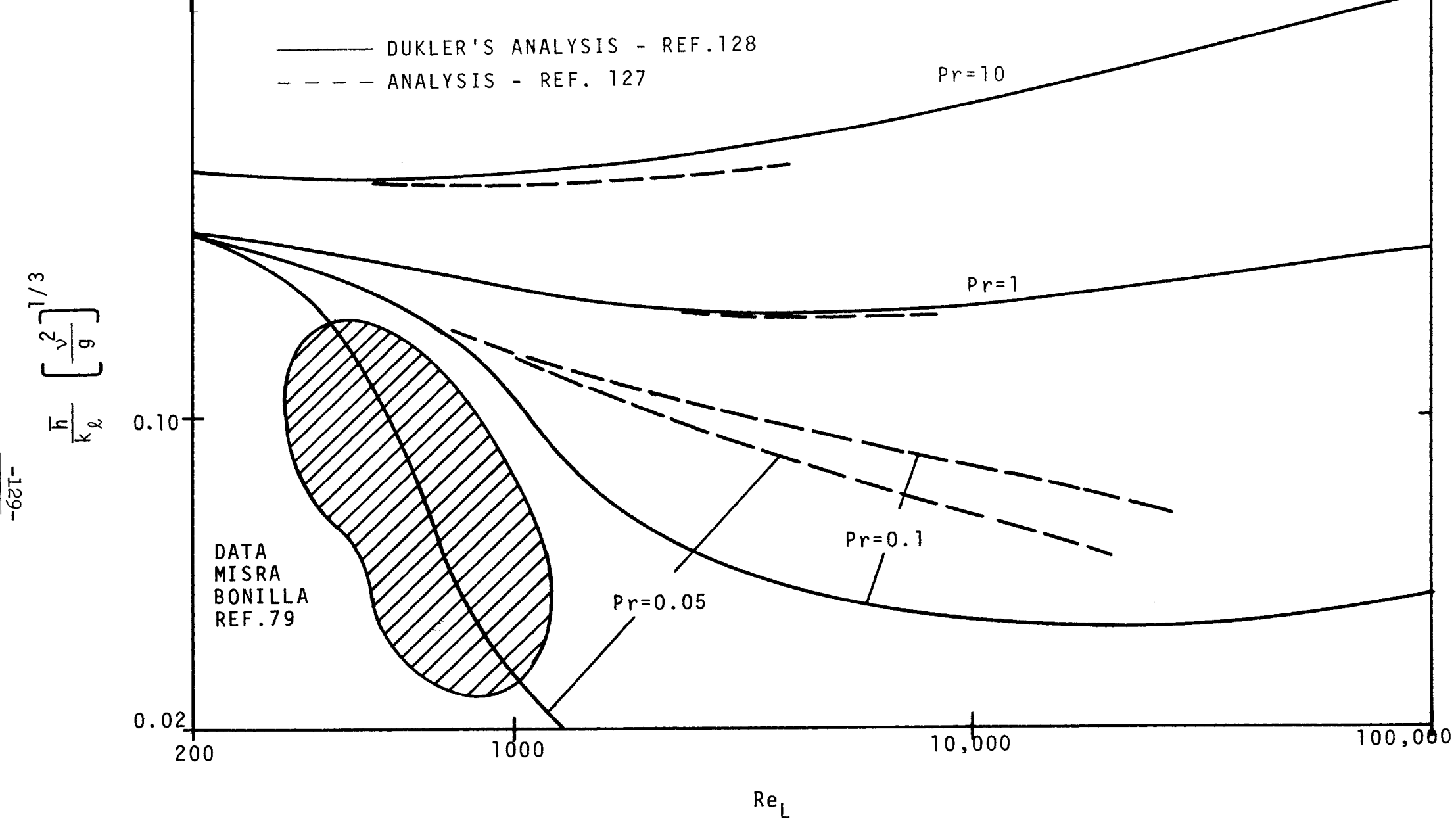

Figure 50. Turbulent Condensation on Vertical Surfaces for Various Prandtl Numbers. (Ref. 127)

VI. MIXTURES

The condensation of mixtures of vapors may include gases which are non-condensable under the conditions present. Mixtures with components of complete mutual solubility of the liquids will behave approximately as simple substances, and the film theories discussed earlier can be used. However, the dew-point temperature of the mixture is used instead of the saturation temperature at the interface. The dew-point temperature depends upon the composition of the vapor, and the mol fraction of the condensed liquid must come from a composition diagram of the constituents. The problem has been theoretically solved for condensation of a binary mixture on a vertical plate under the action of gravity[129].

When one of the components in the gaseous mixture is relatively insoluble in the liquid and does not itself condense, the process is classified as condensation in the presence of a non-condensing gas, and appears to have received the greatest attention in the literature. Discrepancies in the computation of the condensation coefficient using early experimental results have been attributed to the presence of non-condensable gases[38]. Figure 51 shows the relative influence of a non-condensable gas on the steam side heat transfer coefficient. The minimum inert gas concentration was less than 1 ppm. The sensitivity of the heat transfer coefficient increases with heat flux and as the system pressure is lowered[130]. This effect of heat flux is due to the increasing concentration of the non-condensable gas resulting from the convective flow associated with the condensation of the vapor. With no forced convection, an equilibrium condition is established in which the rate of removal of the gas by diffusion and natural convection away from the condensing surface equals the rate at which it is brought to the interface. The resulting increased gas concentration at the interface re-

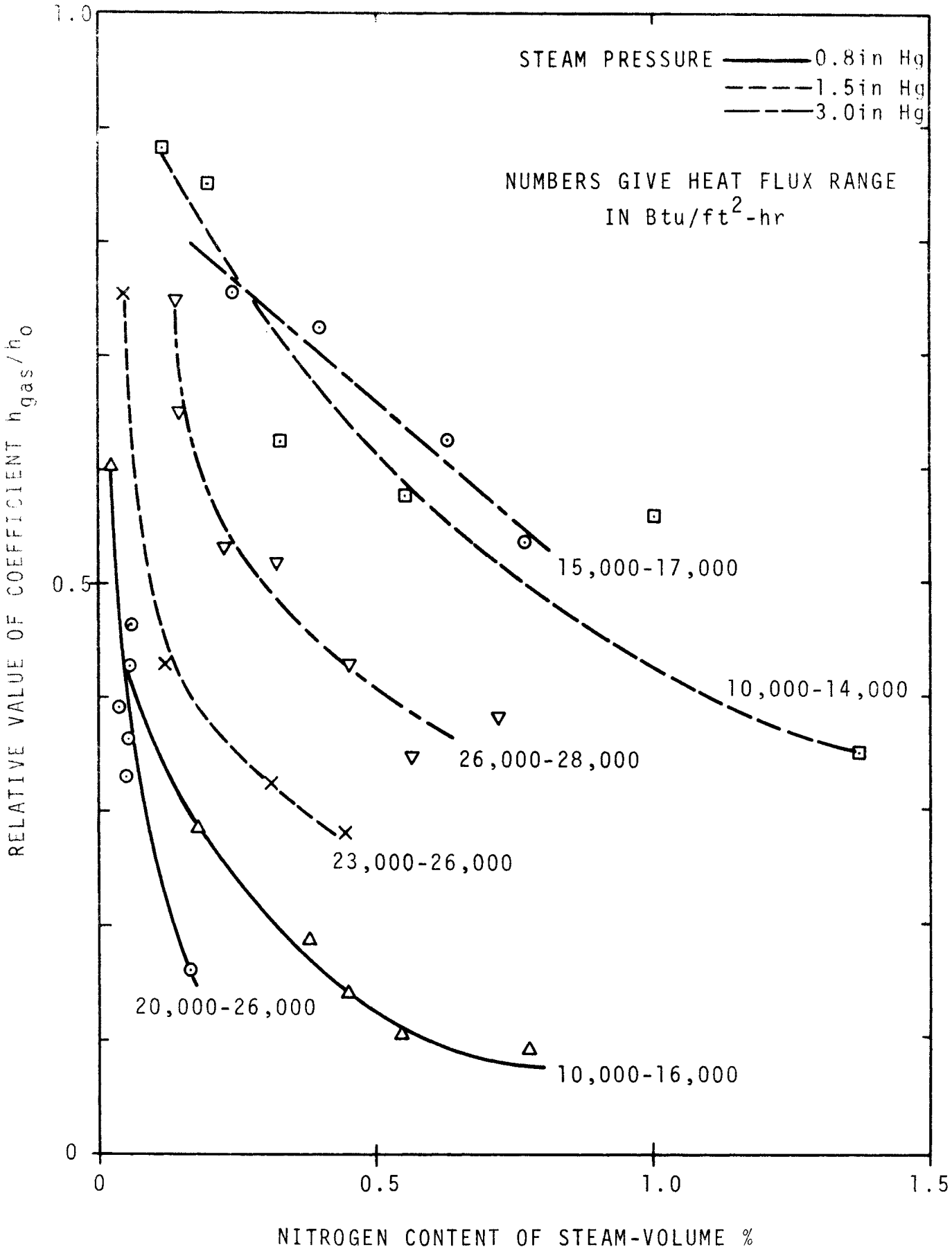

Figure 51. Effect of Non-Condensable Gas on the Steam-Side Heat Transfer Coefficient. (Ref. 130)

duces the partial pressure of the vapor, and hence the vapor condensation temperature. With film condensation the temperature drop across the condensate film is thus smaller, as is the associated heat flux. The increasing concentration of the non-condensable gas as the condensing surface is approached is demonstrated well in the experimental results shown in Fig. 52[63]. The influence of the location of a continuously operating vent on the solid condensing surface subcooling is shown as a function of different heat flux levels. As the vent is brought closer to the surface, the subcooling necessary to maintain the heat flux is reduced, since the non-condensable gas concentration near the surface is reduced. Other experimental work has shown that condensation in the presence of non-condensables can be predicted by diffusion analysis[131].

Several analytical and approximate solutions of forced convection condensation with non-condensables[94,132] show that if the presence of non-condensable cannot be avoided, its detrimental effects can be reduced by forced convection of the vapor, which reduces the local concentration. A recent analytical work includes both gravity and forced convection effects and results in the same conclusion [133].

A number of experimental studies with non-condensables under gravity and forced convection conditions provide empirical correlations for both heat and mass transfer[134, 135, 136, 137]. Other references dealing with non-condensable gases are cited[33, 34, 36, 48, 102, 138-147].

VII. SIMILARITIES BETWEEN BOILING AND CONDENSATION

Based on the discussion of the condensation process it may be observed that many similarities exist between the boiling and condensation phenomena;

a. Nucleate boiling and dropwise condensation are both nucleation governed phenomena. In nucleate boiling the vapor bubbles appear to effectively

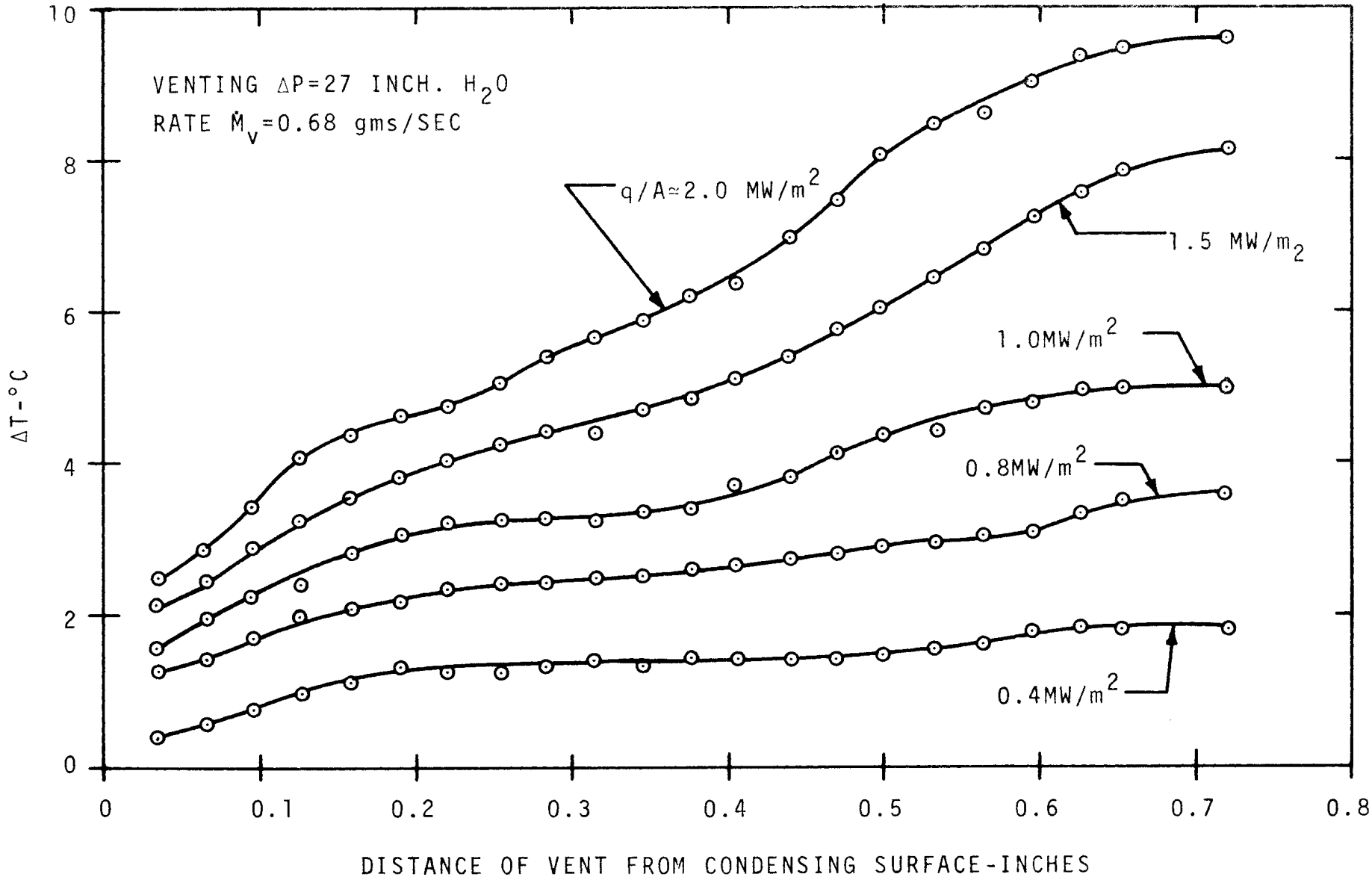

Figure 52. Effect of Vent Position on the Steam-to-Surface Temperature Difference for Fixed Venting Rate. (Ref. 63)

disrupt the boundary layer, and a similar process most likely occurs with dropwise condensation, provided that the drops can be removed before growing too large.

b. For a given ΔT, the heat flux increases as the number of nucleating sites increase, both for nucleate boiling and dropwise condensation.

c. With nucleate boiling, as ΔT increases the number of active sites increase until the population density becomes so great that coalescence takes place, giving rise to the peak or maximum heat flux phenomena. It has not yet been demonstrated that a corresponding peak heat flux exists with dropwise condensation on a steady basis, as ΔT is increased. With nucleate boiling the buoyant forces are large compared to the surface forces which hold the vapor bubble on the surface, thus the departure of the bubbles from the heating surface takes place with facility.

On the other hand, with dropwise condensation the surface forces tending to keep the drop in place are large relative to the gravity forces which might tend to remove it from the cooling surface. It might be anticipated that with a positive droplet removal mechanism (e.g.-centrifugal force), corresponding to the buoyant forces on vapor bubbles, that a peak heat flux will be reached with dropwise condensation as ΔT increases, beyond which coalescence between the drops will increase.

d. With nucleate boiling, when ΔT has been increased sufficiently to produce complete coalescence between vapor bubbles the process of film boiling takes place. Likewise with dropwise condensation, it might be anticipated that when the ΔT is increased such that complete coalescence occurs between adjacent drops, film condensation will be taking place. In practive, film condensation is much more apt to occur than dropwise condensation unless special "promotors" are used, as discussed earlier, because of the lack of a sufficiently effective droplet removal mechanism.

REFERENCES

1. McAdams, W., Heat Transmission, Ch. 13, 3rd Ed., McGraw-Hill (1954).

2. Garrett, W.D., "The influence of monomolecular surface films on the production of condensation nuclei from bubbled sea water", J. Geophysical Research, 73, 5145-5150 (Aug. 1968).

3. Adam, N.K., The Physics and Chemistry of Surfaces, 3rd Ed., Dover Publications (1968).

4. Davies, J.T. and Rideal, E.K., Interfacial Phenomena, Academic Press, (1963).

5. Otto, E.W., "Static and dynamic behavior of the liquid-vapor interface during weightlessness", Preprint 17a, presented at Symposium on Effects of "Zero Gravity" on Fluid Dynamics and Heat Transfer-Part I. AIChE 55th National Meeting, Houston, Texas, February 7-11, 1965.

6. Dupre, A., Theorie Mecanique de la Chaleur, Gauthier-Villars, Paris (1869).

7. Macdougall, G. and Ockrent, C., "Surface energy relations in liquid/solid systems I. The adhesion of liquids to solids and a new method of determining the surface tension of liquids", Proc. Roy. Soc., A180, 151 (1942).

8. Fox, H.W. and Zisman, W.A., "The spreading of liquids on low energy surfaces, II. Modified tetrafluoroethylene polymers", J. Colloid Sci., 7, 109 (1952).

9. Frenkel, J., Kinetic Theory of Liquids, Oxford University Press (1946).

10. Thomson, W., "On the equilibrium of vapor at a curved surface of liquid", Phil. Mag. and J. Sci., 42, 488 (1871).

11. Tolman, R.C., J. Chem. Phys., 17, 333-337 (1949).

12. Wilson, C.T.R., Proc. Roy. Soc. London, 61, 240-243 (1897).

13. Goglia, G.L. and VanWylen, G.J., "Experimental determination of limit of supersaturation of nitrogen vapor expanding in a nozzle", J. Heat Transfer (Trans. ASME), 83, 27-32 (Feb. 1961).

14. Hill, P.G., Witting, H., Demetri, E.P., "Condensation of metal vapors during rapid expansion", J. Heat Transfer (Trans. ASME), 303-317, (Nov. 1963).

15. Volmer, M. and Flood, H., "Tropfchenbildung in Dampfen", Z. Physic Chemie, A170, 273 (1934).

16. Jaeger, H.L., Willson, E.D., Hill, P.G. and Russell, K.C., "Nucleation of supersaturated vapors in nozzles, I. H_2O and NH_3", J. Chem. Phys., 51, 5380-5388 (1969).

17. Lothe, J. and Pound, G.M., "On the statistical mechanics of nucleation theory", J. Chem. Phys., 45, 630-634 (1966).

18. Feder, J., Russell, K.C., Lothe, J. and Pound, G.M., "Homogeneous nucleation and growth of droplets in vapours", Advances in Physics, 15, 111-178 (Jan. 1966).

19. Umur, A. and Griffith, P., "Mechanism of dropwise condensation", J. Heat Transfer (Trans. ASME), 87C, 275-282 (May 1965).

20. Welch, J.F. and Westwater, J.W., "Microscopic study of dropwise condensation", International Developments in Heat Transfer, Part II, ASME, 302-309 (1961).

21. Fatica, N. and Katz, D.L., "Dropwise condensation", Chem. Eng. Progress 45, 661-674 (1949).

22. Trefethan, L., "Drop condensation and the possible importance of circulation within drops caused by surface tension variation", G.E.L. Rept. 58GL47, General Electric Co., Feb. 3, 1958. (In Ref. 25).

23. Lorenz, J.J. and Mikic, B.B., "The effect of thermocapillary flow on heat transfer in dropwise condensation", J. Heat Transfer (Trans. ASME), C92, 46-52 (Feb. 1970).

24. Eucken, A., "Energy and material exchange on boundary surfaces", Naturwissenshaften, 25, 209 (1937). (In Ref. 26).

25. Rohsenow, W.M., Choi, H., Heat, Mass and Momentum Transfer, Prentice-Hall, Inc., New Jersey (1961).

26. Jakob, M., Heat Transfer, John Wiley & Sons, Inc., New York (1949).

27. Emmons, H., "The mechanism of drop condensation", Trans. AIChE, 35, 109 (1939).

28. Jakob, M., "Heat transfer in evaporation and condensation-II", Mech. Eng., 58, 729 (1936).

29. McCormick, J.L. and Westwater, J.W., "Nucleation sites for dropwise condensation", Chem. Eng. Sci., 20, 1021 (1965).

30. Grigull, U., Institute fur Technische Thermodynamik, Technische Hochschule, Munich. Personal Communication (1968).

31. Sugawara, S. and Katsuta, K., "Fundamental study on dropwise condensation", 3rd Int. Heat Transfer Conference (ASME-AIChE), II, 354-361, (1966).

32. Peterson, A.C., Westwater, J.W., "Dropwise condensation of ethylene glycol", Chem. Eng. Progr. Symposium, Ser. 62, 135 (1966).

33. McCormick, J.L. and Westwater, J.W., "Drop dynamics and heat transfer during dropwise condensation of water vapor on a horizontal surface", Chem. Eng. Progr. Symposium, Ser. 62, 120 (1966).

34. Tanner, D.W., Pope, D., Potter, C.J. and West, D., "Heat transfer in dropwise condensation, Part II. Surface chemistry", Int. J. Heat Mass Transfer, 8, 427-436 (March 1965).

35. LeFevre, E.J. and Rose, J.W., "A theory of heat transfer by dropwise condensation", 3rd Int. Heat Transfer Conference (ASME-AIChE), II, 362-375 (1966).

36. LeFevre, E.J. and Rose, J.W., "An experimental study of heat transfer by dropwise condensation", Int. J. Heat Mass Transfer, 8, 1117-1133 (Aug. 1965).

37. Bergles, A.E. and Rohsenow, W.M., "The determination of forced convection surface-boiling heat transfer", J. Heat Transfer (Trans. ASME), 86, 365 (1964).

38. Ruckenstein, E. and Metiu, H., "On dropwise condensation on a solid surface", Chem. Eng. Science, 20, 173 (1965).

39. Schrage, R.W., A Theoretical Study of Interphase Mass Transfer, Columbia University Press, New York (1953).

40. Arpaci, V.S., Conduction Heat Transfer, Addison-Wesley (1966).

41. Sukhatme, S.P. and Rohsenow, W.M., "Heat transfer during film condensation of a liquid metal vapor", J. Heat Transfer (Trans. ASME), 1, 19-28 (Feb. 1966).

42. Kroger, D.G., and Rohsenow, W.M., "Film condensation of saturated potassium vapor", Int. J. Heat Mass Transfer, 10, 1891-1894 (Dec. 1967).

43. Barry, R.E. and Balzhiser, R.E., "Condensation of sodium at high heat fluxes", Proc. 3rd Int. Heat Transfer Conference, II, 318 (Aug. 1966).

44. Nusselt, W., "The surface condensation of steam", Z. Ver. Deut. Ing., 60, 541-569 (1916).

45. Wilhelm, Donald J., "Condensation of metal vapors: Mercury and the kinetic theory of condensation", Argonne National Laboratory, Report ANL-6948 (Oct. 1964).

46. Mortenson, E.M. and Eyring, H., "Transmission coefficients for evaporation and condensation", J. Phys. Chem., 64, 846 (July 1960).

47. Johnstone, R.K.M., Smith, W., "Rate of condensation or evaporation during short exposures of a quiescent liquid", 3rd Int. Heat Transfer Conference, II, 348-353 (1966).

48. Tanner, D.W., Pope, D., Potter, C.J. and West, D., "Heat transfer in dropwise condensation, Part I. The effects of heat flux, steam velocity and non-condensable gas concentration", Int. J. Heat Mass Transfer, 8, 419-426 (March 1965).

49. Mills, A.F. and Seban, R.A., "The condensation coefficient of water", Int. J. Heat Mass Transfer, 10, 1815 (1967).

50. Wenzel, H., "On the condensation coefficient of water estimated from heat-transfer measurements during dropwise-condensation", Int. J. Heat Mass Transfer, 12, 125-126 (Jan. 1969).

51. Fedorovich, E.D. and Rohsenow, W.M., "The effect of vapor subcooling on film condensation of metals", Int. J. Heat Mass Transfer, 12, 1525-1529 (Nov. 1969).

52. List, R., "General heat and mass exchange of spherical hailstones", J. Atmospheric Sci., 20, 189-197 (May 1963).

53. Puzyrewski, R., "Perturbation analysis of condensation controlled by heat transfer on large droplets", Int. J. Heat Mass Transfer, 10, 1717-1726 (Dec. 1967).

54. Wakeshima, H. and Takata, K., "Growth of droplets and condensation coefficients of some liquids", Japan J. Appl. Phys., 2, 792 (Dec. 1963).

55. Zuber, Novak, "Recent trends in boiling heat transfer research, Part I. Nucleate pool boiling", Appl. Mechanics Reviews, 17, 663 (1964).

56. Florschuetz, L.W. and Chao, B.T., "On the mechanics of vapor bubble collapse", J. Heat Transfer (Trans. ASME), 87C, 209-220 (May 1965).

57. Hewitt, H.C. and Parker, J.D., "Bubble growth and collapse in liquid nitrogen", J. Heat Transfer (Trans. ASME), 90, (Feb. 1968).

58. Davies, G.A. and Ponter, A.B., "The prediction of the mechanism of condensation on condenser tubes coated with tetrafluoroethylene", Int. J. Heat Mass Transfer, 11, 375 (1968).

59. Davies, G.A., Mojtehedi, W. and Ponter, A.B., "Measurement of contact angles under condensation conditions; the prediction of dropwise-filmwise transition", Int. J. Heat Mass Transfer, 14, 709-713 (May 1971).

60. Shafrin, E.G. and Zisman, W.A., "Constitutive relations in the wetting of low energy surfaces and the theory of retraction method of preparing monolayers", J. Phy. Chem. 64, 519 (1960).

61. Kosky, P.G., "Tetrafluoroethylene coatings on condenser tubes", Int. J. Heat Mass Transfer, 11, 374 (1968).

62. Hare, E.F. and Zisman, W.A., "Autophobic liquids and the properties of their adsorbed films", J. Phys. Chem., 59, 335 (1955).

63. Citakoglu, E. and Rose, J.W., "Dropwise condensation: Some factors influencing the validity of heat-transfer measurements", Int. J. Heat Mass Transfer, 11, 523-537 (March 1968).

64. Griffith, P. and Lee, M.S., "The effect of surface thermal properties and finish on dropwise condensation", Int. J. Heat Mass Transfer, 10, 697-707 (May 1967).

65. Brown, A.R. and Thomas, M.A., "Filmwise and dropwise condensation of steam at low pressures", Proc. 3rd Int. Heat Transfer Conference, II, 300 (Aug. 1966).

66. Mikic, B.B., "On mechanism of dropwise condensation", Int. J. Heat Mass Transfer, 12, 1311-1323 (Oct. 1969).

67. Scriven, L.E., "On the dynamics of phase growth", Chem. Eng. Sci., 10, 1 (1959).

68. Gose, E.E., Mucciardi, A.N. and Baer, E., "Model for dropwise condensation on randomly distributed sites", Int. J. Heat Mass Transfer, 10, 15-22 (Jan. 1967).

69. Isachencko, V.P., "Mechanism and correlations of heat transfer with dropwise condensation of steam", Teploenergetica, 9, (1962).

70. McCormick, J.L. and Baer, E., "On the mechanism of heat transfer in dropwise condensation", J. Colloid Sci., 18, 208 (1963).

71. Ivanovskii, M.N., Usbbotin, V.I. and Milovanov, Yu. V., "Heat transfer with dropwise condensation of mercury vapor", Thermal Engineering, 14, 114-122 (1967).

72. Roblee, L.H.S., et al "Dropwise condensation of steam at atmospheric and above atmospheric pressures", ONR Tech. Report No. 1, Contract Nonr 3357(02), March 17, 1966.

73. Birt, D.C.P., Brunt, J.J., Shelton, J.T. and Watson, R.G.H., "Methods of improving heat transfer from condensing steam and their application to condensers and evaporators", Trans. Inst. Chem. Engrs., 37, 289-296, (1959).

74. Bromley, L.A., "Effect of heat capacity of condensate", Ind. and Eng. Chem., 44, 2966 (1952).

75. Rohsenow, W.M., "Heat transfer and temperature distribution in laminar film condensation", Trans. ASME, 78, 1645-1648 (1956).

76. Sparrow, E.M. and Gregg, J.L., "Boundary layer treatment of laminar film condensation", J. Heat Transfer, 81, 13-23 (1959).

77. Koh, J.C.Y., Sparrow, E.M. and Hartnett, J.P., "The two phase boundary layer in laminar film condensation", Int. J. Heat Mass Transfer, 2, 69-82 (1961).

78. Chen, Michael Ming, "An analytical study of laminar film condensation: Part 1. Flat plates", J. Heat Trnasfer (Trans. ASME), 83, 48-54 (Feb. 1961).

79. Misra, B. and Bonilla, C.F., "Heat transfer in the condensation of metal vapors", Chem. Eng. Progr. Symposium, 52, 7-21 (1956).

80. Poots, G. and Miles, R.G., "Effects of variable physical properties on laminar film condensation of saturated steam on a vertical flat plate", Int. J. Heat Mass Transfer, 10, 1677-1692 (Dec. 1967).

81. Yang, Kwang-Tzu, "Laminar film condensation on a vertical nonisothermal plate", J. Appl. Mech. (Trans. ASME), 33, 203-205 (Mar. 1966).

82. Matin, Shaikh A., "A similarity solution for the condensate film on a vertical flat plate in presence of variable gravity field", ASME Paper 65-AV-42.

83. Chato, J.C., "Condensation in a variable acceleration field and the condensing thermosyphon", J. Eng. Power (Trans. ASME), 87, 355-360 (Oct. 1965).

84. Spencer, D.L. and Ibele, W.E., "Laminar film condensation of a saturated and superheated vapor on a surface with a controlled temperature distribution", Proc. 3rd Int. Heat Transfer Conference, II, 337 (Aug. 1966).

85. Slegers, L. and Seban, R.A., "Nusselt condensation of n-butyl alcohol", Int. J. Heat Mass Transfer, 12, 237-239 (Feb. 1969).

86. Gerstmann, J. and Griffith, P., "Laminar film condensation on the underside of horizontal and inclined surfaces", Int. J. Heat Mass Transfer, 10, 567-580 (May 1967).

87. Leppert, G. and Nimmo, B., "Laminar film condensation on surfaces normal to body or inertial forces", J. Heat Transfer (Trans. ASME), 90, 178-179 (Feb. 1968).

88. Lewis, E.W., et al, "Boiling of liquid nitrogen in reduced gravity fields with subcooling", ORA Report 07461-20-T, Department of Mechanical Engineering, The University of Michigan, May 1967.

89. Sparrow, E.M. and Siegel, R., "Transient film condensation", J. Appl. Mechanics, 26, 120-21 (1959).

90. Chung, P.M., "Unsteady laminar film condensation on vertical plate", Paper No. 62-HT-23, ASME-AIChE Heat Transfer Conference and Exhibit, Houston, Texas (Aug. 1962).

91. Hassan, K.E. and Jakob, M., "Laminar film condensation of pure saturated vapors on inclined circular cylinders", Trans. ASME, 80, 887 (1958).

92. Sheynkman, A.G. and Linetskiy, V.N., "Hydrodynamics and heat transfer by film condensation of stationary steam on an inclined tube", Heat Transfer-Soviet Research, 1, 90-97 (May 1969).

93. Chen, Michael Ming, "An analytical study of laminar film condensation: Part 2. Single and multiple horizontal tubes", J. Heat Transfer, 83, 55-60 (Feb. 1961).

94. Sparrow, E.M., Minkowycz, W.J. and Saddy, M., "Forced convection condensation in the presence of non-condensables and interfacial resistance", Int. J. Heat Mass Transfer, 10, 1829-1845 (Dec. 1967).

95. Minkowycz, W.J. and Sparrow, E.M., "The effect of superheating on condensation heat transfer in a forced convection boundary layer flow", Int. J. Heat Mass Transfer, 12, 147-154 (Feb. 1969).

96. Jacobs, H.R., "An integral treatment of combined body force and forced convection in laminar film condensation", Int. J. Heat Mass Transfer, 9, 637-648 (July 1966).

97. Linehan, J.H., Petrick, M. and El-Wakil, M.M., "The condensation of a saturated vapor on a subcooled film during stratified flow", AIChE Preprint 3, presented at 11th National Heat Transfer Conference, Minneapolis, Minnesota, Aug. 3-6, 1969.

98. Denny, V.E. and Mills, A.F., "Laminar film condensation of a flowing vapor on a horizontal cylinder at normal gravity", J. Heat Transfer (Trans. ASME), C91, 495-501 (Nov. 1969).

99. Shekriladze, I.G.and Gomelauri, V.I., "Reply to comments on theoretical study of laminar film condensation of flowing vapour", Int. J. Heat Mass Transfer, 13, 942-943 (May 1970).

100. Rosson, H.F. and Myers, J.A., "Point values of condensing film coefficients inside a horizontal tube", Chem. Eng. Progr. Symposium, 61, 190-199 (1965).

101. Hoffman, E.J., "Pressure drop in condensation", ASME Paper 68-WA/HT-28.

102. Silver, R.S. and Wallis, G.B., "A simple theory for longitudinal pressure drop in the presence of lateral condensation", Proc. Inst. Mech. Engrs., 180, Pt.1, 36-40 (1965-66).

103. Ginwala, K., "Engineering study of vapor cycle cooling equipment for zero-gravity environment", WADD Tech. Report 60-776 (Jan. 1961).

104. Lancet, R.T., Abramson, P. and Forslund, R.P., "The fluid mechanics of condensing mercury in a low-gravity environment", Symposium on Fluid Mechanics and Heat Transfer under Low Gravitational Conditions, Lockheed Research Laboratories, Palo Alto, California, 24-25 (June 1965).

105. Albers, J.A. and Macosko, R.P., "Condensation pressure drop of non-wetting mercury in a uniformly tapered tube in 1-g and zero-gravity environments", NASA TN D-3185 (1966).

106. Akers, W.W., Deans, H.A. and Crosser, O.K., "Condensing heat transfer within horizontal tubes", Chem. Eng. Prog., 54 (1958).

107. Akers, W.W. and Rosson, H.F., "Condensation inside a horizontal tube", Chem. Eng. Prog. Symposium, 56 (1960).

108. Baer, S., Maulbetsch, J.S. and Rohsenow, W.M., "Refrigerant forced-convection condensation inside horizontal tubes", Report No. DSR 79760-59, Dept. of Mechanical Engineering, MIT (Nov. 1968).

109. Ananier, E.P., Boyko, L.D. and Kruzhilin, G.N., "Heat transfer in the presence of steam condensation in a horizontal tube", International Developments in Heat Transfer, Part II, 290, ASME (1961).

110. Cavallini, A. and Zecchin, R., "High velocity condensation of organic refrigerants inside tubes", XIII International Congress of Refrigeration paper 2.29, Washington, D.C., Aug. 27-Sept. 3, 1971.

111. Boyko, L.D. and Krushilin, G.N., "Heat transfer and hydraulic resistance during condensation of a steam in a horizontal tube and in a bundle of tubes", Int. J. Heat Mass Transfer, 10, 361-373 (Mar. 1967).

112. Rufer, C.E. and Kezios, S.P., "Analysis of two-phase, one-component stratified flow with condensation", J. Heat Transfer (Trans. ASME), 88, 265-275 (Aug. 1966).

113. Soliman, M., Schuster, J.R. and Berenson, P.J., "A general heat transfer correlation for annular flow condensation", J. Heat Transfer (Trans. ASME), 90, 267-276 (May 1968).

114. Sparrow, E.M. and Gregg, J.L., "A theory of rotating condensation", Trans. ASME, 81, 113 (Mar. 1959).

115. Nandapurkar, S.S. and Beatty, K.O., "Condensation on a horizontal rotating disc", Chem. Eng. Prog. Symposium, 56, 129 (Nov. 1960).

116. Singer, R.M. and Preckshot, G.W., "The condensation of vapor on a rotating cylinder", Proc. 1963 Heat Transfer and Fluid Mech. Institute, Paper No. 14, 205-221 (1963).

117. Nicol, A.A. and Gacesa, M., "Condensation of steam on a rotating vertical cylinder", J. Heat Transfer, Trans. ASME, C92, 144-152 (Feb. 1970).

118. Bromley, L.A., Humphreys, R.F. and Murray, W., "Condensation on and evaporation from radially grooved rotating disks", ASME Paper 65-HT-26.

119. Sparrow, E.M. and Hartnett, J.P., "Condensation on a rotating cone", J. Heat Transfer (Trans. ASME), 83, 101-102 (Feb. 1961).

120. Singer, Ralph M., "Laminar film condensation in the presence of an electromagnetic field", ASME Paper 64-WA/HT-47.

121. Velkoff, H.R. and Miller, J.H., "Condensation of vapor on a vertical plate with a transverse electrostatic field", J. Heat Transfer (Trans. ASME), 87, 197-201 (May 1965).

122. Holmes, R.E. and Chapman, A.J., "Condensation of Freon-114 in the presence of a strong nonuniform, alternating electric field", J. Heat Transfer, (Trans. ASME), 92, 616-620 (Nov. 1970).

123. Frankel, N.A. and Bankoff, S.G., "Laminar film condensation on a porous horizontal tube with uniform suction velocity", J. Heat Transfer (Trans. ASME), 87, 95-102 (Feb. 1965).

124. Yang, Ji Wu, "Effect of uniform suction on laminar film condensation on a porous vertical wall", J. Heat Transfer (Trans. ASME), 92, 252-256 (May 1970).

125. Dent, J.C., "The calculation of heat transfer coefficient for condensation of steam on a vibrating vertical tube", Int. J. Heat Mass Transfer, 12, 991-996 (Sept. 1969).

126. Grober, H., Erik, S. and Grigull, U., Fundamentals of Heat Transfer, McGraw-Hill Book Co. (1961).

127. Lee, J., "Turbulent film condensation", AIChE J., 10, 540-544 (July 1964).

128. Dukler, A.E., "Fluid mechanics and heat transfer in vertical falling film systems", Chem. Eng. Prog. Symposium, 56, 1 (1960).

129. Sparrow, E.M. and Marschall, E., "Binary, gravity-flow film condensation", J. Heat Transfer (Trans. ASME), 91, 205 (May 1969).

130. Tanner, D.W., et al, "Heat transfer in dropwise condensation at low steam pressures in the absence and presence of non-condensable gas", Int. J. Heat Mass Transfer, 11, 181-190 (Feb. 1968).

131. Kroger, D.G. and Rohsenow, W.M., "Condensation heat transfer in the presence of a non-condensable gas", Int. J. Heat Mass Transfer, 11, 15-26 (Jan. 1968).

132. Rose, J.W., "Condensation of a vapour in the presence of a non-condensing gas", Int. J. Heat Mass Transfer, 12, 233-237 (Feb. 1969).

133. Denny, V.E., Mills, A.F. and Jusionis, V.J., "Laminar film condensation from a steam-air mixture undergoing forced flow down a vertical surface", J. Heat Transfer, (Trans. ASME), 93, 297-304 (Aug. 1971).

134. Akers, W.W., Davis, S.H., Jr. and Crawford, J.E., "Condensation of a vapor in the presence of a non-condensing gas", AIChE Preprint 113, 3rd National Heat Transfer Conference ASME-AIChE (Aug. 1959).

135. Lebedev, P.D., Baklastov, A.M. and Sergazin, Zh.F., "Aerodynamics, heat and mass transfer in vapour condensation from humid air on a flat plate in a longitudinal flow in asymmetrically cooled slot", Int. J. Heat Mass Transfer, 12, 833-842 (Aug. 1969).

136. Vizel', Ya. M. and Mostinskiy, I.L., "Mass transfer in vapor condensing from a moving vapor-gas mixture", Heat Transfer-Soviet Research, 1, 97-105 (Mar. 1969).

137. Henderson, C.L. and Marchello, J.M., "Film condensation in the presence of a noncondensable gas", J. Heat Transfer (Trans. ASME), 91, 447-450 (Aug. 1969).

138. Hampson, H., "Condensation of steam on a tube with filmwise or dropwise condensation and in the presence of a noncondensable gas", Int. Developments in Heat Transfer, Part I, ASME, 310-318 (1961).

139. Meisenburg, S.J., Boarts, R.M. and Badger, W.L., "The influence of small concentrations of air in steam on the steam film coefficient of heat transfer", Trans. Am. Inst. Chem. Engrs., 31, 622-38 (1935).

140. Sparrow, E.M. and Lin, S.H., "Condensation heat transfer in the presence of a noncondensable gas", J. Heat Transfer (Trans. ASME), 86, 430-436 (Aug. 1964).

141. Brdlik, P.M., Kozhinov, I.A. and Petrov, N.G., "Experimental investigation of heat and mass transfer during condensation of water vapor from humid air on a vertical surface under natural convection conditions", J. Eng. Physics, 8, 164-166 (Feb. 1965).

142. Marschall, E., "Heat transfer of a condensing vapor in the presence of gases", Kaltetechnik, Klimatisierung, 19, 241-245 (Aug. 1967).

143. Sadek, S.E., "Condensation of steam in the presence of air: experimental mass transfer coefficients in a direct-contact system", I & EC, Fundamentals, 7, 321-324 (May 1968).

144. Stern, F. and Votta, F., Jr., "Condensation from superheated gas-vapor mixtures", AIChE J., 14, 928-933 (Nov. 1968).

145. Taitel, Y. and Tamir, A., "Condensation in the presence of a noncondensable gas in direct contact", Int. J. Heat Mass Transfer, 12, 1157-1169 (Sept. 1969).

146. Ozisik, M. Necati and Hughes, D., "Effects of condensation on the transport of matter from vapor and noncondensable gas mixtures", Nuclear Science and Engineering, 35, 384-393 (1969).

147. Chang, Ki. I. and Spencer, D.L., "Effect of regularly spaced surface ridges on film condensation heat transfer coefficients for condensation in the presence of noncondensable gas", Int. J. Heat Mass Transfer, 14, 502-505 (Mar. 1971).

148. Selin, G., "Heat transfer by condensing vapors outside inclined tubes", Int. Developments in Heat Transfer, II, ASME, 279 (1961).